



**Hydraulics Research**  
Wallingford

MODELLING THE DISPERSAL OF  
EFFLUENTS IN TIDAL WATERS

A review by  
Nicholas Odd

Report No SR 47  
April 1985

Registered Office: Hydraulics Research Limited,  
Wallingford, Oxfordshire OX10 8BA.  
Telephone: 0491 35381. Telex: 848552

© Crown Copyright 1985

Published by permission of the Controller of Her Majesty's Stationery Office.

This report describes work funded by the Department of the Environment under Research Contract PECD 7/7/049. It was carried out by Mr N V M Odd in the Tidal Engineering Department of Hydraulics Research, Wallingford, under the management of Mr M F C Thorn.

## SUMMARY

The report is a short review of the various types of Mathematical Modelling techniques that are available in the UK to simulate and predict the physical dispersal of sewage and trade effluents in tidal waters. The models are assessed in terms of their capability to predict the effect of effluents on Environmental Quality Standards and Environmental Quality objectives, with special reference to mixing zones. The report does not discuss the biochemical or biological aspects of the models.

The main weakness of the types of one-dimensional models of estuaries currently used by Water Authorities in the UK is the neglect of suspended particulate pollutants.

There is a need to test and demonstrate the application of multi-dimensional, multi-process models to a selected number of estuaries in the UK.



## CONTENTS

	Page
1 INTRODUCTION	1
2 MIXING ZONES	2
3 EFFLUENT DISCHARGES IN COASTAL WATERS	3
3.1 Analytical models	4
3.2 Initial dilution	4
3.3 Buoyant spreading	6
3.4 Advection and Turbulent Dispersion	7
3.5 Wind effect	9
3.6 Other factors	9
3.7 2-dimensional numerical models	10
3.8 3-dimensional numerical models	13
4 ESTUARY MODELS	14
4.1 1-dimensional models	14
4.2 Moving element models	15
4.3 Fixed element models	16
4.4 Tide-averaged fixed element models	17
4.5 Seaward boundary conditions	18
4.6 2-dimensional in-depth width averaged models	18
4.7 3-dimensional segmented and layered models	19
5 INTERACTION OF PHYSICAL AND BIOLOGICAL PROCESSES	20
6 DISCUSSION AND CONCLUSIONS	21
7 ACKNOWLEDGEMENTS	26
8 REFERENCES	26

### FIGURES:

1. Different types of tidal receiving waters and effluent distributions

### APPENDICES:

- A Sewage dilution
- B Surface spreading
- C 2-D in-plan model
- D Sewage and solid waste disposal
- E 3-D fine gridded model
- F 1-D moving element model
- G 1-D fixed element model with particulate pollutants
- H 2-D in-depth model
- I 3-D segmented model with photosynthesis



## 1 INTRODUCTION

In 1984, the Department of the Environment commissioned Hydraulics Research Ltd (HR) to make a short review of the various types of mathematical modelling techniques that are available in the UK to simulate and predict the dispersal of sewage and trade effluents in tidal waters. The purpose of the review was to assess the capabilities and limitations of the various types of models that are available for predicting the effect of effluents on Environmental (water) Quality Standards and Environmental Quality Objectives, with special reference to mixing zones. The review includes a general description of the theories employed in the models, but there was insufficient time and money to present the detailed equations, which are copied directly from other reports in the form of appendices.

The brief review only covers the general types of pollution or water quality models that are known by the author to be currently available in the UK. It does not deal with biochemical or biological aspects of the models.

An Environmental Quality Objective (Ref 1) defines the desired state of a body of tidal water in terms of its aquatic ecology and human health. For example, whether it should be able to support various types of fisheries. Environmental Quality Standards define the maximum or minimum levels of floating, dissolved, suspended and adsorbed chemical substances in a tidal water body and its sediments, which are compatible with the desired Environmental Quality Objectives. Emission Standards are the permitted concentrations of toxic chemicals in sewage and trade effluents discharged into a body of tidal water.

One of the main uses of a pollution or water quality model is to predict the effect of changes in the magnitude and distribution of different types of

sewage and trade effluents on the water quality of the tidal water body and its ecosystem. The UK has over a hundred estuaries and thousands of miles of coastline. In the UK there are many wide and relatively deep estuaries formed in sunken glacial valleys, which are exposed to strong tidal mixing due to the relatively high tidal ranges that occur along the UK coast. The UK is also surrounded by shallow seas with relatively strong tidal currents. The sizes of most of the largest estuaries in the UK are out of proportion to the runoff from their existing catchments. For example, the flow of tidal water in and out of the Humber estuary exceeds the peak fluvial flood discharge in the Mississippi river. There are also a large number of smaller and shallower estuaries which have a relatively higher annual fluvial runoff.

There are broadly two types of model

- a) analytical
- b) numerical

Analytical models are based on averaged differential equations (Ref 2) or semi-empirical functions that are solved by classical analytical techniques, which give exact solutions in terms of a few representative variables. Numerical models are based on non-linear differential equations which are applied to a grid covering the study area and which are solved by numerical techniques using computers.

## 2 MIXING ZONES

These are several definitions of a mixing zone. One description of a mixing zone is that it is the region of intense mixing between two bodies of water containing different concentrations of a substance. In fact, the more turbulent body of water usually mixes with and entrains the less turbulent body of water. The initial dilution of a turbulent effluent jet is a process of intense mixing and entrainment of

the ambient flow. However, the area enclosing the identifiable effluent plume is often termed the mixing zone. This is usually only a few kilometers in length and a few hundred metres across.

Another technical description of a mixing zone is the body of water within which most of the effluent is contained. In this context, the whole of the Continental Shelf is a mixing zone for conservative or slowly decaying substances such as Caesium 137.

Particulate pollutants or pollutants adsorbed onto particulate matter tend to be contained within estuaries by gravitational circulation generated by the mixing of river and sea water. Examples of different types of tidal receiving waters and effluent distributions are shown in Fig 1. A reliable pollution model must enclose the whole of the mixing zone for all the effluents under consideration, and simulate the main physical dispersal processes.

### 3 EFFLUENT DISCHARGES IN COASTAL WATERS

An effluent plume is the distribution of floating, dissolved or suspended matter recently discharged from an outfall. The boundary limits of a plume, which should be the zone of rapid mixing, is usually defined rather approximately in terms of either a relative dilution,  $S = C_0/C$  or as an excess concentration over and above the background value  $(C-C_B)$ .

The relative importance of the various physical processes governing the rate of mixing and dispersion of an effluent in a body of tidal water varies with distance from the outfall. It depends upon the geometry of the outfall, the buoyancy and rate of discharge of the effluent, the pattern of tidal flows and wind driven and residual currents and degree of stratification in the ambient flow.

### 3.1 Analytical models

The most common types of analytical model used to describe a single effluent jet discharged from a port on the seabed, separate the mixing process into three distinct phases.

- i) Initial dilution
- ii) Buoyant spreading
- iii) Advection and dispersion.

### 3.2 Initial Dilution

Initial dilution is the process by which the turbulent jet is diluted by entraining the ambient water as it rises to the surface. The main incentive for achieving a high initial dilution for an effluent discharge is to prevent the formation of surface slicks, to reduce the concentration of harmful or toxic pollutants and to minimise the buoyancy of the resulting plume.

The minimum initial dilution of a single jet of non-saline water from a single vertical port (opening) at the boil point in seawater can be calculated for both a condition of slack water (eq 3.1) and with a tidal cross-flow (eq 3.2) reasonably accurately using the semi-empirical theories of Cederwall<sup>(3)</sup> and Wright<sup>(4)</sup>.

$$S = 0.54F \left( \frac{0.38Z}{dF} + 0.68 \right)^{5/3} \quad (3.1)$$

$$S = 0.51 \left( \frac{Z}{d} \right)^2 \frac{U_a}{U_j} \quad (3.2)$$

$$\text{or } S = \frac{0.4 u_a Z^2}{Q} \quad (3.3)$$

Where  $S$  = the minimum dilution of the surface  
 $d$  = the diameter of the Port (m)  
 $Z$  = the depth of water above the outfall (m)  
 $U_j$  = jet velocity at the port m/s  
 $F = U_j \sqrt{g \frac{\Delta\rho}{\rho}} \cdot d$  (Densimetric Froude Number)  
 $\frac{\Delta\rho}{\rho} = 0.026$   
 $U_a$  = the ambient cross-flow velocity (m/s).  
 $Q$  = the discharge through the port ( $m^3/s$ )

The constants (for SI units) were fitted by laboratory experiments. The formulae fit field data measured at outfalls by WRC reasonably well (with slightly different values of the coefficients (Ref 5, Appendix A), and the Southern Water Authority (Refs 6,7)).

The densimetric Froude number should exceed unity for dry season flows to avoid seawater and sediment intruding into the outfall ports. Wright's research showed that the initial dilution is independent of the diameter of the outfall port for a wide range of conditions. Careful attention has to be taken to see that unrealistic levels of turbulence and the effects of viscosity do not unduly influence laboratory results. In the case of field observations, care has to be taken to sample the whole unsteady three-dimensional structure of the plume. There is scope to improve our understanding of the effect of the spacing and orientation of the outfall ports on initial dilution.

Initial dilution of an effluent discharge changes continuously as the depth of water and the tidal velocities vary during a semi-diurnal tidal cycle. The lowest dilutions and highest buoyancy occurs at LW slack when the water depth and tidal velocities are at a minimum.

### 3.3 Buoyant spreading

The methods of modelling the next phase of dispersion of the effluent are more varied, approximate and controversial. Most models assume that the process of initial dilution effectively reduces the buoyancy of the diluted plume to negligible values. In this case, the plume is fairly rapidly mixed through the water column to form a vertically well-mixed plume a short distance from the outfall. It is true that it is usually not possible to identify a plume by measuring salinity distributions, especially at the main run of the tide. However, the author is of the opinion that the above assumption is an over-simplification especially during the LW slack period. The slick of poorly diluted effluent which is discharged at LW slack tends to spread rapidly in a radial direction to form a thin surface layer without losing much buoyancy or becoming much more dilute. Hyden and Larsen showed that the rate of spreading is independent of the initial dilution (Ref 8, Appendix B). The half width of the plume,  $b$ , increases with the  $2/3$  power of the distance from the outfall,  $x$ .

$$b \sim \left[ x \sqrt{\frac{9}{4} \cdot g \frac{\Delta \rho}{\rho} \frac{Q}{U_a^3}} \right]^{2/3} \quad (3.4)$$

Such a thin weakly buoyant slug of polluted surface water can then be transported by the combined effects of wind and tide before it mixes into the main body of underlying water. Plumes from outfalls with multiple ports will merge. Little is understood about the physics of either of these two processes.

With our present knowledge, one has to estimate either the effective initial thickness,  $h$ , or the effective initial half width,  $b_0$ , of the plume. The initial dilution is then used to estimate the other unknown assuming either a top hat (uniform) or Gaussian concentration distribution.

The physical processes occurring in the transition phase of buoyant spreading, between initial dilution by entrainment and spreading by ambient turbulence are not well understood, especially when there is more than one plume. But, from a consideration of continuity, and the application of Wright's dilution equation one can show that the product of the effective half width and the effective thickness of the plume, after initial dilution, is related to the depth of water,  $Z$ , and the number,  $n$ , of ports; assuming they are spaced so that the plumes start to interact at the water surface.

$$b_o h \approx \frac{n}{4} Z^2 \quad (3.5)$$

The cross-sectional area and hence the dilution of a combined plume increases or decreases approximately linearly with the number of operating ports. If some ports become blocked the initial dilution becomes worse.

### 3.4 Advection and Turbulent Dispersion

At the next phase of the dispersion of a plume, which is reached at some distance from the outfall, the lateral and vertical spreading process is governed by ambient turbulence in the tidal stream. The concentrations of dissolved pollutants are often assumed to take on a Gaussian profile in both a vertical and lateral direction. The concentrations in the plume can be estimated by solving the advection dispersion equations by analytical techniques (Ref 9) in terms of  $x$ ,  $y$  and  $z$ ; the distance measured along, laterally and vertically from the centre line of the plume, respectively. The values of the coefficient of horizontal,  $K_y$ , and vertical,  $K_z$ , dispersion in UK waters are usually in the range  $0.5 - 10 \text{ m}^2/\text{s}$  and  $10^{-4} - 10^{-2} \text{ m}^2/\text{s}$ , respectively. If the plume remains as a

thin buoyant layer, as may occur after slack water,  $K_y$  may be set to zero. If the plume is well-mixed through the depth one only needs to consider lateral spreading. However, the plume will spread and distort in a different fashion if it moves into shallower or deeper water. In this case, one has to solve the two-dimensional depth averaged equations for the conservation of the pollutant using numerical techniques. Considering the case where the depths are uniform or the plume is a thin layer, then as the plume widens larger eddies can cause mixing within it so that the value of  $K_y$  will tend to increase with distance from the outfall.

Conditions often reach a quasi-steady state on the main run of the flood and ebb tides. In this case, there is a simple analytical solution with constant velocities and constant initial dilutions.

Unfortunately, this is not usually a critical design condition because initial dilution is at a maximum. In contrast, the slug of poorly diluted effluent discharged at slack water tends to form into a circular spreading patch moving along the centre line of the plume. The distribution of pollution in this patch can be estimated by the same type of analytical technique as applied to a single spreading patch. Such isolated patches of poorly diluted effluent are released four times a day, and they are the most likely cause of pollution on nearby beaches.

The changing position of the centre line of a plume in a tidal current can be determined directly from float track observations in the field or from a physical scale model. Alternatively, they can be predicted by using a two-dimensional or three-dimensional mathematical model. Observations are satisfactory, provided you have already one or two preferred sites for the outfall. The floats can be set at any level. But it is unlikely that the observations will cover the full range of critical design conditions as

regards tide and wind. The use of a 2-dimensional tidal model allows one to determine the path or track of particles of water from any position and any type of tide. A 3-dimensional model can also be used to predict the effect of a cross wind on a plume track. This can not be done using a 2-dimensional depth averaged model.

### 3.5 Wind effect

The most common method of allowing for wind drift is to add vectorally a current which is usually 1-3% of the speed of the wind and in the same direction. This method does not allow for the Ekman effect in which the direction of the drift varies with depth below the surface, or the generation of return flow at depth where an onshore wind blows into a beach (a critical design condition). The non-linear interaction of tide and wind may carry a plume or slug of poorly diluted effluent directly onto a nearby beach. But non-linear interactions may also rapidly disperse the pollutant by shearing and mixing the plume in three dimensions.

### 3.6 Other factors

The concentration of pollutants in the mixing zone defined by an effluent plume are also affected by whether the pollutant is: floating, such as an oil slick; suspended, in which case it tends to settle into the lower layer and possibly even on to the bed; or if it had a high mortality as in the case of coliforms in sunlit saline waters. Oil slicks may either evaporate or sink. Floating rubbish tends to move in the direction of prevailing winds. Suspended particles usually flocculate in salt water and may either settle into the lower layers or become part of the suspended load of the estuary. Its eventual distribution is then governed by the tidal currents and circulations within the region as a whole (Ref 10). The mortality rates for coliforms are probably the most uncertain factor in predicting the dispersion of sewage plumes.

The analytical plume model is best suited to evaluating the distribution of pollutants in single small buoyant plume in a coastal region of approximately uniform depth (Fig 1(a)).

### 3.7 2-dimensional in-plan numerical models

2-dimensional in-plan numerical models have been used to predict the dispersion and interaction of several large discharges in shallow (1-20 m) vertically well mixed semi-enclosed coastal waters, which are wide in respect to their length (Fig 1(b)) (Appendix C).

The study zone is covered by either a uniform or a nested set of variable grid sizes. The grids may be square as used in finite difference methods or polygons as used in finite element models. The finest grids are located so as to cover the area surrounding the focal point of interest such as the discharge point from an outfall. In the case of finite element models, the grid can be chosen to either match the bathymetry and the coastline, the pattern of tidal currents or the shape of the plume but not all three at once. Whereas finite difference models use uniform elements within each grid. A finite element grid which is chosen to fit the bathymetry is very unlikely to be ideal for resolving the shape of a moving plume. The grid size needed to resolve a plume is usually an order of magnitude finer than that needed to resolve the tidal currents. Finite element models tend to be very expensive to use to simulate unsteady tidal current patterns. Neither type of model is suitable for simulating wind drift effects. This is because a depth-averaged model does not allow for a return flow at depth. Results from a tidal flow model are used to drive a pollution model. The pollution model may have exactly the same grid as the flow model or it may use a finer grid by interpolating the flow results.

The pollution model solves the 2-dimensional depth-averaged equations for the conservation of each pollutant. Each outfall is represented by a loading into a single element of the model. The initial dilution predicted by this type of model depends entirely on the volume of the outfall element. There is no difficulty in modelling mortality or the prescribed chemical interaction of several dissolved pollutants or re-aeration through the water surface. But the model only deals with depth-averaged values.

The rate of dispersion of a pollutant which is well mixed through the depth, depends on both the rate of mixing between adjacent elements and on the relative movement of different filaments in the flow. The former mixing process is probably most important in the immediate vicinity of the outfall where the concentration gradients are highest. The method of solution used in all numerical models tends to smooth the solution in the region of steep gradients. The degree of numerical smoothing or mixing depends on the solution technique and the size of the grid. In general, 2-dimensional models cannot be expected to predict the concentration of pollutants accurately close to the outfall. The finer the grid the more accurate the model.

The process of lateral turbulent exchange in tidal flows is not well understood. The most common method is based on the use of the concept of a coefficient of lateral eddy diffusivity, which is usually assumed to be equal to the coefficient of lateral eddy viscosity as used in the flow model. The value of the coefficient of lateral eddy viscosity is normally adjusted approximately by trial and error so that it gives the correct pattern of tidal eddies. The size of eddies (unconstrained by the local geometry of the coastline) and the speed of rotation depends in part on the rate of exchange of momentum from the main flow to the eddy. The coefficients of lateral eddy

viscosity and diffusivity vary approximately in the range 1-10  $\text{m}^2/\text{s}$ . They are usually assumed to be constant over the area of each grid.

Another method, employed by the Water Research Centre (Appendix D), disperses the pollutant between model elements by using random walk techniques (Ref 10). This method attempts to simulate the type of random motions that occur in turbulent flows. The method has embedded in it empirical coefficients which control the rate of lateral mixing. The model has the advantages of a Lagrangian method in that it is not troubled by numerical dispersion effects. Unlike the Fickian diffusion methods previously mentioned, the random walk method gives a different answer each time the model is run. The results of several runs are used to establish a statistical average and range of variability of pollutant concentrations in the plume. More recently, WRC have used the results from the single run with a larger number of particles (25,000). The model records the location and time of release of each particle for a single tidal cycle using a grid size of about 100m. The effect of decaying coliforms released on previous tidal cycles is taken into account by assuming the pattern of particles is the same each tide. The random walk method is more expensive to use than the standard diffusion method.

All 2-dimensional models are expensive methods to use to investigate single small isolated plumes when compared to the analytical methods; especially if new field data is needed to calibrate the flow model.

2-dimensional depth-averaged numerical models are best suited to:

- a) predict the dispersion of single very large intermittent or steady discharges of effluents into vertically well-mixed turbulent tidal flows in enclosed tidal waters. In this case, the

effluent is rapidly mixed through the depth and the shape of the plume is often heavily distorted or even divided by the pattern of unsteady tidal currents (Ref 11).

- b) To simulate the cumulative effect of a number of large discharges on water quality of a semi-enclosed body of coastal water Fig 1(b) Ref 12).

2-dimensional numerical pollution models are not suited to simulate conditions in which surface wind drift effects are important or when the plume remains buoyant for a significant period.

### 3.8 3-dimensional Numerical models

3-dimensional or multi-layer models use the same in-plan grid as the 2-dimensional models. The water body can be divided into a number of unequally spaced layers. At present, HR's 3-dimensional model (Appendix E) can only handle a single grid with about 62 x 62 elements in plan and 4-10 layers within each element.

The wind effect is introduced simply by applying a stress to the water surface. The model correctly reproduces the effect of Coriolis at all depths in the flow. It will simulate the two-layer residual flow pattern set up by an on-shore wind. A 3-dimensional flow model can actually reproduce the tracks of particles on the surface.

A 3-dimensional model will also correctly simulate the vertical and horizontal structure of a large buoyant plume. The plumes behave correctly because the model simulates the damping of vertical turbulent exchange at the underface of the buoyant plume. At present, this type of fine grid model is most suited to simulate the dispersion of dissolved, or particulate

(settling) pollutants from small to medium river outfalls into coastal regions (Fig 1(c)). It is also ideally suited for simulating the hot water plume formed by large coastal power stations (Ref 13).

#### 4 ESTUARY MODELS

Estuaries are mixing zones. They receive a variety of pollutants from upland rivers and from outfalls sited along their banks.

##### 4.1 1-dimensional models

Many estuaries are narrow with respect to their length (Fig 1(d)) and fairly well-mixed over their cross-section. This means that all variables only vary as a function of time or distance along the estuary and they can be treated as 1-dimensional problems. In that case, all the calculations are made in terms of values averaged over the cross-section.

The prerequisite of a 1-dimensional water quality model is a knowledge of the tidal flows in the estuary. This may be determined from a cubature using closely spaced tidal level observations and cross-sections from the estuary but, 1-dimensional hydro-dynamic models can simulate tidal flows for a much wider range of tidal and fluvial flow conditions. A hydro-dynamic model can also predict the effect of new engineering works, such as barrages, dredging and the re-distribution or reduction of fluvial flows on water movements in an estuary.

1-dimensional models may be used to simulate and predict the following processes in estuaries:

- a) Salinity intrusion
- b) Oxygen and nutrient balance
- c) Heat balance

- d) Inter-tidal fixed element models will also simulate mud transport (turbidity) and the movement of adsorbed and suspended particulate pollutants.

Mathematical models can now handle branched and looped tidal channel systems. The results are used to solve the advective diffusion equation for the conservation of pollutants in the estuary. There are three methods of solving the conservation equations using

- a) moving elements
- b) fixed elements
- c) tide averaged models.

#### 4.2 1-dimensional moving element models

In the moving element method, the volume of water in the tidal channel is divided into elements of constant volume, which move up and down the estuary with the tide (Ref 14 and 15) (Appendix F). The model calculates the concentration of pollutants in each constant volume element as a function of time. Effluents are added to the correct moving element as it passes each outfall. The method is extremely elegant and gives a very rapid answer for repeating tides with a steady fluvial discharge.

The results are usually output in terms of long term average conditions at half-tide. The method has been used as a planning tool for the Thames Estuary for many years (Ref 16).

The longitudinal mixing between the elements is represented in terms of an equal and opposite exchange discharge, which is not easily related to the physics of mixing processes between fixed elements in estuaries. However, moving element models are usually calibrated using salinity observations. The method

avoids the problem of numerical mixing by spreading the effluents between the elements according to their position at different phases of the tide.

The method requires a high level of mathematical skill to apply the method to a branched (or looped) channel network like the Yorkshire Ouse system (Ref 17), where the elements divide and rejoin (travel side by side with lateral mixing) at the junctions. The method has even been applied to a 2-dimensional in-plan models of bays and two layer models of estuaries. However, in these cases it assumes that particles of water move backwards and forwards along the same paths every tidal cycle. Residual circulations have to be imposed on the system.

The main disadvantage of the method is that it requires the tidal flows to be processed in a special manner, which is not very well suited to analysing conditions during unsteady fluvial flows. The other drawback is that the method is not well suited to calculating the erosion, transport and deposition of particular pollutants.

#### 4.3 1-dimensional fixed element models

A fixed element model generally uses the same computational grid as the flow model, which divides the tidal channel into small elements spaced along its length (Ref 18). The volume and rate of flow through each element varies during the tidal cycle. The pollution model can be driven with either a repeating neap-spring tidal cycle of flows with a constant fluvial discharge; or it can be run with a changing pattern of fluvial flows. The longitudinal mixing is treated as a Fickian process with a coefficient of effective longitudinal dispersion, which can vary with distance along the channel and with the river discharge. The mixing process in the model is usually calibrated by using salinity observations.

A fixed element model tends to consume considerably more computer time than a well set up steady state moving element model. Care has to be taken to make sure that numerical dispersion introduced by the solution technique is small compared to physical dispersion by using small element lengths and time steps. The method can handle particular pollutants (Ref 19, Appendix G), which settle on the bed at slack water, and discontinuous flows through barrages and from storm water outfalls. The fixed element model is well suited to quick ad-hoc engineering feasibility studies involving changes to the shape of an estuary.

#### 4.4 Tide-averaged fixed element models

Physically, the simplest model is a tide-averaged fixed element model. In this case, the model solves the conservation equations for a tide-averaged condition with constant volume fixed elements (Ref 20). Both the advective and dispersive processes by which the tidal motion spreads an effluent over the length of a tidal excursion are represented in the model by a coefficient of effective longitudinal dispersion. Salinity observations are used to define the value of the coefficients and the model is calibrated in terms of mixing processes by using salinity observations.

Tide-averaged fixed element models do not predict the position of peaks in pollution concentrations that occur at high water and low water slack as accurately as either the moving element or fixed-element inter-tidal models.

#### 4.5 Seaward boundary conditions

The prescribed seaward boundary conditions may have a significant influence on the results from a 1-dimensional model. Ideally, the boundary should be located at a section which is remote from the region of interest. In the moving element model and tide-averaged fixed element models, the only means of losing pollutant to the ocean is by the agency of the net residual fluvial flow out of the boundary and by turbulent mixing between the most seaward element and the ocean. This latter term can be large even if the longitudinal concentration gradients are small at the boundary, because the coefficient of longitudinal mixing (or equivalent mixing flows) increase rapidly at the mouth of an estuary (Ref 21).

The boundary conditions for an inter-tidal fixed element model are slightly different in that you only need to prescribe the concentration of pollutants on the incoming water on the flood tide. This means that this type of model can simulate - but also overestimate - the loss of pollutants removed from the mouth an estuary by longshore tidal currents. In this case, only part of the water leaving the estuary on the ebb tide is returned on the following flood tide. A model may always be extended into the open sea to avoid losing pollutants from the calculation area at low water.

#### 4.6 2-dimensional in-depth width averaged models

In this type of model, the estuary is divided into layers as well as elements along the estuary. The model can simulate variations in pollutant concentrations both as a function of depth and distance along the estuary. They are most suited to simulating conditions in deep partially stratified canalised estuaries (Ref 23).

The interfaces may move up and down with the rising and falling tide to maintain a fixed number of layers. Or, they may be fixed in space with the water level moving up and down through the surface layers. If the tidal range is small compared to the depth the motion of the surface can often be contained within a single surface layer. Fixed layered models simulate the physical processes of gravitational circulation and vertical mixing more accurately than moving layer models. A fixed layer model is probably more suited to simulating estuaries with deep and shallow areas.

The pollution models may be run either independently (Appendix H) or inter-actively with the tidal flow model. A layered model is ideally suited for simulating gravitational circulation, stratification and the transport of particulate pollutants in deep, partially mixed estuaries. There is less empiricism in the manner of simulating longitudinal dispersion in these types of models than with 1-dimensional area averaged models.

#### 4.7 3-dimensional segmented and layered models

This type of model (Ref 24),(Appendix I) is most suited to simulating conditions in an enclosed body of tidal water, which may be divided into a relatively small number (say 20) horizontally well-mixed segments of uneven but approximately equal size and with differing water quality objectives.

The whole model area is divided into unevenly spaced layers which subdivide each segment. The hydrodynamics of the model are more approximate than a uniform fine gridded 2-D or 3-D model. But it can simulate a 3-D gravitational circulation from a number of different lateral freshwater inflows. This type of model may be run in a tide-averaged or inter-tidal mode.

Due to the relatively small number of elements (50-150) it is possible to use this type of model to simulate the interacting effect of the oxygen balance and nutrient balance on the major constituents of the marine ecosystem (Appendix I). The model can also simulate full seasonal cycles in its tide-averaged mode. It is ideally suited for determining the effect of emission standards of individual outfalls or groups of outfalls on average water quality standards and water quality objectives in different zones of an estuary or region of semi-enclosed coastal water.

## 5 INTERACTION OF PHYSICAL AND BIOLOGICAL PROCESSES

The water quality and ecosystem of a body of estuarine or coastal water is maintained by several interacting physical and biological sub-systems as follows;

- (i) hydrodynamics  
(transport, dilution and dispersion of pollutants),
- (ii) suspended particulate transport  
(light penetration, transport and settlement of particulate and adsorbed pollutants),
- (iii) salt and thermal balance  
(gravitational circulation, vertical mixing, biological activity),
- (iv) oxygen and nutrient balance  
(biological activity)
- (v) ecosystem  
(nutrient recycling, oxygen balance, bioturbation),

(vi) toxic pollutants in heavy metals  
(biological activity).

HR have developed a series of multi-dimensional models incorporating the WRC oxygen balance model and the IMER ecosystem model. But they have not been tested by comparison with field observations in a UK estuary.

## 6 DISCUSSION AND CONCLUSIONS

If a model is to be used to predict the effect of changes in the quality, magnitude and distribution of sewage and trade effluents on water quality in tidal waters, it must simulate all the processes and interactions that are relevant to a particular location. Few of the currently available models are sufficiently versatile to include all the aforementioned sub-systems.

There are a wide range of analytical and multi-dimensional numerical hydrodynamic models available to drive an equally wide range of water quality models, which can be applied to simulate and predict conditions in UK tidal waters.

The best type of hydrodynamic to match six common types of receiving waters and outfall configuration, shown in Fig 1 and given below.

CHOICE OF MATHEMATICAL MODELS TO SIMULATE DISPERSAL OF  
POLLUTANTS IN COASTAL WATERS

<u>Type of receiving water and effluent distribution</u>	<u>Type of model</u>
(a) Small isolated outfall on an open coast: biodegradable pollutant	Semi-empirical analytical models
(b) Multiple outfalls in shallow semi-enclosed vertically well-mixed tidal waters with strong tidal currents. (or whole seas)	2-D in-plan numerical model (element size 100-5000 m) (area 400-100,000 km <sup>2</sup> )
(c) Large isolated buoyant discharges into open sea (small river outfall large power station)	3-D fine gridded numerical model. (element size 10-100 m) (area 0.5 - 40 km <sup>2</sup> )
(d) Multiple outfalls in narrow cross-sectionally well mixed turbid estuaries	1-D numerical (channel) model (moving or fixed element) (element size 200-2000 m) (length of system 20-250 km)
(e) Multiple outfalls in narrow stratified estuaries	2-D in-vertical numerical model. (5-25 layers) (20-50 km of channel)
(f) Multiple outfalls in deep (10-20 m) weakly stratified semi-enclosed tidal waters	3-D segmented and layered numerical model. (each segment 1-100 km <sup>2</sup> 3-6 layers) or 2-D 2-layer numerical model.

An analytical plume model is best suited to evaluating the distribution of pollutants in single small buoyant plume in a coastal region of approximately uniform depth.

There are many different versions of analytical plume model depending on the type of flow data and the assumptions made by the modeller. The least well understood physical processes appears to be the buoyant spreading of merging plumes and the transition to vertically well mixed conditions with a cross wind.

In the authors opinion, most attention should be given to modelling the behaviour of the surface pool of poorly diluted effluent which is discharged at slack tide.

All 2-dimensional model are expensive methods to use to investigate single small isolated plumes when compared to the analytical methods; especially if new field data is needed to calibrate the flow model.

2-dimensional depth-averaged numerical models are well suited to predict the dispersion of single very large intermittent or steady discharges of effluent as in turbulent tidal flows where the effluent is rapidly mixed through the depth and the shape of the plume is often heavily distorted or even divided by the pattern of unsteady tidal currents.

Such models also well suited to simulate the cumulative effect of a number of discharges on the water quality of a semi-enclosed body of coastal water.

2-dimensional depth-averaged numerical pollution models are not well suited to simulating conditions in which surface wind drift effects are important or when the plume remains buoyant for a significant period.

The model grid must be fine enough to resolve the structure of the plume. At present there has been insufficient experience with the random walk technique to say whether its use makes a significant improvements of the results compared with a normal solution of the advective diffusion equations.

The main uncertainty in most 2-dimensional models is how to define the value of the coefficient of lateral turbulent diffusivity as a function of known hydrodynamic variables.

At present, few of the multi-dimensional models have been applied to UK estuaries. Instead, moving element and fixed element versions of the 1-dimensional oxygen balance model are used to simulate and predict conditions in all types of estuaries, regardless of their shape or vertical and lateral variations in water quality.

A weakness of most existing water quality models is the neglect of suspended particulate pollutants. Particulate BOD plays a major role in suppressing dissolved oxygen levels during spring tides in many estuaries. For example, the Trent, Mersey, Usk and probably even the Thames Estuary.

The transport of polluted particulate matter can usually only be simulated in a multi-layer model, which resolves the vertical structure of the flow, (except in the case of the tributaries to the Severn estuary). The physical dispersion of heavy metals and most radio active wastes are controlled by the mud transport regime.

The other weakness of most water quality models is the neglect of the interaction between the oxygen, and nutrient balance, and the primary production in the estuary.

UK have proved that it is technically possible to construct and use multi-dimensional models which simulate interaction of these processes.

The hindrance to their application as planning tools in the UK is

- (a) Lack of knowledge of the biochemical behaviour of particulate matter.
- (b) The lack of examples of the application of the new types of models to the UK estuaries.
- (c) The reluctance of Water Authorities to invest significant funds in modelling work as compared to field monitoring exercises.
- (d) The unsuitability of most Water Authority Computers for numerical modelling work.
- (e) The difficulty of Water Authorities employing suitably qualified staff for the intermittent use of models for planning purposes.

In the author's opinion, there is a need for;

- (a) A commitment by the Water Authorities to use the latest modelling techniques as part of their planning studies.
- (b) More laboratory and field data on the biochemical behaviour of particulate pollutants.
- (c) Trial application and testing of multi-dimensional models to a selected number of UK estuaries.
- (d) The development and documentation of a reliable set of standard types of models incorporating

particulate pollutants and selected parts of the ecosystem.

- (e) To find means of providing the Water Industry access to specialised computer facilities with expert support staff.

If research funds were available, HR would be willing to cooperate with WRC, IMER and one of more Water Authorities to apply some of the new types of multi-dimensional multi-process models to a few selected UK estuaries.

## 7 ACKNOWLEDGEMENTS

The author acknowledges the helpful cooperation of the staff of the Water Research Centre, ICI's laboratory at Brixham, Southern Water Authority, Welsh Water Authority and the North West Water Authority in providing information to make this brief review of water quality models used in the UK.

## 8 REFERENCES

- 1 Water Research Centre. Emission Standards in relation to water quality objectives. WRC Technical Report No TR 17, June 1976.
- 2 Chatwin, P C and C M Allen Mathematical Models of Dispersion in Rivers and estuaries. Ann Rev Fluid Mech 1985, 17: 119-149.
- 3 Cederwall. Hydraulics of Marine Waste Water Disposal. Hyd. Div. Chalmers. Inst. of Tech. Gotoborg. Report No 42, January 1968.
- 4 Wright, S J. Mean behaviour of buoyant jets in a cross-flow. J of Hyd. Div. ASCE, 1977, 103 (HY5), 499-513.
- 5 Munro, R. Sewage Dilution between Outfall and Shore. Paper present to Symposium on Sea

Outfalls, Exeter June 1983. The Public Health Engineer, 12 April 1984.

- 6 Bennett, N S. Design of sea outfalls - the lower limit concept of initial dilution. Proc. ICE, Part 2, 1983, 75, p 113.
- 7 Hydraulics Research Report EX 1264. Sandown long sea outfall - Isle of Wight. Estimation of coliform distributions in the effluent plume. Dec. 1984.
- 8 Hyden, H and Lassen, I. Surface spreading Paper No 28, Symposium on discharge of sewage from sea outfalls. WRC Sept 1974.
- 9 Hunter, J R. The prediction of pollutant concentrations, Report U81-3. Marine Science Laboratories, Menai Bridge, Sept 1981.
- 10 Allen C M. Numerical simulation of contamination dispersion in estuary flows. Proc R Soc Lond A 381, 179-194 (1982).
- 11 Hydraulics Research and Southern Water Authority. HR Report EX 1201. Solent and Eastney Outfall Mathematical model, 1984.
- 12 Chalmer, M L, Gameson, A L H, Rodger, J G and Odd N V M. Model Study of Pollution in Hong Kong Harbour. Int. Sym. Waste Water Engineering and Management at Canton, March 1984.
- 13 Cooper, A J. Development and application of a 3-D DAP Numerical Model of Estuaries. HR Report SR 38, March 1985.
- 14 Mollowney, B M. One-dimensional Models of Estuarine Pollution. Water Pollution Research Technical Report No 13, HMSO, 1972.

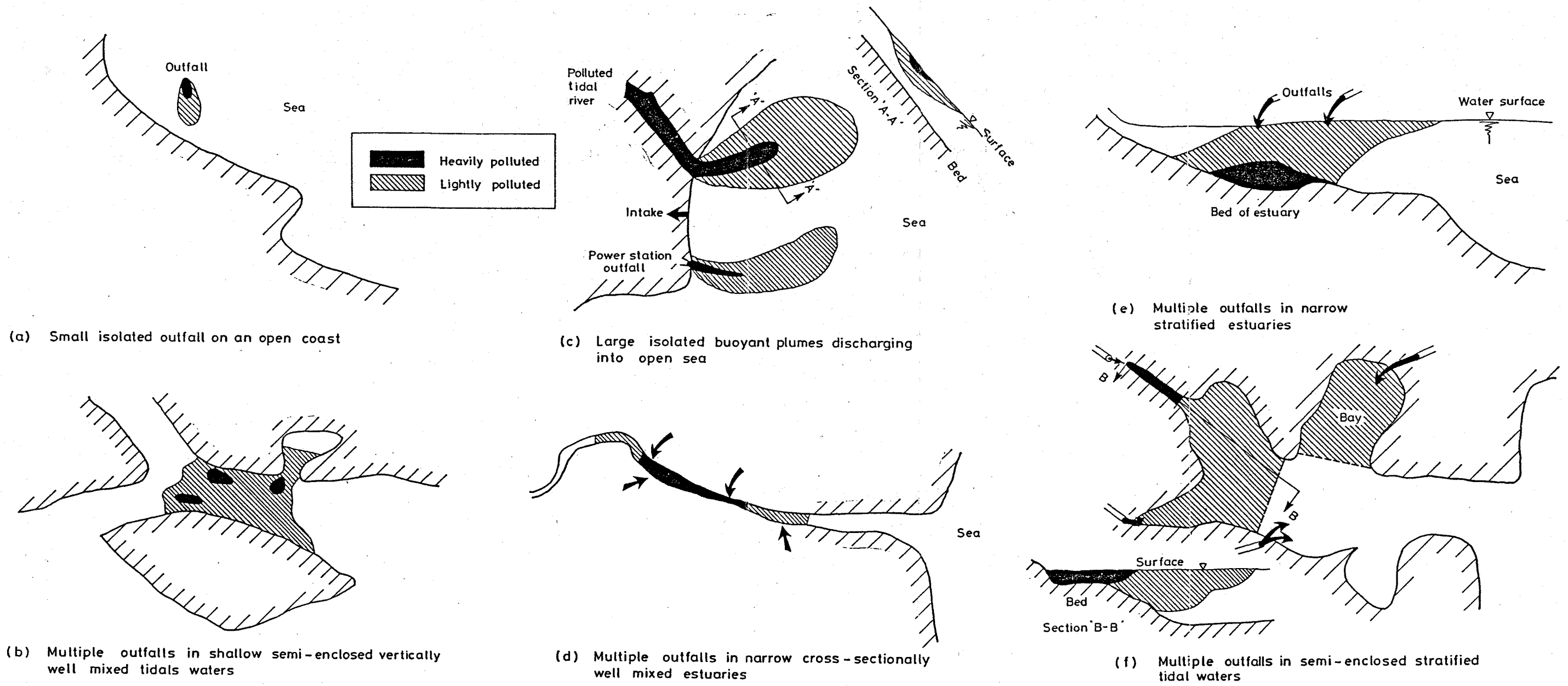
- 15 Mollowney, B M. Moving co-ordinate systems, in estuaries. WRC Technical Report TR 13, April 1976.
- 16 Barrett, M J. Mollowney, B M, Casapieri, P. The Thames Model: An assessment, Proc. Wat. Tech. 1978, Vol 10, Nos 5/6, p 409, Pergamon Press.
- 17 Gameson, A L H (Editor). The Quality of the Humber Estuary 1961-81. Published by the Yorkshire Water Authority on behalf of the Humber Estuary Committee, 1982.
- 18 Maskell, J M and Odd, N V M. HR Report IT 171. A mathematical model of the oxygen balance in a well-mixed estuary. Dec 1977.
- 19 Maskell, J M. The Effect of Particulate BOD on the Oxygen balance of a muddy estuary. EBSA symposium Estuarine Management and Quality Assessment, Dublin, Sept 1982.
- 20 Radford, P J, Uncles, R J, Morris, A W (1981). Simulating the impact of technological changes on dissolved cadmium distributions in the Severn Estuary. Water Research 15, p 1045-1052.
- 21 HR Report EX 868. Shannon Estuary Thermal Study. March 1979.
- 22 Brady, J A. Operational use of estuary models of the Northumbrian Water Authority. Paper No 4 WRC/IH joint colloquia on Residual flows to rivers and estuaries, Oct 1980.
- 23 Hobbs, G D and Fawcett A. Two-dimensional Estuarine Models. Proceedings Sym on Mathematical and Hydraulic Modelling of estuarine pollution. WPRL, April 1972.

24 HR Report EX 1045 Tolo water quality model  
QUEST 1: a three-dimensional water quality model  
and algal growth model. 1982.



FIGURE.





Different types of tidal receiving waters and effluent distributions

Fig 1



APPENDICES.



APPENDIX A

SEWAGE DILUTION

EXTRACT FROM

WRC PAPER 1984

Munro, R. Sewage Dilution between Outfall and  
Shore. Paper present to Symposium on Sea  
Outfalls, Exeter June 1983. The Public Health  
Engineer, 12 April 1984.



## INTRODUCTION

The effectiveness of long sea outfalls at diluting a sewage flow makes it difficult to measure the concentration of the sewage in waters near the shore. Often the chief difficulty is that other sources of the bacterial indicators used to assess the concentration of sewage make a much greater contribution near the shore than does the long sea outfall. It could be concluded that such outfalls are unnecessarily long and that shorter outfalls would have achieved reasonable design criteria, but how could the designers have known beforehand? It is common practice to use some form of predictive mathematical model for design purposes. It is important however that such models should have been validated on some existing long sea outfalls.

Since 1962 the Water Research Centre (or Water Pollution Research Laboratory prior to 1974) has been developing models of bacterial dispersion while placing great emphasis on their field validation. It was hoped that statistical analyses of field measurements of bacterial concentration would determine the parameters associated with the greatest pollution at several sites and sampling positions, though concurrently the programme of research included detailed measurements of effluent dispersion and bacterial decay for use in deterministic models of bacterial dispersion. The wealth of data gathered and the wide variety of real conditions encountered ensured that neither the statistical nor the deterministic modelling approach may be considered verified, but many lessons have been learned and have been published in detailed technical reports<sup>1,2</sup>. This paper attempts to illustrate through a few examples the dilution expected for sewage discharged offshore as it disperses, and reference is made to some more comprehensive models of extreme conditions for poor dilution at the shore. The methods are not claimed to be universally applicable, but they are based on detailed observations of some actual outfalls.

The EC directive on the quality of bathing water<sup>3</sup> is of relevance to a dilution target when designing an outfall, for, though the directive applies only to certain identified beaches, no other standards for bathing waters are nationally recognized in the UK. It would not be easy to specify which parameter in the directive would be the most stringent, but the imperative value for faecal coliforms of 2000 per 100 ml would require a reduction in concentration from levels commonly found in sewage by a factor of about 10 000. In general some reduction in bacterial concentration of sewage is achieved by decay, but this cannot always be relied upon, for example at night or during dull overcast conditions.

## INITIAL DILUTION

In the surface "boil" over an outfall the concept of dilution is fairly simple because the contribution from earlier discharges is small and can be taken account of as a steady background. However where dilutions are large the boil is far from steady and sometimes dilutions are measured from time-average concentrations at a point. Such dilutions would normally be greater than those referred to here, which are based on quick samples where the concentration seems highest. Results of surveys are well described in the literature<sup>4</sup> and for most outfalls the initial dilution can be calculated with reasonable accuracy. Dilution can be increased for a given sewage flow by building a longer outfall into deeper water or by splitting up the flow into more discharge ports, but the former may be expensive and the latter may eventually lead to blockage. The main incentive for achieving a high initial dilution is the prevention of slicks<sup>5</sup> in most sea conditions, and once sewage has been diluted it cannot be reconcentrated. It is sometimes said that poor initial dilution could lead to a stable surface field, but experience at Sidmouth where dilutions between 5 and 20 are common was that the plume dispersed laterally and vertically and the concentrations measured at the shore showed high dilution.

The Water Research Centre has always recommended that outfalls be designed to operate at low discharge velocities at the dry weather flow. At low velocities the dilution,  $S$ , expected at the surface a height  $Y$  above a discharge port with a flow  $Q$  of sewage into quiescent sea water is given by<sup>6</sup>

$$S = 0.091 \left[ \frac{\Delta \rho Y^3}{Q^2} \right]^{1/3} \quad (1)$$

where the sea-water density is a factor  $(1 + \Delta)$  times that of the sewage and  $g$  is the gravitational acceleration. Units need to be consistent.  $\Delta$  is usually taken as 0.026.

In moving water also it should be possible to express the initial dilution independently of the size of the outlet for low outlet velocities. This has been done by Wright<sup>7</sup> using dimensional analysis techniques with the result for a current of speed  $U$

$$S = 0.3 U Y^{3/2} / Q \quad (2)$$

The constant was fitted by observations and appears to fit data collected at outfalls by the Water Research Centre reasonably well.

At modern outfalls with diffuser systems discharging screened or comminuted sewage the diameters of outlet ports tend to be about 0.2 m and outlet velocities corresponding to the dry weather flow are about 0.4 m/s leading to a flow from a port of 0.013 m<sup>3</sup>/s. Thus dilutions at slack water in a water depth of 15 m are nearly 100 while in a current of 0.2 m/s this would be increased to around 1000. For most long sea outfall schemes, such dilutions would be considered adequate aesthetically, but when higher sewage flows have to be discharged, because of the diurnal flow pattern or storm flows, the achievable dilution is usually reduced. Whether initial dilution criteria should be linked with the hydraulic maximum flows is a matter worthy of some discussion, preferably based on surveys where long sea outfalls operate.

## NATURAL DISPERSION IN THE SEA

After discharge near the sea-bed and a large initial dilution, the sewage/sea-water mixture has a density very close to that of sea-water and it is probably transported identically. Natural turbulence (generated by currents at the sea-bed and breaking waves at the surface) ensures that as a patch of sewage is advected by the current it is mixed through an increasing volume. Although dispersion, for example of smoke from a chimney, is obviously not a smooth process it is useful to consider it as a steady mixing of adjacent waters characterized by dispersion coefficients because these can be used to make predictions (based on well-defined postulates) of sewage concentration when velocities in the sea and sewage flows are specified.

The calculation of dispersion coefficients from field measurements usually makes use of the formula<sup>8</sup> describing the effect in one dimension of a dispersion coefficient  $K$  on concentration  $C(x, t)$  at time  $t$  after a quantity  $M$  of material was released at position  $x = 0$ ,

$$C(x, t) = \frac{M}{\sqrt{4\pi Kt}} \exp \left[ -\frac{x^2}{4Kt} \right] \quad (3)$$

The objective is to find the value of  $K$  giving the best overall description of the observations. The Water Research Centre estimated dispersion rates from a series of eight releases in March 1977 of radioactive Bromine 82 through the long sea outfall at West Bay, Dorset. The discharges to the sea lasted about 20 minutes and the patches were monitored for an average of six hours in a wide variety of sea conditions. The dispersion coefficients measured were in the direction perpendicular to the shoreline and in the vertical because these coefficients determine the rate of dilution in a sewage plume elongated parallel to the shore by the tidal currents. The horizontal dispersion coefficients ranged from 0.3 to 7 m<sup>2</sup>/s with a median (from 7 values) of 1.4 m<sup>2</sup>/s while the vertical dispersion coefficients ranged from less than 1 to 60 cm<sup>2</sup>/s with a median

(from 5 values) of 11 cm<sup>2</sup>/s. There was no correlation between the two coefficients. The vertical coefficient was well correlated with roughness of the sea.

Observed dispersion coefficients can be used in equation (3) to show dilutions in sewage plumes: some average conditions at West Bay where the measurements were made illustrate the methods. A typical value of the sewage flow was about 0.03 m<sup>3</sup>/s and the tidal current speed parallel to the shore averaged about 0.2 m/s. Thus when a 1 m thick slice of water perpendicular to the shore moves past the outfall at the average velocity the quantity of sewage discharged into it would be 0.15 m<sup>3</sup>. It is reasonable to assume for the calculation that this volume of sewage stays within the slice because, for a continuous discharge, exchanges with adjacent slices have minimal net effect. Initially it can be assumed that the sewage patch has been introduced at the surface as a hypothetically concentrated point source. More sophisticated models could take account of the initial distribution, but the methods would show negligible difference after a few hours' dispersion.

Assuming a lateral dispersion coefficient of 1.4 m<sup>2</sup>/s, the concentration at the point in the slice where the 0.15 m<sup>3</sup> of sewage was injected would be  $0.15/\sqrt{4\pi} \times 1.4t$  m<sup>3</sup> of sewage per m<sup>2</sup> surface area, when  $t$  is expressed in seconds, because  $\exp(0) = 1$ . Four hours after the start this can be evaluated as 0.000 298 m<sup>3</sup> of sewage in a water column of cross-sectional area 1 m<sup>2</sup>. An effective plume width can be calculated by dividing the amount of sewage present in the slice by its concentration on the central column. Here the value is about 500 m.

The distribution in the water column can also be calculated using equation (3) assuming that the vertical dispersion coefficient of 11 cm<sup>2</sup>/s (0.0011 m<sup>2</sup>/s) has operated for four hours. Because equation (3) assumes no boundary to dispersion it has to be adapted to the case of dispersion being prevented by the water surface. Where the pollutant starts at the surface, and the theory assumes that half the material moves up above the surface, it can be allowed for simply by doubling the estimates of concentration made by equation (3). Thus the concentration at the point in the slice where the sewage was injected 4 h previously becomes  $0.000\ 298 \times 2/\sqrt{4\pi} \times 0.0011 \times 4 \times 3600$  m<sup>3</sup> of sewage per m<sup>2</sup>, calculated as 0.000 042 2, a dilution of about 24 000. As for the lateral width of the sewage field, an effective depth of the field can be obtained by dividing the total quantity of sewage in the central water column by its peak concentration. This leads to an effective depth of 7 m. When the result approaches the total depth the plume cannot deepen and the best estimate of concentration is obtained by dividing the total amount present in the column by the depth.

Since it is unlikely that the sewage plume from the 1340 m outfall would approach bathing waters at West Bay in four hours' drift, there would appear to be no danger of high concentrations of bacterial indicators of sewage pollution on the beach there. However the calculation has been made using average values of many parameters, and other choices can show considerably reduced dilution, particularly for large discharges near slack water. Quickly it becomes advantageous to do the calculations on a computer which can show the results of many sets of assumptions.

#### DILUTION AT THE SHORE

For sewage outfalls worldwide, an important objective is to achieve high dilution of any sewage reaching bathing waters at the shore. Often this is expressed as a bacterial concentration which may be exceeded only infrequently, posing difficulties for the designer as information on the distribution of currents conveying sewage quickly to the shore is seldom available. However wind records covering many years can usually be obtained and it is often assumed that strong onshore winds move a sewage plume towards the shore at about 2 per cent of the wind speed. Great care must be taken with such models that the assumptions made are self-consistent and that when several worst-condition parameters are combined the probability of such a combination is more than infinitesimal.

When currents at the surface have a shorewards component, the water level at the shore would rise unless compensated by subsurface water moving offshore. It has been shown<sup>9</sup> that, for a balanced current system with vertical dispersion continuously redistributing decaying sewage bacteria through the water depths, the numbers of bacteria reaching the shore are strongly dependent on vertical diffusion for parameters typical of long sea outfalls in the UK. Further work<sup>10</sup> at Sidmouth, Devon, where the outfall is 430 m long, showed that strong onshore winds could be roughly allowed for by assuming that the sewage was blown one-third of the way ashore, but then it dispersed normally as if discharged through an outfall whose length had been cut by one third. If the sewage plume had been moved to the shore, as many designers assume, concentrations about 30 times greater than those observed would have been predicted.

For longer outfalls even greater factors of overestimate in the concentrations can be expected when plumes are assumed to be blown to the shore *en masse*.

As prediction of low diluting conditions still needs much evidence, complete reliance should not yet be placed in models, though of course they can be used to estimate some limiting values. Extrapolation of measurements of dispersion of labelled patches to much longer times and over large areas is still a dubious activity. A more convincing method to measure the response at the shore to an injection of a microbial tracer with the sewage or at a proposed discharge point. A great virtue of microbial tracers is that a large number (10<sup>11</sup> is not uncommon) of organisms may be discharged and sample volumes of 100 ml may be analysed. Sufficient numbers should be released to ensure a measurable response at the shore and sampling needs to be round the clock if the main peak is to be sampled. When such responses are used to estimate the dilution of a continuous discharge of sewage between outfall and shore the results have a firm basis. However the exercise needs to be carried out many times if the more polluting situations are to be covered.

#### CONCLUSIONS

Long sea outfalls with a diffuser arrangement in deep water cause the sewage to be diluted about 100-fold in less than a minute from release to the sea even at slack water and dilution by 1000-fold may be expected for typical tidal currents. A point needing careful consideration on design criteria for outfalls is to what extent the lower dilution obtainable at high storm flows should influence design of the outfall.

In the sewage plume dilution increases as turbulent mixing widens and deepens the plume. Typical widths and depths after four hours are about 500 m and 7 m respectively.

Many outfalls are designed on the basis of calculations assuming that the sewage plume can be advected bodily towards the shore by onshore winds, leading to prediction of high bacterial concentrations at the shore for otherwise acceptable outfall sites, and these outfalls are designed longer than necessary. Some modelling work has shown that when consistent current regime is used the sewage is not conveyed directly to the shore. At Sidmouth, for which many data were available, a model which roughly described the observations was to consider that strong onshore winds effectively reduced the outfall to two-thirds of its length. Although mathematical modelling allows study of many hypotheses, the only way to estimate with confidence how much (or how little) dilution may be expected for a particular outfall is to use large additions of microbial tracers. When models can be sharpened up by these data, more reliance on models will be justified.

#### REFERENCES

- (1) Gameson, A. L. H., Monitoring at West Bay, Dorset, in *Coastal Discharges—Engineering Aspects and Experience*, Thomas Telford Ltd., 1981, 197-200.
- (2) Gameson, A. L. H., *Investigations of Sewage Discharges to Some British Coastal Waters. Chapter 5. Bacterial Distributions, Part 4*, Water Research Centre, Technical Report TR 176, 1982.
- (3) Munro, D., Observed and predicted coliform distributions near sea outfall, in *Discharge of Sewage from Sea Outfalls* (ed. A. L. H. Gameson), Pergamon Press, 1975, 353-362.
- (4) Commission of the European Communities, Council Directive of 8th December 1975 concerning the quality of bathing water. *Official Journal*, No. L31, 5th February 1976.
- (5) Agg, A. R., *Investigations of Sewage Discharges to Some British Coastal Waters, Chapter 6. Initial Dilution*, Water Research Centre, Technical Report TR 99, 1978, (a) Equation 6.31.
- (6) Newton, J. R., Factors affecting slick formation at marine sewage outfalls, in *Pollution Criteria for Estuaries* (ed. P. R. Helliwell and J. Bossanyi), Pentech Press, London, 1975, 12.1-12.16.
- (7) Wright, S. J., Mean behaviour of buoyant jets in a crossflow. *Journal of the Hydraulics Division, American Society of Civil Engineers*, 1977, 103 (HY5), 499-513.
- (8) Crank, J., *The Mathematics of Diffusion*, Oxford University Press, 1956.
- (9) Munro, D. and Mallowney, B. M., The effect of a bottom counter-current and vertical diffusion on coliform concentrations at the shore due mainly to wind-induced onshore currents, *Rapport et Procès-verbaux des Réunions Conseil International pour l'Exploration de la Mer*, 1974, 167, 37-40.
- (10) Munro, D., *Influence of Wind on Coliform Counts at the Shore Sidmouth*, Water Research Centre, Technical Memorandum TR 109, 1975.

APPENDIX B

SURFACE SPREADING

EXTRACT FROM

WPRL TECHNICAL REPORT 13

Hyden, H and Lassen, I. Surface spreading Paper  
No 28, Symposium on discharge of sewage from sea  
outfalls. WRC Sept 1974.



The surface spreading phase starts when the vertical motion of a diluted waste-water plume ceases, and ends when the difference in density between the diluted waste water and the surrounding waters is no longer a significant factor for the pattern of motion.

The object of this paper is to describe what may be expected to happen when diluted waste water at the rate of  $Q$  arrives at the water surface—or is trapped at an intermediate level—with almost the same horizontal velocity,  $U_0$ , as the main current. Due to the relative difference in density,  $\Delta$ , the diluted waste water will try to spread in all directions.

### Buoyancy Spread without Vertical Turbulent Diffusion

A description of the buoyancy spread has already been published<sup>1</sup>. It was found that the spreading of waste water due to density differences was chiefly determined by the buoyancy flux and to a large extent was unaffected by dilution and diffusion. The theory was inexact in many details, but was expected to give results of the correct order of magnitude. Calculations for outfalls from larger cities showed that places normally considered sheltered from the outfall zone by a region of considerable turbulent diffusion could in some cases be polluted by poorly diluted waste water and that the influence of wind could add significantly to this effect.

The sheet of waste water formed on top of the main current is supposed to have a uniform thickness,  $h$ , in the direction perpendicular to the main current. A density front will advance with a velocity  $v = k\sqrt{\Delta gh}$  relative to the main current,  $g$  being the gravitational acceleration and  $k$  a constant between 1 and 1.4. With the notation of Fig. 1 the front condition states that

$$U_0 \sin \theta = k\sqrt{\Delta gh}. \quad (1)$$

When turbulent diffusion is neglected, the continuity equation is

$$2BhU_0 = Q. \quad (2)$$

Integration yields

$$\frac{B}{B_0} = 1 + \left(\frac{3x}{2B_0}\right)^{2/3} \quad (3)$$

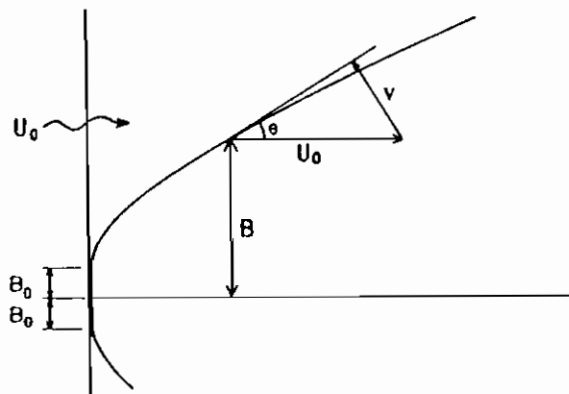


FIG. 1. Plan view of plume boundary in steady current of velocity  $U_0$

where  $x$  is the distance from the upper edge of the plume, and  $B_0$  is the initial half-width of the sewage field, chosen so that the front velocity at this section equals the velocity of the main current:

$$B_0 = \frac{k^2 \Delta g Q}{2U_0^3}. \quad (4)$$

Only the product of  $\Delta$  and  $Q$ , being equivalent to the buoyancy flux, appears in Equations 3 and 4. For a homogeneous recipient the spread is evidently not dependent on the initial dilution. Normally  $B_0$  is larger than the diameter of the rising jet of waste water or the width of the outlet of cooling-water. If not, the equation of spreading (Equation 3) will have to be modified, but the dependence of the buoyancy flux will remain.

### Turbulent Diffusion

Vertical exchange was then considered, both the case of one-sided vertical diffusion from the top layer to the underflowing recipient, and that of symmetrical turbulent exchange between these layers.

It was found that the variation of  $B$  with  $x$  was little affected by turbulent diffusion so long as the surface layer existed. The width,  $B$ , of the surface field may therefore be calculated according to Equation 3. Further, the transport of density deficit,  $T$ , was found to depend mainly on the level of turbulence in the receiving water. In the case of symmetrical exchange the dilution,  $S$ , was determined by

$$S^{-1} = 1 - \frac{Mx}{B_0} \left\{ 0.78 \left( \frac{x}{B_0} \right)^{2/3} + 1 \right\} \quad (5)$$

where  $M$  is the dimensionless exchange rate given by

$$M = \frac{T \Delta g B_0}{U_0^3}. \quad (6)$$

An evaluation of the distance over which the waste water is able to spread due to density effects requires the knowledge of the turbulent exchange mechanism.

Turbulent diffusion between two layers of slightly different density has been studied theoretically and experimentally by the Authors, and some preliminary results have been published<sup>2</sup>. It has been shown<sup>3</sup> that in homogeneous water the diffusion is mainly determined by the larger eddies and that a density gradient will act as an eddy filter reflecting these eddies. Consequently in the presence of a density difference between two layers the turbulent mixing between them will be strongly damped.

By dimensional analysis it was found that the turbulent diffusion across an interface, as expressed by the velocity of exchange,  $u_e$ , can be described by the functional relationship

$$u_e(\nu w)^{-1/4} = F(N_1, N_2, N_3) \quad (7)$$

where  $\nu$  = kinematic viscosity,  $w$  = energy dissipation rate per unit mass and  $N_1, N_2, N_3$  are dimensionless parameters defined by

$$N_1 = L(\nu^3/w)^{-1/4}, \quad (8)$$

$$N_2 = t(w/\nu)^{1/2}, \quad (9)$$

$$N_3 = \frac{\rho w}{\Delta \rho g} (\nu w)^{-1/4}, \quad (10)$$

where  $L$  = eddy size characterizing the energy supply,  $t$  = time,  $\rho$  = density, and  $\Delta \rho$  = density difference.

It was further argued that if  $L$  is larger than the largest eddy size that can contribute to the turbulent diffusion, and if the process may be considered quasi-stationary, then Equation 7 can be simplified to

$$u_e(\nu w)^{-1/4} = F_1(N_3). \quad (11)$$

In order to support the theoretical results, laboratory experiments were carried out using different types of agitators<sup>2</sup>. The results can be summarized by the equation

$$u_e(\nu w)^{-1/4} = N_3^{4/3}/G \quad (12)$$

where  $G$  is a constant depending on the type and the positions of the agitators. Thus, for each type of agitator the experimental result (Equation 12) agrees with the theoretical result (Equation 11).

APPENDIX C

2-D IN-PLAN MODEL

EXTRACT FROM

HYDRAULICS RESEARCH LTD

REPORT EX 1254 AND 1201



## TIDEFLOW-2D MODEL DETAILS, EX 1254

The HR TIDEFLOW-2D model is two-dimensional: the computed velocities being depth-averaged.

The model utilises finite difference techniques to solve the following equations which represent the physical concept of conservation of mass and Newton's Laws of Motion:

Conservation of mass:

$$\frac{\partial \zeta}{\partial t} + \frac{\partial}{\partial x}(ud) + \frac{\partial}{\partial y}(vd) = 0$$

Conservation of momentum:

$$\frac{\partial u}{\partial t} + u \frac{\partial u}{\partial x} + v \frac{\partial u}{\partial y} = -g \frac{\partial \zeta}{\partial x} + \Omega v - fuq/d + D \nabla^2 u$$

$$\frac{\partial v}{\partial t} + u \frac{\partial v}{\partial x} + v \frac{\partial v}{\partial y} = -g \frac{\partial \zeta}{\partial y} - \Omega u - fvq/d + D \nabla^2 v$$

where:

- $\zeta$  is the water surface elevation relative to mean sea level (m)
- $h$  is the bed level relative to the same datum (m)
- $d$  is the total water depth  $\zeta + h$  (m)
- $u, v$  are the depth averaged velocity components (m/s) referred to Cartesian co-ordinates  $x$  and  $y$
- $t$  is time (sec)
- $g$  is the acceleration due to gravity ( $m/s^2$ )
- $f$  is the friction factor
- $\Omega$  is the Coriolis parameter ( $t^{-1}$ )
- $D$  is the horizontal eddy viscosity coefficient ( $m^2/s$ )
- $q$  is the water speed  $(u^2 + v^2)^{1/2}$  (m/s)
- $\nabla^2$  is  $\partial^2/\partial x^2 + \partial^2/\partial y^2$  ( $m^{-2}$ )

The equations incorporate the assumptions that the flow is incompressible and well mixed, that vertical accelerations are

negligible (hydrostatic pressure assumption), and that a quadratic friction law is valid.

The friction factor  $f$  is defined using the rough channel law,

$$(8f)^{-\frac{1}{2}} = 2 \log_{10} (14.8d/k_s)$$

The roughness length,  $k_s$ , is related to the size of the protuberances on the bed, either directly in the form of particle sizes (especially in the case of shingle and stones etc) or indirectly in the form of ripple lengths (in the case of fine particles, ripple lengths are about 1000 times median grain size (see for example Yalin\*)).

The formula for the eddy viscosity coefficient,  $D$  is not well determined: Fischer\* discusses various formulae. Fortunately the solutions to the equations are not in general critically dependent on  $D$  and an initial estimate based on Fischer's discussion, can be taken as:

$$D = 0(u^*d)$$

where  $u^*$  is a typical shear velocity.

The size of  $D$  does have an effect on the size of tidal eddies and so, by comparing model eddy sizes with observations, the value of  $D$  used could be roughly confirmed as being reasonable.

Output from a model run consists of tide levels and the two components of the current for each model cell. These are stored in the computer at frequent intervals during the tide and subsequently processed to yield computer plots of model flow patterns and particle tracks and curves of tide level and current speed and directions during the tide.

The stored results are also available if required for use as input to other elements of the TIDEWAY system to study sediment transport and the dispersion of cooling water and pollution.

## Pollution Model, EX 1201

Both the Dissolved Oxygen/Biological Oxygen Demand models and coliform models use the depth averaged equation describing the transport and diffusion of a non conservative quantity. These equations can be written as

### Dissolved Oxygen

$$\frac{\delta dDO}{\delta t} + \frac{\delta (duDO)}{\delta x} + \frac{\delta (dvDO)}{\delta y} = \frac{\delta}{\delta s} (dD_s \frac{\delta DO}{\delta s}) + \frac{\delta}{\delta n} (dD_n \frac{\delta DO}{\delta n}) + K_c C \quad (1)$$

### Biological Oxygen Demand/Coliforms

$$\frac{\delta dC}{\delta t} + \frac{\delta duC}{\delta x} + \frac{\delta dVC}{\delta y} = \frac{\delta}{\delta s} (dD_s \frac{\delta C}{\delta s}) + \frac{\delta}{\delta m} (dD_m \frac{dC}{dm}) - K_c C + L \quad (2)$$

where  $u, v$  are the depth averaged component of velocity  
 $DO$  concentration of Dissolved Oxygen  
 $C$  Biological Oxygen Demand or Coliforms concentration.  
 $DOD$  Dissolved Oxygen deficit = saturated concentration -  $DO$  concentration  
 $K_a$  reaeration rate  
 $K_c$  reaction rate of pollutant/mortality rate for coliforms  
 $L$  loading of remaining oxygen demand  
 $d$  water depth  
 $D_s$  longitudinal (shear flow) oxygen demand  
 $D_n$  lateral diffusion coefficient due to turbulence  
 $x, y$  cartesian coordinates  
 $(S, n)$  intrinsic coordinates parallel and normal to flow direction  
 $t$  time

The Dissolved Oxygen/Biological Oxygen Demand model solves both equations 1 & 2. The Coliform model solves only equation 2.

In model, non-isotropic dispersion can be used to produce greater dispersion in the mean flow direction.

Numerical solutions of this equation are unfortunately prone to numerical noise and diffusion. In order to minimise these effects the model uses an explicit, upstream finite difference representation of the advection terms, with flux corrections to restore second order accuracy.

The upstream difference operators  $\Delta_x$  and  $\Delta_y$  are defined as:

$$\Delta_x(duc) = (H(u_e)c_k + H(-u_e)c_e)(du)_e - (H(u_w)c_w + H(-u_w)c_k)(du)_w \quad (2)$$

$$\Delta_y(dvc) = (H(v_n)c_k + H(-v_n)c_n)(dv)_n - (H(v_s)c_s + H(-v_s)c_k)(dv)_s \quad (3)$$

In terms of the Heaviside unit function:

$$H(x) = 1 \quad x > 0 \quad H(x) = 0 \quad x < 0 \quad (4)$$

where suffices n, s, e and w refer to cells north, south, east and west of cell k.

To determine the form of the truncation error we use the Heaviside properties:

$$x H(x) + x H(-x) = x \quad x H(x) - x H(-x) = x \quad (5)$$

and re-write the upstream difference operators as:

$$\Delta_x(du\bar{I}) = \delta_x(du\mu_x(C)) - \frac{1}{2}\delta_x(du\delta_x(C)) \quad (6)$$

$$\Delta_y(dv\bar{I}) = \delta_y(dv\mu_y(C)) - \frac{1}{2}\delta_y(dv\delta_y(C)) \quad (7)$$

In terms of standard central differences  $\delta_x$  and  $\delta_y$  and averaging operation  $\bar{x}$  and  $\bar{y}$ .

Thus the upstream difference method introduces first order truncation errors:

$$\frac{1}{2} \frac{\partial}{\partial x} d \left( u \Delta s \frac{\partial c}{\partial z} + \Delta t \frac{\partial c}{\partial t} \right) + \frac{1}{2} \frac{\partial}{\partial y} d \left( v \Delta s \frac{\partial c}{\partial y} + v \Delta t \frac{\partial c}{\partial t} \right) \quad (8)$$

on the right hand side of the advection diffusion equation (1). That is to say the representation of advection is formally first order accurate in

space. Note that the truncation error has the structure of a diffusive term with numerical diffusion coefficients  $\frac{1}{2} \Delta u$  and  $\frac{1}{2} \Delta v$ .  $\Delta$  is the grid spacing.

The flux correction method (Boris, J P and Book D L. "Flux corrected Transport III. Minimal error FCT Algorithms". J Comp Phys, 20, pp 397 - 431 (1976)) is simply to subtract out just the right amount of diffusions to cancel the numerical diffusion generated by the upstream differences. The net result is to produce a second order accurate representation of the advection terms.

The corrections to eliminate numerical diffusion - anti-diffusion corrections - cannot be included in the numerical scheme without careful consideration. The effect of including them is to transfer heat up the temperature gradient and there is a tendency for existing temperature extremes to be increased or for new extremes to be formed. However, it is a simple matter in the program to limit the anti-diffusion flux so that the generation of extremes is avoided. There are two possible levels of constraint: to prevent new minima only or to prevent both new maxima and minima from being formed, but only the former is included in the current model. The net result of the selective anti-diffusion is to include strong diffusion in those areas where otherwise error waves would have been generated, but have no effect where the temperature gradient is smooth.



APPENDIX D

SEWAGE AND SOLID WASTE DISPOSAL  
SEA OUTFALL PERFORMANCE  
WATER RESEARCH CENTRE  
PUBLICITY 1985



## SEA OUTFALL PERFORMANCE

Computer models are being developed to simulate the dispersion of sewage from point sources in coastal areas, taking reasonable account of local topography. The results, displayed as coloured maps of the local sea area with each colour representing a band of concentration of faecal coliform bacteria, can be used to compare the effects of different discharge options at sensitive bathing beaches for a variety of tidal conditions, dispersion coefficients, and decay rates.

Tidal currents and water levels are evaluated over a tidal cycle using a hydrodynamic model; these results are used in a dispersion model to move the bacteria released from selected sources while concentrations are being reduced through dispersion and diurnally varied decay. After running the dispersion model over several tidal cycles, estimates of concentration in small cells over the sea area are stored at hourly intervals over a whole day, and a display program can present the results for any pair of discharge options as a series of coloured maps. In the interests of economy the models ignore variations in velocity and concentration through the water column and the estimates made represent averages over the water depth.

At present some of the important mechanisms in the dispersion of bacteria in the sea are imperfectly understood, therefore these models are approximate when providing absolute values. However the results can be accepted as adequate for comparing design options and they give a quantitative basis on which to judge improvement against water quality criteria and scheme costs.



APPENDIX E

3-D FINE GRIDDED MODEL  
EXTRACT FROM  
HYDRAULICS RESEARCH LTD  
REPORT IT 254



## 1 Introduction

Two-dimensional depth-integrated models of flow and transport are frequently used to study harbour, estuary and coastal problems. Unfortunately such models cannot account for the important circulations in the vertical which may result from wind or stratification. Sometimes it is possible to use a laterally integrated (x-z-t) model to resolve the vertical circulation (see Ref 1) but only at the expense of losing the horizontal circulations. Often the flow pattern is truly three-dimensional and only a 3D model can give an accurate representation.

A 3D model has been developed by Hydraulics Research. This model has been used to produce patterns of wind-driven circulation in three dimensions and it should also be possible to model the effects of stratification. The model will be useful for many kinds of study involving pollution, heat or sediment as fewer idealisations are made than in 2D models.

## 2 Equations of motion

The governing equations of the model are:

Conservation of water volume

$$\frac{\partial u}{\partial x} + \frac{\partial v}{\partial y} + \frac{\partial w}{\partial z} = 0 \quad (1)$$

Conservation of momentum in the x and y directions

$$\begin{aligned} \frac{\partial u}{\partial t} + u \frac{\partial u}{\partial x} + v \frac{\partial u}{\partial y} + w \frac{\partial u}{\partial z} + \\ \frac{1}{\rho} \frac{\partial p}{\partial x} = \Omega v + \nu_H \nabla^2 u + \frac{1}{\rho} \frac{\partial \tau_x}{\partial z} \end{aligned} \quad (2)$$

$$\begin{aligned} \frac{\partial v}{\partial t} + u \frac{\partial v}{\partial x} + v \frac{\partial v}{\partial y} + w \frac{\partial v}{\partial z} + \\ \frac{1}{\rho} \frac{\partial p}{\partial y} = -\Omega u + \nu_H \nabla^2 v + \frac{1}{\rho} \frac{\partial \tau_y}{\partial z} \end{aligned} \quad (3)$$

where the hydrostatic pressure is

$$p = -g \int_z^{\eta} \rho dz \quad (4)$$

and

$$\rho = 1000 + 0.76s \quad (5)$$

Conservation of salt

$$\frac{\partial s}{\partial t} + \frac{\partial}{\partial x}(us) + \frac{\partial}{\partial y}(vs) + \frac{\partial}{\partial z}(ws) = k_H \nabla^2 s + \frac{\partial f_s}{\partial z} \quad (6)$$

where

x, y, z are Cartesian co-ordinates, z vertically upwards (m)

u, v, w are the corresponding velocity components (m/s)

t is time (s)



APPENDIX F

1-D MOVING ELEMENT MODEL  
EXTRACT FROM  
WATER RESEARCH CENTRE  
TECH REPORT 13 (1972)  
AND HUMBER ESTUARY COMMITTEE

Mollowney, B M. Moving co-ordinate systems, in estuaries. WRC Technical Report TR 13, April 1976.

Gameson, A L H (Editor). The Quality of the Humber Estuary 1961-81. Published by the Yorkshire Water Authority on behalf of the Humber Estuary Committee, 1982.



# One-Dimensional Models of Estuarine Pollution

In recent years the benefits of applying mathematical modelling techniques to problems of estuarine pollution have been widely recognized. For estuaries where the variations in concentrations of dissolved substances over the depth and between the centre and sides are not large in comparison with those over the length, the calculation of the distribution of pollutants can be treated as a problem in one dimension, the average concentration of a substance over the cross-section being expressed as a function of distance along the length of the estuary. However, the variations in concentration over the cross-section, when combined with the variations in velocity, give rise to a longitudinal mass transport called longitudinal dispersion.

In this paper a numerical time-dependent model is described in which the flood and ebb of the tide are specifically represented and in which longitudinal dispersion is represented as a diffusion process. The estuary is considered as a series of segments moving upstream and downstream with the tidal velocity, and the concentrations occurring in each segment are calculated at any instant during the tidal cycle by solving the equations of conservation of volume and of mass of pollutant. If the exact time variation during the tidal cycle is not required, but only the changes from one tidal cycle to the next, then by taking a time average of the equations over a tidal cycle a model may be derived which is useful for looking at seasonal variations. Also, the steady-state model commonly used in pollution studies is now seen as resulting from long-term averaging of the equations applied to a moving segment. Thus a unified approach to one-dimensional modelling of estuarine pollution has been achieved. Since all these models are based on the concepts of conservation of water volume and pollutant mass the relevant equations will first be derived.

## One-dimensional equations of conservation of volume and pollutant

### Cross-section averaging and longitudinal dispersion

Consider the mass transport of a substance through a cross-section of an estuary at some time  $t$  during the tidal cycle. Let  $u(x, y, z, t)$  be the instantaneous velocity of the water perpendicular to the cross-section and  $c(x, y, z, t)$  the concentration of the substance at any point in the cross-section where the longitudinal, lateral, and vertical co-ordinates are  $x, y, z$  respectively. Further, let the mean values of  $u$  and  $c$  over the cross-section be  $U$  and  $C$ , and the departures from the means be  $u'$  and  $c'$ . Then the mass transport of substance per unit time through the cross-section of area  $A(x, t)$ , is given by

$$\int_A uc \, dA = \int_A (U + u')(C + c') \, dA = AUC + \int_A u'c' \, dA \quad (1)$$

since the integrals of  $Uc'$  and  $Cu'$  are zero. The term  $AUC$  is the mass transport per unit time due to the net flow, and the final integral is that due to the correlation between variations in velocity and concentration over the cross-section. A dispersion coefficient  $D(x, t)$  may be defined which expresses this additional transport per unit area per unit concentration gradient, so that

$$\int_A u'c' \, dA = -DA \frac{\partial C}{\partial x} \quad (2)$$

where the negative sign indicates mass transport in the direction of decreasing concentration<sup>1</sup>.

### Conservation equations

The equations of conservation of volume and of pollutant can now be written down for any longitudinal portion of an estuary. At the tidal limit ( $x = 0$ ) let the fresh-water flow be  $Q_0(t)$  and the concentration of pollutant be  $C_0(t)$ ; let the rates of entry of fresh water and pollutant to the estuary from tributaries, effluents, and other sources be respectively  $q(x, t)$  and  $m(x, t)$  per unit length; finally let the total volume of water from the tidal limit to any point  $x$  be  $V(x, t)$  and the mass of pollutant therein be  $P(x, t)$ .

The equation of volume conservation is

$$\frac{\partial V}{\partial t} = Q_0 + \int_0^x q \, dx - AU. \quad (3)$$

Differentiating partially with respect to  $x$ , and noting that  $\partial V/\partial x = A$ , gives the volume conservation in differential-equation form:

$$\frac{\partial A}{\partial t} = q - \frac{\partial}{\partial x} (AU). \quad (4)$$

Similarly, the equation of pollutant conservation is

$$\frac{\partial P}{\partial t} = Q_0 C_0 + \int_0^x m dx - \int_A uc dA, \quad (5)$$

which, by substituting for the last expression by means of Equations 1 and 2, gives

$$\frac{\partial P}{\partial t} = Q_0 C_0 + \int_0^x m dx + DA \frac{\partial C}{\partial x} - AUC. \quad (6)$$

Differentiating as before, and noting that  $\partial P/\partial x = AC$ , gives

$$\frac{\partial}{\partial t} (AC) = m + \frac{\partial}{\partial x} \left( DA \frac{\partial C}{\partial x} \right) - \frac{\partial}{\partial x} (AUC). \quad (7)$$

If the substance is decaying at a rate,  $k$ , proportional to its concentration, then  $-kAC$  is added to the right-hand side of Equation 7.

### Solutions of equations

If either  $A$  or  $U$  is known as a function of  $x$  and  $t$ , the other can be determined from Equation 4. If neither is known, they can both be found by the simultaneous solution of Equation 4 and the corresponding equation which may be derived from the conservation of momentum. In any case, if  $D$  and the boundary and initial values of  $C$  are known,  $C$  can be found by solving Equation 7. Although analytical solutions of such equations are available for simple functional forms of  $A$ ,  $U$ , and  $D$ , numerical methods of solution are used for most practical pollution calculations. Some special properties of Equations 4 and 7 which make their numerical solution easier will now be described.

The tidal velocity may be defined as

$$U_T = U - \frac{Q}{A}, \quad (8)$$

where

$$Q(x, t) = Q_0 + \int_0^x q dx \quad (9)$$

= total land-water flow.

Since  $AU = AU_T + Q$ , Equation 3 may be written as

$$\frac{\partial V}{\partial t} + AU_T = 0; \quad (10)$$

or, since  $\partial V/\partial x = A$ ,

$$\frac{\partial V}{\partial t} + U_T \frac{\partial V}{\partial x} = 0. \quad (11)$$

This equation implies that if a particle is moving with the velocity  $U_T$  the volume upstream remains constant. Thus let  $x(a, t)$  be the position of such a particle at time  $t$ ,  $a$  being its initial position. Let the volume upstream of the particle be  $v(a, t)$  which is equal to  $V(x(a, t), t)$ . Its rate of change is then

$$\frac{\partial v}{\partial t} = \frac{\partial V}{\partial t} + \frac{\partial V}{\partial x} \frac{\partial x}{\partial t} \quad (12a)$$

$$= \frac{\partial V}{\partial t} + U_T \frac{\partial V}{\partial x}, \text{ since } \frac{\partial x}{\partial t} = U_T \quad (12b)$$

$$= 0, \text{ from Equation 11.} \quad (12c)$$

By combining Equations 4 and 7 and substituting for  $AU$  as before, we get (after some manipulation)

$$\frac{\partial C}{\partial t} + U_T \frac{\partial C}{\partial x} = \frac{1}{A} \left\{ \frac{\partial}{\partial x} \left( DA \frac{\partial C}{\partial x} - QC \right) + m \right\}. \quad (13)$$

If, in the previous paragraph, volume is replaced by salinity,  $S$ , then  $v(a, t)$  becomes  $S(x(a, t), t)$ , and it is seen from Equation 12b that the time rate of change of salinity of a particle of water moving with the tidal velocity is  $\partial S/\partial t + U_T \partial S/\partial x$ . (Equation 12c is inapplicable here since Equation 11 is not true when  $V$  is replaced by  $S$ .) It follows from Equation 13 that, if no salt enters in the land water, the condition that the salinity of the particle remains constant is that

$$DA \frac{\partial S}{\partial x} = QS, \quad (14)$$

or that the transport of salt by dispersion at any point is exactly balanced by that of the land-water flow. If this condition is approximately satisfied, plotting observed data for the salinity of samples taken at various places at any state of tide against the volume upstream will give points within a fairly narrow band about a curve. This was the basis of the method developed by the Laboratory to adjust data (not only for salinity, but also for dissolved oxygen and other properties) for the Thames Estuary to a particular tidal state<sup>2</sup>. All this suggests that the variations experienced by a particle moving with the tidal velocity are much less than those at a fixed point, so that Equation 13 may be more easily solved if it is applied to such a particle. A numerical model using this approach will now be described.

### General numerical time-dependent model

For the purposes of the numerical model the estuary is considered as a series of uniformly mixed segments. Let the positions of the boundaries of the segments at any time  $t$  be  $X_0(t), X_1(t), \dots, X_i(t), \dots, X_n(t)$  where  $i$  is a general suffix and  $n$  is the total number of segments. If the boundaries are moving with the tidal velocity,  $U_T$ , defined by Equation 8, then

$$\frac{dX_i}{dt} = U_T, \text{ for } i = 0, 1, 2, \dots, n. \quad (15)$$

#### Equation of conservation of volume for a segment

The equation of conservation of volume for the segment  $X_{i-1}$  to  $X_i$  (the  $i$ th segment) is

$$\frac{d}{dt} \Delta V_i = A_{i-1}(U_{i-1} - U_{T_{i-1}}) - A_i(U_i - U_T) + \Delta Q_i, \quad (16)$$

where  $\Delta V_i$  is the volume of the segment,  $\Delta Q_i$  is the integral of  $q$  with respect to  $x$  (from  $X_{i-1}$  to  $X_i$ ), and  $A_i$  is the cross-sectional area and  $U_i$  the velocity of the water at  $X_i$ . From Equations 8 and 9

$$\begin{aligned} A_i(U_i - U_T) &= Q_i \\ &= \text{land-water flow at } X_i. \end{aligned} \quad (17)$$

Substituting Equation 17 in Equation 16 we see that

$$\frac{d}{dt} \Delta V_i = 0, \quad (18)$$

i.e. the volume of a segment is constant in time. As a corollary the volume upstream of  $X_i$  is constant in time and this provides a simple way of calculating  $X_i$  as a function of time. This is illustrated graphically in Fig. 1. In the upper part the volume  $V(x, t)$  is plotted against distance,  $x$ , for three different values

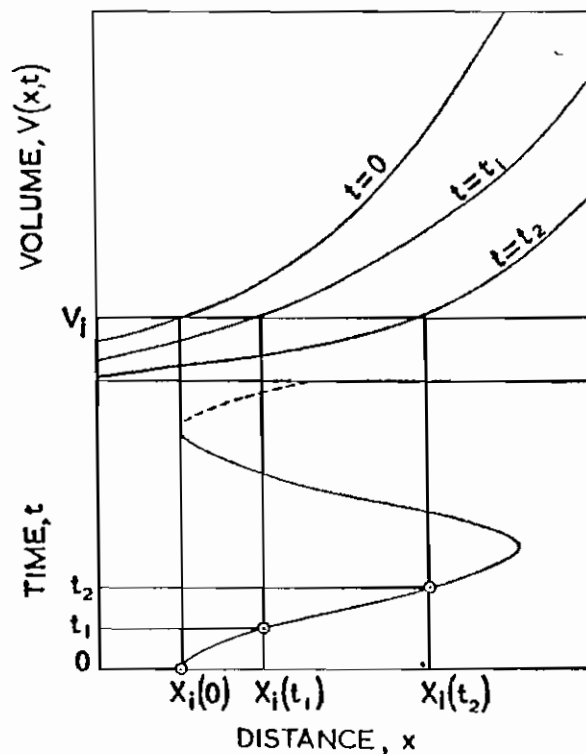


FIG. 1. Diagrammatic representation of movement of particle moving with tidal velocity during tidal cycle

of time,  $t$ . A line of constant volume, say  $V = V_i$ , defines the points  $X_i(0)$ ,  $X_i(t_1)$ ,  $X_i(t_2)$  which are plotted against time in the lower half of the figure. The resultant curve is labelled by the volume  $V_i$ , which is the volume upstream of  $X_i(0)$  at  $t = 0$ .

#### Equation of conservation of substance in a segment

From Equation 1 the mass transport per unit time through the boundary at  $X_i$  is made up of two terms: the transport due to the net flow and that due to longitudinal dispersion. If the segment is moving with the tidal velocity  $U_T$  the net flow at  $X_i$  is  $Q_i$  from Equation 17. If  $C_i(t)$  is the concentration in the  $i$ th segment at any instant, then the mass transport per unit time at  $X_i$  due to the net flow is  $Q_i C_i$ . Longitudinal dispersion is simulated<sup>3</sup> by assuming a continuous exchange of water between adjacent segments by equal and opposite flows,  $F_i$ . The mass transport per unit time at  $X_i$  due to dispersion is  $F_i(C_i - C_{i+1})$ . This is essentially a finite-difference approximation to the model where longitudinal dispersion is assumed to be a diffusion process with

$$F_i = \frac{2D_i A_i}{X_{i+1} - X_{i-1}}, \quad (19)$$

where  $D_i$  is the diffusion (dispersion) coefficient at  $X_i$ . The advantages of this representation are that it is easy to visualize and  $A$  no longer appears explicitly in the equations. The equation of conservation of the substance, assuming a decay at a rate proportional to the concentration, for the  $i$ th segment is then

$$\Delta V_i \frac{dC_i}{dt} = Q_{i-1} C_{i-1} + F_{i-1}(C_{i-1} - C_i) - Q_i C_i + F_i(C_{i+1} - C_i) - K_i \Delta V_i C_i + M_i, \quad (20)$$

where  $K_i$  is the decay rate and  $M_i$  is the integral of  $m$  through the segment.

#### Solution of Equation 20

If there are  $n$  segments covering the estuary there will be  $n$  equations similar to Equation 20 for  $i = 1, 2, 3, \dots, n$ . This set of differential equations can be solved at discrete time intervals using the Crank-Nicholson approximation<sup>4</sup>. This involves integrating Equation 20 from  $t = (r-1)\Delta t$  to  $t = r\Delta t$  where  $r$  is an integer taking values 1, 2, 3,  $\dots$ , and  $\Delta t$  is the time step, and approximating the integral with respect to time on the right-hand side by the trapezoidal rule. Equation 20 becomes

$$\begin{aligned} \Delta V_i (C_i^r - C_i^{r-1}) = & \frac{\Delta t}{2} \{ Q_{i-1}^r C_{i-1}^r - Q_i^r C_i^r + F_{i-1}^r (C_{i-1}^r - C_i^r) + F_i^r (C_{i+1}^r - C_i^r) - K_i \Delta V_i C_i^r \} + \\ & + \frac{\Delta t}{2} \{ Q_{i-1}^{r-1} C_{i-1}^{r-1} - Q_i^{r-1} C_i^{r-1} + F_{i-1}^{r-1} (C_{i-1}^{r-1} - C_i^{r-1}) + F_i^{r-1} (C_{i+1}^{r-1} - C_i^{r-1}) - K_i \Delta V_i C_i^{r-1} \} + M_{add}^i. \end{aligned} \quad (21)$$

where  $C_i^r$  is the concentration in the  $i$ th segment at  $t = r\Delta t$ ,  $F_i^r$  and  $Q_i^r$  are average values at  $X_i$  during the time step  $(r-1)\Delta t$  to  $r\Delta t$  and  $M_{add}^i$  is the total mass of substance added to the segment during the time step. This equation can be arranged to give one of the form

$$\alpha_i C_{i-1}^r + \beta_i C_i^r + \gamma_i C_{i+1}^r = \delta_i (C_{i-1}^{r-1}, C_i^{r-1}, C_{i+1}^{r-1}). \quad (22)$$

To start a calculation, the concentration of a substance is given initial values. The set of algebraic equations (22) is solved either directly<sup>4</sup> or by the iterative Gauss-Seidel method<sup>5</sup>; the values obtained are then used as initial values for the next time step, and so on. The boundary values  $C_0(t)$ ,  $C_{n+1}(t)$  are assumed to be known throughout the calculation.

#### Estimation of the mixing exchange, $F_i$

In the preceding paragraphs it was assumed that the mixing exchanges,  $F_i$ , were known as a function of time. In general, estimates of these exchanges are found by fitting calculated to observed salinity distributions. As an example of this technique, calculated variations in salinity during an average tidal cycle at a number of positions in the Thames Estuary are compared in Fig. 2 with observations made on a hydraulic model<sup>6</sup> operated with steady-state conditions simulating a tide with a range of 4.4 m at Southend and a fresh-water flow of 34 m<sup>3</sup>/s at Teddington. For this calculation it was assumed that the mixing exchange during the time step  $(r-1)\Delta t$  to  $r\Delta t$  was given by

$$F_i^r = \frac{Q_i^r (S_i - S_0)}{S_{i+1} - S_i}, \quad (23)$$

where  $S_0$  is the salinity of the fresh-water inflow,  $S_i$  the salinity of the  $i$ th segment when it is high water at Southend,  $t = 0$ , and  $r$  is an integer taking values 1, 2, 3,  $\dots$ . If  $F_i^r$  is substituted into Equation 21 and it is assumed that  $C_i^0 = S_i$ , then it is found that  $C_i^r = S_i$ , i.e. the salinity of the  $i$ th segment is constant in time. This, perhaps, can more easily be seen from Equation 14 and the subsequent

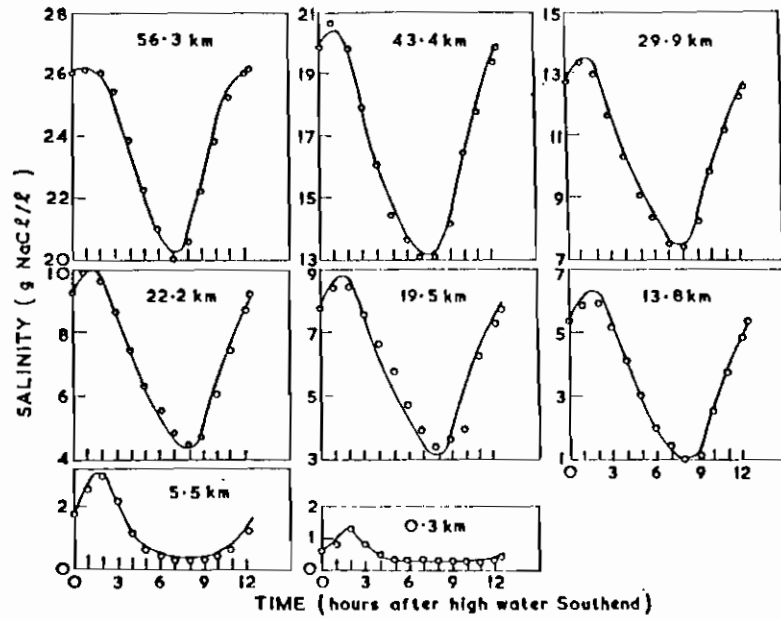


FIG. 2. Comparison of salinity variations during average tidal cycle in Thames Estuary, obtained from mathematical model (curves) and from hydraulic model (circles)  
*Fresh-water flow 34 m<sup>3</sup>/s at Teddington*

discussion. The overall agreement between the mathematical and hydraulic models shows that the assumptions were reasonable in this case.

#### Calculation of temperature distributions

It is convenient to consider the temperature of an estuary at any point to be composed of two parts—that existing in the absence of artificial heating and the increment attributable to cooling-water discharges<sup>7</sup>. If it is assumed that the rate of loss of heat to the air from the *i*th segment is proportional to the surface area,  $R_i(t)$ , and to the temperature rise,  $\theta_i(t)$ , then the equation governing the temperature rise is (by analogy with Equation 20)

$$\Delta V_i \frac{d\theta_i}{dt} = Q_{i-1} \theta_{i-1} + F_{i-1} (\theta_{i-1} - \theta_i) - Q_i \theta_i + F_i (\theta_{i+1} - \theta_i) - g R_i \theta_i + H_i, \quad (24)$$

where  $g$  is the heat exchange coefficient and  $H_i$  is the rate at which artificial heat is added to the *i*th segment. Equation 24 is solved in a similar way to Equation 20.

#### Dissolved oxygen and associated substances

The oxygen equivalents of the concentrations of organic carbon ( $B$ ), organic nitrogen ( $N_1$ ), ammoniacal nitrogen ( $N_2$ ), and oxidized nitrogen ( $N_3$ ) are calculated simultaneously with that of dissolved oxygen (DO) ( $O_2$ ). The oxidation processes in an estuary can be represented as shown in Fig. 3; a block

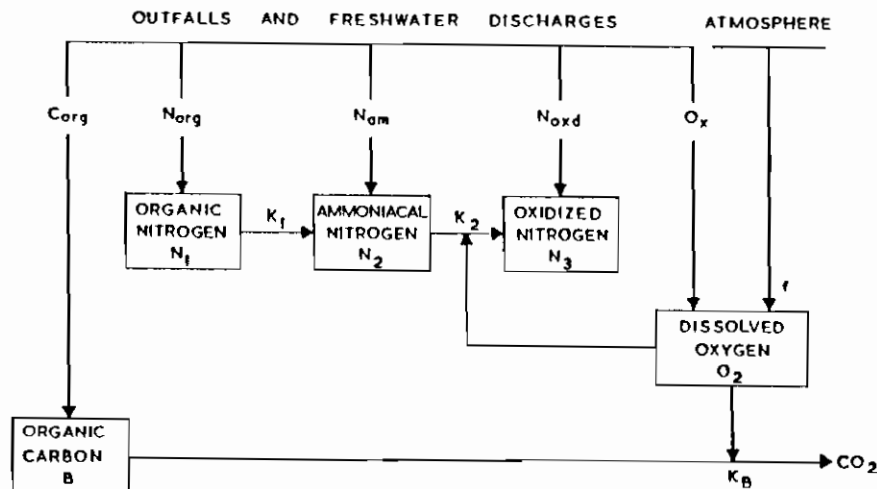


FIG. 3. Schematic diagram showing sources and sinks of dissolved oxygen and associated substances in absence of denitrification

represents the mass of the substance in a segment of the estuary and the arrows show its sources and sinks. For each substance, the source includes direct waste inputs and formation from other substances, and the sink is the chemical or biological breakdown. As an example, the sources of ammoniacal nitrogen are outfalls and the hydrolysis of organic nitrogen, and the sink is the oxidation of ammonia to oxidized nitrogen. The destruction and formation of the substance may be represented either by first-order kinetics or by more detailed bacterial growth kinetics<sup>8,9</sup>. When all loads and concentrations are expressed in terms of their oxygen equivalents<sup>9</sup> the equations for the *i*th segment assuming first-order kinetics are

$$\Delta V_i \frac{dB_i}{dt} = \Delta V_i \left( \frac{\partial B_i}{\partial t} \right)_{O.F.} - K_{B_i} \Delta V_i B_i + C_{org_i}, \quad (25)$$

$$\Delta V_i \frac{dN_{1i}}{dt} = \Delta V_i \left( \frac{\partial N_{1i}}{\partial t} \right)_{O.F.} - K_{1_i} \Delta V_i N_{1i} + N_{org_i}, \quad (26)$$

$$\Delta V_i \frac{dN_{2i}}{dt} = \Delta V_i \left( \frac{\partial N_{2i}}{\partial t} \right)_{O.F.} - K_{2_i} \Delta V_i N_{2i} + K_{1_i} \Delta V_i N_{1i} + N_{am_i}, \quad (27)$$

$$\Delta V_i \frac{dN_{3i}}{dt} = \Delta V_i \left( \frac{\partial N_{3i}}{\partial t} \right)_{O.F.} + K_{2_i} \Delta V_i N_{2i} + N_{oxd_i}, \quad (28)$$

$$\Delta V_i \frac{dO_{2i}}{dt} = \Delta V_i \left( \frac{\partial O_{2i}}{\partial t} \right)_{O.F.} + f_i R_i (O_{a_i} - O_{2i}) - K_{B_i} \Delta V_i B_i - K_{2_i} \Delta V_i N_{2i} + O_{x_i}, \quad (29)$$

$$\text{where } \Delta V_i \left( \frac{\partial C_i}{\partial t} \right)_{O.F.} = Q_{i-1} C_{i-1} - Q_i C_i + F_{i-1} (C_{i-1} - C_i) + F_i (C_{i+1} - C_i)$$

= flux into the *i*th segment due to land-water flow and dispersion,

$K_{B_i}, K_{1_i}, K_{2_i}$  represent the first-order decay rates,

$C_{org_i}, N_{org_i}, N_{am_i}, N_{oxd_i}, O_{x_i}$  are the rates of addition to the *i*th segment from outfalls and tributaries,

$f_i$  is the reaeration coefficient, and

$O_{a_i}$  is the air-saturation value of oxygen for the *i*th segment.

These equations are solved in a similar way to Equation 20. If the DO is low then Equations 27-29 may be modified to allow for restricted oxidation of ammonia and denitrification of oxidized nitrogen.

## Discussion

This model has been programmed in ALGOL for use in a theoretical study to assess the effect of the proposed Thames Barrier on the distributions of DO and temperature in the estuary during steady fresh-water flow and tidal conditions<sup>9</sup>. The programme has been extended to deal with variable fresh-water flow, variable tidal conditions such as those in the spring-to-neap cycle, and time-varying pollution loads.

An alternative model to the one just described is obtained by moving the segments with the velocity of the water—though it has the property that the number of segments needed to cover an estuary whose cross-sectional area increases towards the sea, increases in time.

## Time-average and steady-state models

### Time-averaging over a tidal period

If the change in concentration of a substance from one tidal cycle to the next is of more interest than the exact time variation during the tidal cycle then by averaging the equations over a tidal period a model may be derived which is useful for calculating the effects of seasonal changes due to varying fresh-water flow and temperature. The actual method of averaging is to some extent arbitrary but in order to be specific the time average  $\bar{\varphi}(t)$  at time *t* of a function  $\varphi(t)$  is defined to be

$\frac{1}{T} \int_t^{t+T} \varphi(t) dt$  where *T* is the tidal period. When this averaging is applied to Equation 20 we get

$$\frac{\Delta V_i}{T} \int_t^{t+T} \frac{dC_i}{dt} dt = \frac{1}{T} \int_t^{t+T} \left\{ Q_{i-1} C_{i-1} + F_{i-1} (C_{i-1} - C_i) - Q_i C_i + F_i (C_{i+1} - C_i) - K_i \Delta V_i C_i + M_i \right\} dt. \quad (30)$$

The left-hand side of Equation 30 is equal<sup>10</sup> to  $\Delta V_i d\bar{C}_i/dt$ , and if  $C_i$  is a slowly varying function of time then, to a good approximation,

$$\frac{1}{T} \int_t^{t+T} \left\{ -Q_i C_i + F_i (C_{i+1} - C_i) \right\} dt = -\bar{Q}_i \bar{C}_i + F_i (\bar{C}_{i+1} - \bar{C}_i). \quad (31)$$

Equation 30 now becomes

$$\Delta V_i \frac{dC_i}{dt} = \bar{Q}_{i-1} C_{i-1} + F_{i-1} (C_{i-1} - C_i) - \bar{Q}_i C_i + F_i (C_{i+1} - C_i) - K_i \Delta V_i C_i + \bar{M}_i. \quad (32)$$

Also, on averaging the equation of continuity of volume (Equation 16),

$$\frac{d}{dt} \Delta V_i = \bar{Q}_{i-1} - \bar{Q}_i + \overline{\Delta Q}_i \quad (33)$$

$$= 0 \text{ from Equation 18.} \quad (34)$$

Equations 33 and 34 can be used to determine  $\bar{Q}_i$  if  $\bar{Q}_0$  and  $\overline{\Delta Q}_i$  are known. It is useful to consider the functions  $\overline{\Delta Q}_i$  and  $\bar{M}_i$  in more detail:  $\Delta Q_i$  is the volume added to the  $i$ th segment per unit time by tributaries and outfalls that it passes as it moves up and down the estuary; if the tide is repeating itself exactly with period  $T$  then  $\overline{\Delta Q}_i$  and  $\bar{M}_i$  are constant in time, but in general they will vary even for a constant rate of addition because of the spring to neap cycle.

#### Steady-state model

If Equation 20 is averaged over  $N$  tidal cycles where  $N$  is an integer we again get Equation 32, but now with

$$C_i = \frac{1}{NT} \int_t^{t+NT} C_i dt. \quad (35)$$

If the fresh-water flow,  $Q_0$ , and the rates of entry,  $M_i$  and  $\Delta Q_i$ , are steady over a long period then variations in concentration arise only from the effect of the spring-to-neap cycle and other cycles of longer period. If  $NT$  is at least a lunar cycle these variations will either be removed or very much reduced by the averaging. Then to a good approximation

$$\frac{dC_i}{dt} = \frac{1}{NT} \int_t^{t+NT} \frac{dC_i}{dt} dt = \frac{C(t+NT) - C(t)}{NT} \quad (36)$$

$$= 0. \quad (37)$$

Equation 20 then becomes

$$\bar{Q}_{i-1} C_{i-1} + F_{i-1} (C_{i-1} - C_i) - \bar{Q}_i C_i + F_i (C_{i+1} - C_i) - K_i \Delta V_i C_i + \bar{M}_i = 0. \quad (38)$$

The equation of continuity of volume is

$$\bar{Q}_{i-1} - \bar{Q}_i + \overline{\Delta Q}_i = 0. \quad (39)$$

The time at which these equations are taken to apply is arbitrary as all the quantities  $\bar{Q}_i$ ,  $F_i$ ,  $C_i$ ,  $\overline{\Delta Q}_i$ , and  $\bar{M}_i$  are constant. However, in order to do a calculation a particular tidal state has to be assumed, such as high water mean tide or low water neap tide. The volume at the chosen tidal state is plotted against position; the estuary is segmented and the volume of each segment is read off. The contribution of each outfall to  $\overline{\Delta Q}_i$  and  $\bar{M}_i$  is calculated from the product of the rate of input and the proportion of the time the  $i$ th segment spends in passing the outfall. The segments affected by the outfall are determined by the maximum and minimum volumes upstream of the outfall during the period. When  $\overline{\Delta Q}_i$  has been calculated,  $\bar{Q}_i$  is obtained from Equation 39 using the average fresh-water flow into the estuary during the period. The observed salinity is plotted against the volume upstream at the time and position of sampling, and an average value,  $\bar{S}_i$ , for the period is given to each segment. The mixing exchanges  $F_i$  are calculated from the relation  $F_i = \bar{Q}_i (\bar{S}_i - S_0) / (\bar{S}_{i+1} - \bar{S}_i)$ , where  $S_0$  is the salinity of the fresh-water inflow. Equation 38 is solved either by direct elimination or by an iterative method<sup>5</sup>.

#### Comparison between equilibrium condition calculated by the time-dependent model and that by the steady-state model

In Fig. 4 are compared the distributions of temperature rise calculated by the time-dependent model and by the steady-state model using data from the Thames Estuary. The temperature rise from a continuous discharge of 2000 CHU/h from a single outfall 10 km below London Bridge has been calculated by both models assuming a steady fresh-water flow of 34 m<sup>3</sup>/s, a tide of mean range of 4.4 m, and a heat exchange coefficient of 3.7 cm/h. The open circles are the average values in a moving segment over a tidal period—the range being indicated by the stalks—from the time-dependent model 60 tidal cycles after starting from zero initial values. The two curves are results from the steady-state model;

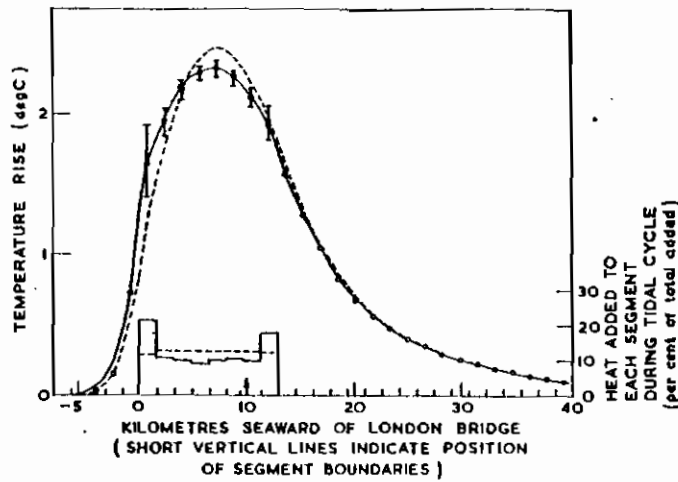


FIG. 4. Comparison of temperature rise calculated from steady-state model (curves) for two distributions of heat from a single outfall with that from time-dependent model (circles) using data from Thames Estuary. Broken curves, uniform heat addition over tidal cycle. Continuous curves, heat addition proportional to time spent passing outfall (indicated by arrow). Circles and vertical bars, average and range of values in moving segment during tidal cycle for time-dependent model. Tidal state, high water at Southend

the broken curve was calculated after assuming a uniform distribution of heat to the affected segments (shown in the lower part of the figure by the corresponding broken line), while the continuous curve used a distribution (shown in the lower part by the corresponding continuous line) calculated from the time spent by each segment passing the outfall. The comparison shows that for conditions of steady flow and tidal range, results almost identical with those of the time-dependent model are given by the steady-state model if the distribution of effluents is properly taken into account.

#### ACKNOWLEDGEMENTS

It is a pleasure to acknowledge the helpful criticism offered by colleagues particularly Mr A. L. H. Gameson, Mr M. J. Barrett, and Mr D. Munro.

#### REFERENCES

- HOLLEY, E. R., and HARLEMAN, D. R. F. Dispersion of pollutants in estuary type flows. Hydrodynamics Laboratory, Massachusetts Institute of Technology, Cambridge, Mass., Report No. 74, 1965, p. 21.
- DEPARTMENT OF SCIENTIFIC AND INDUSTRIAL RESEARCH. Effects of polluting discharges on the Thames Estuary. Water Pollution Research Technical Paper No. 11, H.M. Stationery Office, London, 1964.
- DOWNING, A. L. Some aspects of the work of the Water Pollution Research Laboratory. Association of River Authorities Year Book, 1966, p. 73.
- ROSENBROCK, H. H., and STOREY, C. Computational techniques for chemical engineers. Pergamon Press, London, 1st Edn., 1966, p. 167.
- LAPIDUS, L. Digital computation for chemical engineers. McGraw-Hill, New York, 1962, p. 259.
- GREATER LONDON COUNCIL. Thames Flood Prevention. First Report of Studies, 1969, p. 69.
- GAMESON, A. L. H., HALL, H., and PREDDY, W. S. Effects of heated discharges on the temperature of the Thames Estuary. *Engineer, Lond.*, 1957, 204, 816, 850, and 893.
- DOWNING, A. L., and KNOWLES, G. Nitrification in treatment plants and natural waters: some implications of theoretical models. *Proc. 5th Int. Conf. Wat. Pollut. Res., San Francisco & Hawaii, 1970*, Vol. 1, 1-8.
- BARRETT, M. J., and MOLLOWNEY, B. M. Pollution problems in relation to the Thames Barrier. *Phil. Trans. R. Soc. Lond. A.*, 1972, 272, 213.
- OKUBO, A. Equations describing the diffusion of an introduced pollutant in a one-dimensional estuary. In 'Studies on Oceanography', University of Tokyo Press, 1964, p. 216.

In introducing his paper Mr Mollowney emphasized its novel features. He advocated the use of a frame of reference moving with the tidal velocity for the numerical solution of the advection-diffusion equation for a one-dimensional estuary. This was done by moving the segments, into which the estuary was assumed to be divided, upstream and downstream with the tide so that the volume upstream of a given segment boundary was constant in time. By then applying the principles of conservation of volume and of mass of pollutant, the concentrations in each moving segment at small increments of time could be obtained. He pointed out that by

averaging the conservation equations applied to a moving segment over a period of a tidal cycle the time-dependent non-tidal model could be derived and by taking a time average over a longer period the steady-state model could be derived. He said that in this concept of the steady-state model it was still necessary to know the tidal movement during the tidal cycle in order to calculate the contribution made by the outfalls to each moving segment. He concluded by showing a comparison (Fig. 4) between results from the steady-state model and the time-dependent model for steady flow and tidal range conditions. This demonstrated that, when the distribution of effluent over the segments was taken into account, the steady-state model gave results almost identical with the time averages in the moving segments of the time-dependent model.

#### CONTRIBUTION BY MR. J. P. J. O'KANE

(Following Mr Mollowney's presentation, Mr J. P. J. O'Kane (University College, Dublin) made a lengthy contribution which he later elaborated and submitted in writing. This contribution is reproduced in full.)

It has long been recognized that the oscillatory flow produced by the tide in an estuary, is largely responsible for the variations in water quality within a tidal period. Many intuitive discussions of this have been presented, but the precision which a mathematical formulation of such insights might provide has been slow in forthcoming. The present discussion reviews recent progress in this direction.

#### Oscillating reference frames

The independent variables  $x$  and  $t$  in the convective-diffusion equation (13) represent a fixed reference frame for an observer on the bank of the estuary. Any measurements he takes are always referred to the  $(x, t)$  frame: a position  $x$  and a time  $t$ . Now consider a notional observer who can move so as to maintain a constant volume of water between himself and the head of the estuary. His motion defines a new reference frame which oscillates back and forth when viewed from the bank, i.e. from the  $(x, t)$  frame. Will the estuary appear to behave differently and perhaps more simply to this oscillating observer? To answer this question mathematically requires (a) the equations of transformation from one frame to the other and their differential properties, and (b) the transformation of the convective-diffusion equation (13), which, in its usual form, is

$$\frac{\partial C}{\partial t}(x, t) + U(x, t) \frac{\partial C}{\partial x}(x, t) = \frac{1}{A(x, t)} \cdot \frac{\partial}{\partial x} \left\{ D(x, t) \cdot A \cdot \frac{\partial C}{\partial x} \right\} - \frac{qC}{A}(x, t) + \frac{m}{A}(x, t), \quad (40)$$

from an expression concerning the rates at which things happen in the  $(x, t)$  frame to the corresponding expression in the oscillating frame. If (b) produces a simpler equation after transformation, then (a) allows us to make use of it.

Two very similar oscillating frames are possible:  $(V, t)$  and  $(x', t)$  depending on whether position on the oscillating frame is labelled with the volume  $V$  of the estuary or some equivalent position of that volume,  $x'$  on the bank. Position on the original  $(x, t)$  frame, i.e. on the bank, is labelled with a standardized measuring rod. Time in all three frames is labelled with the same standardized clock.

#### The $(V, t)$ reference frame

##### Equations of transformation and their differential properties

The defining equation which interrelates the  $(x, t)$  and  $(V, t)$  frames is the volume function itself:

$$V = V(x, t). \quad (41)$$

The frame is labelled with the volume of water in the estuary. Specify  $x$  and  $t$ , and a point,  $V$ , on the new frame is determined. The inverse transformation from the volume frame to the bank  $x = x(V, t)$  is determined implicitly. The other implicit function  $t = t(V, x)$  shows that the 2 frames behave as a clock. The Author's Fig. 1 is a graphical solution of Equation 41 for these 2 implicit equations of transformation. The differential properties of the transformation are found from the standard rules for partial derivatives. There are 6 possible first-order derivatives of which 4 are implicitly defined by Equation 41.

The derivative  $(\partial V / \partial x)_t = A$  is the *coefficient of distortion* of the oscillatory stretching transformation. It shows that the ratio of the length of a small piece of the volume frame, measured in  $V$  units, to its length measured in  $x$  units, is equal to the cross-sectional area. The derivative

$$\left( \frac{\partial x}{\partial t} \right)_V = - \frac{(\partial V / \partial t)_x}{(\partial V / \partial x)_t} = - \frac{(\partial V / \partial t)_x}{A} \quad (42)$$

is the velocity of a fixed point  $V$  on the oscillating frame as observed from the bank  $x$ ;  $(\partial V / \partial t)_x$  is the velocity of a point  $x$  on the bank as observed from the volume frame  $V$ . Equation 42 shows that the *dual velocities* are interrelated by the coefficient of distortion of the transformation. Substituting Equation 10 into Equation 42 gives

$$\left( \frac{\partial x}{\partial t} \right)_V = U_T. \quad (43)$$

This is the continuous form of Equation 15 and is a direct proof of the Author's assertion that when travelling with the tidal velocity an observer on the bank maintains constant volume.

The ranges over which points on the bank and volume frames oscillate are called the *tidal excursions*  $E_V(x)$  and  $E_x(V)$ , and have dimensions  $[L^3]$  and  $[L]$  respectively. The most important tidal excursion  $E_V(x)$  is the maximum distance measured in  $V$  units through which a point  $x$  on the bank will move during half a tidal cycle ( $\frac{1}{2}T$ ), so that

$$E_V(x) = \max_x V(x, t) - \min_x V(x, t); -\frac{1}{2}T \leq t \leq +\frac{1}{2}T. \quad (44)$$

The other tidal excursion is

$$E_x(V) = \max_x x(V, t) - \min_x x(V, t); -\frac{1}{2}T \leq t \leq +\frac{1}{2}T. \quad (45)$$

If an outfall is discharging solute at  $x$  then  $E_V(x)$  is the length of estuary (in  $V$  units) that is smeared during half a tidal cycle when other transport mechanisms are small. Likewise, if a patch of oil is at  $V$  then  $E_x(V)$  is the length of bank that is smeared during half a tidal cycle when change in storage is the sole transport mechanism in the estuary.

The reciprocals of the velocities,  $(\partial t / \partial V)_x$  and  $(\partial t / \partial x)_V$ , are called *residence distributions* and are defined on the tidal excursions  $E_V(x)$  and  $E_x(V)$ ;  $(\partial t / \partial V)_x$  is the differential time a point  $x$  (an outfall) spends at any point  $V$  within  $E_V(x)$  as  $x$  oscillates back and forth. This is the more important of the two residence distributions since matter is normally discharged from the bank to the estuary and not in the reverse direction. From Equations 42 and 43 or otherwise we have

$$\left(\frac{\partial t}{\partial V}\right)_x = \frac{-1}{AU_x}. \quad (46)$$

The residence distributions always exhibit singularities at the ends of the tidal excursions where  $U_T = 0$  at slack tide.

If an outfall is discharging solute at  $x$  then the instantaneous concentration per unit 'length' of  $V$  at a point  $V$  opposite  $x$  is equal to the product of the discharge rate and the ordinate of the residence distribution,  $(\partial t / \partial V)_x$ , at the point  $(x, V)$ .

These differential properties of the  $(V, t)$  frame have obvious numerical approximations in Fig. 1.

Simple examples of oscillating  $(V, t)$  frames for estuaries of exponential or uniform geometry can be constructed easily<sup>11</sup>. Their properties provide many insights into the nature of oscillatory motion in estuaries of one dimension.

#### Transforming the convective-diffusion equation

Shinohara *et al.*<sup>12</sup> have shown that the transformed convective-diffusion equation in the  $(V, t)$  frame is

$$\frac{\partial C}{\partial t}(V, t) + Q'(V, t) \frac{\partial C}{\partial V}(V, t) = \frac{\partial}{\partial V} \left\{ A'^2(V, t) \cdot D'(V, t) \cdot \frac{\partial C}{\partial V} \right\} - q'(V, t) \cdot C + m'(V, t). \quad (47)$$

The primes on  $Q'$ ,  $A'$ ,  $D'$ ,  $q'$ , and  $m'$  indicate that the functional dependence of these parameters on  $(V, t)$  is not the same as that for  $(x, t)$  with  $V$  simply replacing  $x$ . The correct form is obtained by substituting for  $x$  the implicit equation of transformation  $x = x(V, t)$ ;  $q'$  and  $m'$  have also been transformed to rates of injection of water and solute per unit 'length' of  $V$ . Hence  $\partial Q' / \partial V = q'$ . Noting that

$$\frac{\partial}{\partial V}(Q'C) = Q' \frac{\partial C}{\partial V} + q'C, \quad (48)$$

Equation 47 can be written as

$$\frac{\partial C}{\partial t}(V, t) = \frac{\partial}{\partial V} \left\{ A'^2 D' \frac{\partial C}{\partial V} - Q'C \right\}' + m'(V, t). \quad (49)$$

This corresponds to Equation 14 transformed to the  $(V, t)$  frame. Note that  $V$  and  $Q$  must correspond; flood rises due to  $Q$  must appear in  $V$  in the upper reaches of the estuary.

Integrating Equation 49 over an oscillating segment  $\Delta V_i = V_i - V_{i-1}$ , and ignoring  $m'$  for the moment, gives

$$\frac{\partial}{\partial t} \int_{V_{i-1}}^{V_i} C(V, t) dV = -Q'C \Big|_{V_{i-1}}^{V_i} + D'A'^2 \frac{\partial C}{\partial V} \Big|_{V_{i-1}}^{V_i}; \quad i = 1, \dots, n. \quad (50)$$

The term on the left-hand side is  $\Delta V_i d\hat{C}_i/dt$  where  $\hat{C}_i(t)$  is the average concentration in segment  $i$  defined as

$$\hat{C}_i(t) = \frac{1}{\Delta V_i} \int_{V_{i-1}}^{V_i} C(V, t) dV. \quad (51)$$

However, the terms on the right-hand side contain the concentrations and concentration gradients at the boundaries of segment  $i$ . In order to close the system of equations, assumptions relating  $\hat{C}_i(t)$ ,  $C(V_i, t)$ , and  $(\partial C / \partial V)|_{V=V_i}$  must be introduced. The Author has implicitly assumed that

$$\begin{aligned} C(V_i, t) &= \hat{C}_i(t); & C(V_{i-1}, t) &= \hat{C}_{i-1}(t); \\ \frac{\partial C}{\partial V} \Big|_{V=V_i} &= \frac{2(\hat{C}_{i+1} - \hat{C}_i)}{V_{i+1} - V_{i-1}}; & \frac{\partial C}{\partial V} \Big|_{V=V_{i-1}} &= \frac{2(\hat{C}_i - \hat{C}_{i-1})}{V_i - V_{i-2}}. \end{aligned} \quad (52)$$

Other assumptions are possible<sup>13,14</sup>. Substituting above gives

$$\Delta V_i \frac{d\hat{C}_i}{dt} = Q'_{i-1} \hat{C}_{i-1} - Q'_i \hat{C}_i + F'_i (\hat{C}_{i+1} - \hat{C}_i) - F'_{i-1} (\hat{C}_i - \hat{C}_{i-1}) \quad (53)$$

where

$$F'_i = 2D'(V_i, t)A'^2(V_i, t)/(V_{i+1} - V_{i-1}); \quad Q'_i = Q'(V_i, t). \quad (54)$$

These are more accurate forms of Equations 19 and 20 and are not restricted to uniformly mixed segments as stated in the paper and belied by Fig. 4. Since the Author's data in Fig. 2 are invariant with time when plotted in the  $(V, t)$  plane,  $F_i$  is a constant so that  $D'A'^2$  is a function of  $V$  only, under conditions of constant  $Q'$  in Equation 53.

The concentration of solute per unit 'length' of  $V$  due to an outfall at  $x$  discharging at a rate  $m(t)$  is  $(\partial t / \partial V)_x m(t)$ . Integrating this over  $\Delta V_i$  and assuming that  $m(t)$  is constant gives

$$\int_{V_{i-1}}^{V_i} m \left( \frac{\partial t}{\partial V} \right)_x dV = \int_{t(V_{i-1}, x)}^{t(V_i, x)} m(\tau) d\tau = [t(V_i, x) - t(V_{i-1}, x)]m. \quad (55)$$

This is merely the total amount discharged while  $x$  lies within  $\Delta V_i$  and is used by the Author in both the time-dependent and steady-state models as shown in the bottom of Fig. 4. If  $\Delta V_i$  straddles the end of the tidal excursion,  $E_V(x)$ , then some small changes are necessary above. The singularities in  $(\partial t / \partial V)_x$  are always smoothed out in this discrete approximation. However they reappear as  $\Delta V_i$  becomes smaller and smaller. Hence the range of the stalks (vertical bars), and possibly their averages as well, at the ends of  $E_V(x)$  in Fig. 4, will increase as  $\Delta V_i$  is reduced. The Author might like to present his very interesting results as lines of constant concentration in the  $(V, t)$  plane, for different values of  $\Delta V_i$ , so as to highlight the nature of the oscillations implied by the stalks and also to show whether they extend beyond  $E_V(x)$ .

The uniform distribution of input in Fig. 4 can be better interpreted as the product of the residence distribution  $(\partial t / \partial V)_x$  and a variable heat source modulated so as to have a concentration directly proportional to its reciprocal, the velocity  $(\partial V / \partial t)_x$ . Hence the singularities are associated with zero discharge. The broken curve in Fig. 4 is therefore the average and steady-state concentration resulting from the modulated discharge of the given heat load. The Author might like to present his results in the  $(V, t)$  plane for this case also. The Author's result confirms that intermittent discharge far (in terms of  $E_V(x)$ ) from the seaward boundary can be counter-productive. This can be anticipated by simply using the residence distribution and appropriate bounds on its singularities.

### The $(x', t)$ reference frame

A full description of the  $(x', t)$  frame has been published<sup>11</sup> with historical references and examples. The  $(V, t)$  reference frame is mentioned in the Thames Report<sup>2</sup> but was completely superseded by the equivalent half-tide position or  $(x', t)$  frame. Only the salient points will be presented here in order to contrast the Author's use of the  $(V, t)$  frame with the Laboratory's earlier use of the  $(x', t)$  frame.

#### Equations of transformation and their differential properties

Position in the  $(V, t)$  reference frame was labelled with the volume of water in the estuary. Position in the  $(x', t)$  frame is labelled with the position on the bank,  $x'$ , of that volume at some arbitrary time, say  $t = 0$ ;  $x$  and  $x'$  are by definition coterminous at  $t = 0$ . Let  $V'$  be the volume function in the  $(x', t)$  frame. Hence the identity

$$V'(x', t) \equiv V(x', 0). \quad (56)$$

Since the volume of water must be the same in both the  $(x, t)$  and  $(x', t)$  frames, the equation

$$F(x, x', t) = V(x', 0) - V(x, t) = 0 \quad (57)$$

implicitly determines the required transformation of coordinates from one frame to the other:

$$x = x(x', t); \quad x' = x'(x, t); \quad t = t(x, x'). \quad (58)$$

A simple graphical method of solving Equation 57 for Equations 58 is available<sup>11</sup>. The differential properties of the  $(x', t)$  frame are similar to those for the  $(V, t)$  frame. As before, velocities, tidal excursions, and residence distributions occur in pairs.

#### Transforming the convective-diffusion equation

It can be shown<sup>11</sup> that the transformed convective-diffusion equation in the  $(x', t)$  frame is

$$\frac{\partial C}{\partial t}(x', t) + \frac{Q'(x', t)}{A'_0} \frac{\partial C}{\partial x'} = \frac{1}{A'(x', t)} \frac{\partial}{\partial x'} \left\{ A' D' \left( \frac{A'}{A'_0} \right)^2 \frac{\partial C}{\partial x'} \right\} - \frac{q' C}{A'_0} + \frac{m'}{A'_0} + W' \quad (59)$$

where  $W'$  is an extra term which can probably be neglected and  $A'_0 = A(x', 0) = A'(x', 0)$ . As before a great simplification has been achieved in the advective term. If the estuary is of exponential shape then  $A'(x', t)$  becomes a function of  $x'$  only and hence equals  $A'_0$  and  $W' = 0$ . Hence Equation 59 becomes

$$\frac{\partial C}{\partial t}(x', t) = \frac{1}{A'_0} \frac{\partial}{\partial x'} \left\{ A'_0 D'(x', t) \frac{\partial C}{\partial x'} - Q'(x', t) C \right\} + \frac{m'}{A'_0}(x', t). \quad (60)$$

The labelling of the  $(x', t)$  frame at  $t = 0$  can correspond with high water or low water or half-tide at an arbitrary point on the bank. The time of labelling must not, however, vary from point to point. In the Thames Report<sup>2</sup> the time of labelling is a function of position. This adds extra terms to the differential properties of the transformation and complicates rather than simplifies the transformed solute equation (60).

### Comparison of frames

The solute equation is simplest in the  $(V, t)$  frame. Both the  $(x', t)$  and  $(V, t)$  frames successfully remove almost all the tidal harmonics originally present in the  $(x, t)$  frame. When data, which have been collected uniformly on the  $(x, t)$  frame, are transferred to the  $(V, t)$  frame, they are stretched increasingly towards the sea according to the coefficient of distortion  $(\partial V/\partial x)_t = A$ . This is visually undesirable and does not occur in the  $(x', t)$  frame;  $x'$  is a more natural coordinate than  $V$ .

The Author clearly regards the  $(V, t)$  frame as an auxiliary frame in the calculations. This writer contends that oscillating frames are the natural frames on which to record and represent estuarine behaviour in the longitudinal dimension.

### REPLY TO MR J. P. J. O'KANE

Mr Mollowney thanked Mr O'Kane for his most interesting contribution. His use of the two reference frames  $(x, t)$  and  $(V, t)$  was particularly enlightening. However, there were a number of points on which they held different views.

Mr O'Kane had shown that there were two distinct ways of describing the transformation  $(x, t) \longleftrightarrow (V, t)$ . The first was from the viewpoint of an observer on the bank who watched the elements of volume moving past the outfalls with the tidal velocity. This was the view used explicitly in the paper. In the second way the water was considered to be stationary (ignoring the fresh-water flow for the moment) and the banks and outfalls oscillated back and forth. This was the viewpoint of an observer fixed in the oscillating frame. In deriving Equations 53 and 54 (which were basically the same as Equations 19 and 20) this viewpoint had been used; but these equations could also be derived using the first point of view. Thus by defining  $X_i(t)$  as  $x(V_i, t)$  and  $X_{i-1}(t)$  as  $x(V_{i-1}, t)$ , and integrating Equation 13 from  $X_{i-1}$  to  $X_i$ , one obtained

$$\int_{X_{i-1}}^{X_i} A \left( \frac{\partial C}{\partial t} + U_r \frac{\partial C}{\partial x} \right) dx = (DA \frac{\partial C}{\partial x} - QC) \Big|_{X_{i-1}}^{X_i} + \int_{X_{i-1}}^{X_i} m dx. \quad (61)$$

It could be shown that the left-hand side was equal to  $\frac{d}{dt} \int_{X_{i-1}}^{X_i} AC dx$ . This could then be written as  $\Delta V_i (\hat{d}\hat{C}_i/dt)$ ,  $\hat{C}_i$  being the average concentration in segment  $i$  and defined by

$$\hat{C}_i(t) = \frac{1}{\Delta V_i} \int_{X_{i-1}}^{X_i} AC dx. \quad (62)$$

In these equations  $C = C(x, t)$ . (It would have been more consistent if Mr O'Kane had used  $C'(V, t)$  instead of  $C(V, t)$  in his discussion.) The right-hand side of Equation 61 could be expanded by assuming that

$$C(X_i, t) = \hat{C}_i, \quad C(X_{i-1}, t) = \hat{C}_{i-1}, \quad (63)$$

and

$$DA \frac{\partial C}{\partial x} \Big|_{X_i} = \frac{2D_i A_i}{X_{i+1} - X_{i-1}} (\hat{C}_{i+1} - \hat{C}_i). \quad (64)$$

Substituting these relations gave Equation 19 with  $F_i$  defined as in Equation 20. As Mr O'Kane had pointed out, the expressions for  $F_i$  and  $F_i'$  (from Equation 54) ought to agree but did not. However, it was not possible from the derivation given to say which was the more accurate formula because the derivations were not rigorous but at most just plausible.

Mr O'Kane gave the transformed convective diffusion equation in the  $(x', t)$  frame as Equation 59. The Author had found that a simpler form of the transformed equation was

$$A' \frac{\partial C'}{\partial t} = \frac{\partial}{\partial x'} \left\{ \left( \frac{D' A'^2}{A'^2} \right) A' \frac{\partial C'}{\partial x'} - Q' C' \right\} + m' \quad (65)$$

where the primes on  $C'$ ,  $A'$ ,  $A'_o$ ,  $m'$ ,  $Q'$  indicated that the functional dependence was on  $(x', t)$ .

### ADDITIONAL REFERENCES

11. O'KANE, J. P. J. A kinematic reference frame for estuaries of one dimension. *Proc. International Symposium on Mathematical Models in Hydrology, Warsaw, 1971*. Inst. Ass. Hydrol. Sci., 1973, Vol 2. (In press).
12. SHINOHARA, K., TSUBAKI, T., AWAYA, Y., and FARAMOTO, K. Numerical analysis on the salinity intrusion in the tidal estuary of well-mixed type. *Proc. Symp. int. Assn. Hydraul. Res., Tokyo, 1970*, p. 165.

13. THOMANN, R. V. Mathematical model for dissolved oxygen. *J. sanit. Engng Div. Am. Soc. civ. Engrs*, 1963, **89** (SA5), 1.
14. KEELING, C. D., and BOLIN, B. The simultaneous use of chemical tracers in oceanic studies. Pt. I. General theory of reservoir models. *Tellus*, 1967, **19**, 566.

# Mathematical Modelling

The Humber Estuary Committee requested the Water Research Centre (WRC) to develop mathematical models of the Humber tidal system with dissolved oxygen as the main parameter. A suite of models has been completed and transferred to the Yorkshire Water Authority which is operating them on behalf of the authorities concerned with the management of the system.

Two types of model have been produced – water-quality models to predict the distributions of dissolved oxygen (and related substances) for any given pattern of polluting load and environmental conditions, and a hydrodynamic model to calculate water levels and water movements throughout the system from a knowledge of the variation in level at the seaward end and the fresh-water flow in the rivers.

In fact three water-quality models have been developed – a fixed-segment time-dependent model, a moving-segment steady-state model<sup>1</sup>, and a moving-segment time-dependent model. Both the fixed-segment model and the moving-segment steady-state model calculate the steady-state (or equilibrium) distributions arising from steady fresh-water inflows and polluting discharges (outfalls and inputs at tidal limits). The fixed-segment model was the first model to be developed (in 1976) but has now been superseded by the moving-segment model which produces a much more efficient solution to the mathematical equations than the fixed-segments approach. The moving-segment time-dependent model is used to calculate the effect of varying fresh-water flow and discharges.

The hydrodynamic model, which is based on a computer program obtained from the Hydraulics Research Station (HRS), is used to generate the variations in system geometry for input to the water-quality models.

## D1 Representation of System

The Humber system is slightly stratified, but the variations in concentration of dissolved substances over the depth and between the centre and the sides are not large in comparison with those over the length. Consequently, it is possible to treat the dispersion of pollutants as a problem in one dimension, the average concentration of a substance over a cross-section being expressed as a function of distance along the estuary.

To provide the most effective tool for the future management of the system, it was necessary to take into account the ebb and flow of the tide, and the branching of the estuary at Trent Falls into the tidal waters of the Ouse and Trent, and of the Ouse into the tidal waters of the Wharfe, Aire, and Don. Accordingly, the system is represented by five one-dimensional channels: the main channel comprising the Ouse and the Humber, and four tributary channels. Positions are measured from Trent Falls as origin along the centre line of the channels. In the water-quality models the flux arising from the variations in velocity and concentration (from their mean values) over a cross-section is represented by a one-dimensional

diffusion process, and in the hydrodynamic model the stress or friction at the bed is assumed to be a function of the mean velocity over the cross-section.

## D2 Water-Quality Models

### (a) Basic Principles

In essence, each model consists of a series of equations which specify the rate at which the concentration of a pollutant at a point in the estuary is changed by the processes to which it is exposed; these include tidal motion, displacement by the land-water flow, dispersion by mixing, degradation under the action of microorganisms, and transformations by chemical reactions. The basic equation governing the mass balance of a substance, concentration  $C$ , at distance  $x$  along the estuary at any instant in time,  $t$ , during the tidal cycle may be written as

$$\frac{\partial}{\partial t} (AC) + \frac{\partial}{\partial x} (AUC) = \frac{\partial}{\partial x} \left( DA \frac{\partial C}{\partial x} \right) - kAC + m, \quad (1)$$

where  $A(x,t)$  is the cross-sectional area,  $U(x,t)$  is the water velocity,  $D(x,t)$  is a longitudinal dispersion coefficient,  $k(x,t)$  is a decay rate-constant for the substance, and  $m(x)$  is the steady rate of addition of the substance per unit length of estuary. The corresponding equation of conservation of volume is

$$\frac{\partial A}{\partial t} + \frac{\partial}{\partial x} (AU) = q, \quad (2)$$

where  $q$  is the rate of entry (per unit length) of water from tributaries and discharges.

Although Equation 1 may be solved at a fixed point,  $x$  by stepping forward in time until a steady state is reached, both velocity and concentration at a given position in an estuary vary over wide limits during a tidal cycle, and in order to achieve sufficient accuracy in numerical computation it is generally necessary to use a very small time-step. For this and other reasons, it is preferable to adopt a different concept and to apply the equation of conservation of mass and volume to a point moving with the tidal velocity. By this means the tidal velocity term is eliminated from the numerical computation of substance concentration, reducing numerical dispersion and allowing a more efficient method of solution.

For the numerical solution of Equations 1 and 2 the estuary is imagined to be divided by vertical partition (extending from one bank to the other) into a series of segments which oscillate upstream and downstream with the tidal velocity in such a way that the volume landwards of a given boundary remains constant. The movement of the segments is determined from knowledge of the volume of water landwards of given positions during a tidal cycle. As each segment passes the position of an outfall it receives an increment of pollution given by the rate of discharge of the substance multiplied by the time taken for the segment to pass the outfall. To satisfy continuity there is a seaward flow through each segment boundary equal to the total landward water flow. Longitudinal dispersion is represented as

continuous exchange of water between adjacent segments, and values of the dispersion coefficient are obtained by assuming a balance at any instant between the mass of salt transported by the land-water flow and that transported by mixing. It will be appreciated that although segment volumes are constant, their lengths, depths, and surface areas vary throughout a tidal cycle. During the ebb tide, segments from the tributaries enter the main channel and allowance is made for lateral mixing between the segments in the tributary and in the main channel.

Under conditions of steady fresh-water inflow, steady rates of discharge of the substance, and a periodic tide, the steady-state solution is a periodic function of time having a period of one tidal cycle. A very good approximation to the solution, and one which does not vary with time, has been obtained by averaging over the tidal period. The equation which describes this time-averaged steady-state solution is found by averaging the mass-balance equation (Equation 1 applied to a moving point) over the tidal period and setting the average of the time-derivative to zero. This gives an equation of the form

$$F_{i-1}(C_{i-1} - C_i) + F_i(C_{i+1} - C_i) + Q_{i-1}C_{i-1} - Q_iC_i - k_i\Delta V_i C_i + M_i + F_i^Y(C_i - C_i) = 0, \quad (3)$$

where  $F_i$  is the longitudinal and  $F_i^Y$  the lateral mixing flow in the  $i$ 'th segment,  $Q_i$  the fresh-water flow out of the segment,  $k_i$  the rate of decay,  $\Delta V_i$  the segment volume, and  $M_i$  the mass of substance received from discharges. A similar equation is derived for the segments in the tributaries.

The cumulative volume in each channel at 0730 on 22 June 1978 (high water at Immingham) was plotted against distance and divided into 144 segments, distributed as follows: Wharfe 8, Aire 13, Don 16, Trent 43, and Ouse-Humber 64. The boundaries of the segments were chosen to be at the same positions as the cross-sections of the hydrodynamic model (approximately 2-km intervals); thus the moving frame and fixed frame coincide at 0730 on 22 June 1978. The upstream boundary of each channel is treated as a segment of zero volume - a point where concentrations are specified and held constant. The solution of the simultaneous equations is done essentially by a method of elimination and back substitution.

#### 'b) Oxygen Balance

Calculations of the distribution of dissolved oxygen from knowledge of the polluting load entering the estuary in sewage and industrial effluents and in the water entering at the tidal limits, requires that the distributions of organic carbon, organic nitrogen, and ammoniacal and oxidised nitrogen be found simultaneously. For instance, organic nitrogen hydrolyses to ammonia, which in turn oxidises to nitrate which may subsequently be reduced in one other part of the system.

As in earlier estuary studies, the course of oxidation of carbonaceous material in the majority of effluents to the sewer system is represented by a composite exponential derived on the assumption that the organic matter undergoing oxidation consists of two components, referred to as 'fast' and 'slow' carbon to distinguish the relative rates of uptake. The equation used is

$$y = E_c (1 - p_f e^{-kt} - p_s e^{-kt/5}), \quad (4)$$

where  $y$  is the oxygen uptake by time  $t$ ,  $k$  the standard rate-constant of 0.23 per day at 20°C,  $p_f$  the proportion of the organic material oxidising at the rate  $k$ ,  $p_s$  the proportion oxidising at the slow rate  $k/5$ , and  $E_c$  the total oxygen uptake. The relationship between  $E_c$  and the 5-day BOD at 20°C,  $B$ , is

$$E_c = B / (1 - p_f e^{-5k} - p_s e^{-k}). \quad (5)$$

Organic nitrogen which is in combination with organic carbon is assumed to be converted to ammonia at the same rate as carbon is oxidised.

During the oxidation of organic carbon, ammonia is assimilated by the bacteria and there is an increase in organic nitrogen resulting from the growth of bacterial cells. It is assumed that the rate of assimilation of ammonia and production of organic nitrogen is proportional to the rate of uptake of dissolved oxygen by the organic carbon compounds.

When ammonia is present in water containing more than a certain concentration of dissolved oxygen, it is oxidised through nitrite to nitrate, and when nitrate is present in water containing less than a certain concentration of oxygen it is utilised in the oxidation of carbon compounds. Although much less is known than could be wished about the precise conditions under which these processes occur, reasonable simulations have been obtained in other studies by assuming that

- ammonia is oxidised at a rate proportional to its concentration,
- the oxidation of ammonia is retarded when the oxygen content falls to 5% saturation,
- when ammonia oxidation ceases, and organic carbon remains to be oxidised, nitrate is reduced to molecular nitrogen at a rate sufficient to maintain the oxygen level at 5% saturation, and
- when nitrate is exhausted the dissolved-oxygen concentration is allowed to fall to zero.

The oxygen balance in each segment is represented by seven equations: those for fast and slow carbon, fast and slow organic nitrogen, ammonia, oxidised nitrogen, and dissolved oxygen. In addition it is necessary to know salinity and temperature. The distributions of fast and slow carbon, and fast and slow organic nitrogen are calculated by solving equations of the form of Equation 3, choosing the appropriate loads and rate-constant. The equation for ammonia has additional terms representing the formation of ammonia from the hydrolysis of organic nitrogen, loss by assimilation during the oxidation of the organic carbon compounds, and the restriction on the rate of oxidation of ammonia when the concentration of dissolved oxygen is limiting. The equation for oxidised nitrogen takes account of formation by oxidation of ammonia, loss by denitrification, and reduction to nitrogen gas to satisfy carbonaceous demand when dissolved oxygen is limiting. The equation for dissolved oxygen takes account of the oxygen uptake by the carbonaceous compounds and by ammonia, the oxygen made available by the restriction of oxidation of ammonia and the reduction of nitrate where appropriate, and the exchange at the air/water interface. It should be noted that all the rate-constants are functions of temperature and satisfy an equation of the form

$$k = K (1 + a/100)^{T-20}, \quad (6)$$

where  $k$  is the value of the constant at temperature  $T$ °C,

K is the value at 20°C, and a is a temperature coefficient (per cent per degC). The values of a for the various substances are as follows:

Organic carbon	Organic nitrogen	Ammonia	Nitrate
5.0	5.0	8.8	7.0

The method of calculation is to assume initially that there will be no restriction on the oxidation of ammonia, and no reduction of nitrate. Each equation is thus solved in turn, starting with that for fast carbon, and followed by those for slow carbon, fast and slow organic nitrogen, ammoniacal and oxidised nitrogen, and finally that for dissolved oxygen. If the minimum calculated concentration of dissolved oxygen is not less than 5% saturation, the calculated distributions are the solutions required. If values less than 5% occur then it is necessary to recalculate the last three terms using an iterative procedure.

### (c) Calibration and Validation

In order to calibrate and validate the model it was necessary to collect, collate, and process a large quantity of data on hydrography, water quality, polluting loads, and fresh-water flow. Also it was necessary to make respirometric measurements in the laboratory of the consumption of oxygen by river water and by effluents from the major discharges.

Data for the calculation of cross-sectional area and surface width were obtained from three sources. The British Transport Docks Board (BTDB) made available the results of a detailed survey from Trent Falls to Spurn Head carried out in 1966. Soundings for the tidal Trent were obtained from drawings, supplied by the Severn-Trent Water Authority (STWA), relating to a survey in the late 1950's, and data for the tidal Ouse and its tributaries (from a survey in 1967) were available from HRS computer files. From these records the variations in cross-sectional area and surface width with respect to water level were calculated at intervals of approximately 2 km corresponding to the segment boundaries of the hydrodynamic model.

Data on the variation in tidal level were obtained from level recorders maintained by BTDB, STWA, and the Yorkshire Water Authority (YWA). The variation in estuarine geometry during a tidal period was computed from this information.

Two intensive fixed-point surveys of the tidal waters of the Humber system were carried out by YWA, STWA, and the Anglian Water Authority (assisted by WRC) during 16-18 May and 20-22 June 1978 specifically to provide data to calibrate and validate the model (see Sections 1.8 and 7.4). Twenty-nine sampling stations were manned for 13-hour periods to cover complete tidal cycles. The stations were distributed as follows: Trent (6 including the tidal limit), Ouse system (16 including tidal limits) and Humber (7). The main determinands were temperature, dissolved oxygen, chloride or salinity, nitrogen compounds, suspended solids, and BOD. Measurements were at two-hourly intervals at the tidal limits, shortening progressively to half-hourly just above Trent Falls and throughout the Humber. The composition of the river water entering at the tidal limits, and the composition and flow of the principal discharges, were measured intensively by the water authorities during 8-18 May and 12-22 June 1978 to provide data on

boundary values and polluting loads (Section 3.1). Fresh-water flows entering the tidal system are gauged by the various water authorities at Skelton (Ouse), Flint Mill (Wharfe), Beal (Aire), Hadfields (Don), and North Muskham (Trent). The daily flows at the tidal limits were calculated from the gauged flows by adjusting for the contribution from tributaries above and below the tidal limit as follows. The recorded daily flow at Skelton was increased by 30 MI/d (0.35 m<sup>3</sup>/s), that at Flint Mill by 20 MI/d, and that at Beal by 6 MI/d. The gauging station at the tidal limit of the Don at Doncaster was temporarily inoperative and the flow was assumed to be three times that at Hadfields. The flow at Cromwell Weir in the Trent was taken to be the same as that at North Muskham.

The measurements of water quality made at the sampling stations during the intensive surveys were transformed to the moving frame by calculating which segments were passing the sampling stations at the times of sampling. In effect, this was done by calculating the volume upstream of the sampling point at the time of sampling and by interpolation in the graph of the cumulative volume versus distance at 0730 on 22 June 1978 to get an equivalent distance; water-quality data were then plotted against those distances. For example the distributions obtained for salinity are shown in Fig. 63 for the June survey. The curves plotted through the data represent the mean distribution (fitted by eye) during the tidal period and it may be seen that the overall scatter (which derives in part from real-time variations in the moving frame and in part from sampling errors) is small. As a measure of goodness of fit the standard error of estimate, SE, was calculated from

$$SE = \left[ \frac{1}{N} \sum (P_i - O_i)^2 \right]^{1/2} \quad (7)$$

where  $P_i$  = predicted data,  $O_i$  = observed data, and  $N$  = number of data points. The value found for SE from the June salinity data was 0.9 g/kg on 479 data points, while the corresponding value for the May survey was 0.6 g/kg on 292 points. The observed and fitted mean distributions of temperature gave values of SE of 0.6 degC for June and 0.7 degC for May.

The observed distributions of dissolved oxygen, ammoniacal and oxidised nitrogen were plotted in a similar manner (Figs 39, 40, and 64 for June and Figs 37, 38, and 65 for May). Most of the data lie in a narrow band about a curve, suggesting that the movement of water is satisfactorily represented and that the variations in salinity, temperature, dissolved oxygen, ammoniacal nitrogen, and oxidised nitrogen in a given volume of water during a tidal period are comparatively small. This confirms one of the basic assumptions of the moving-segment approach. By contrast much larger variations were seen in the distributions of organic nitrogen, BOD, and suspended solids. Even in these cases, however, a mean curve through the data gives a reasonable representation of the distribution in the estuary for much of the time.

The model was calibrated using the observed data for fresh-water flow, polluting loads, and water quality relating to the June survey, and validated using data for the May survey. The results obtained for the Ouse-Humber and Trent were presented in Figs 39 and 40 for the June survey and in Figs 37 and 38 for May and discussed in the accompanying text (pp 24-26). Results for the Wharfe, Aire and Don are presented in Fig. 64 for June and in Fig. 65 for May. Calibration of the model consisted in varying the reaeration coefficient, the horizontal mixing in the fresh-water region, and the oxidation rate for ammonia; all other constants were

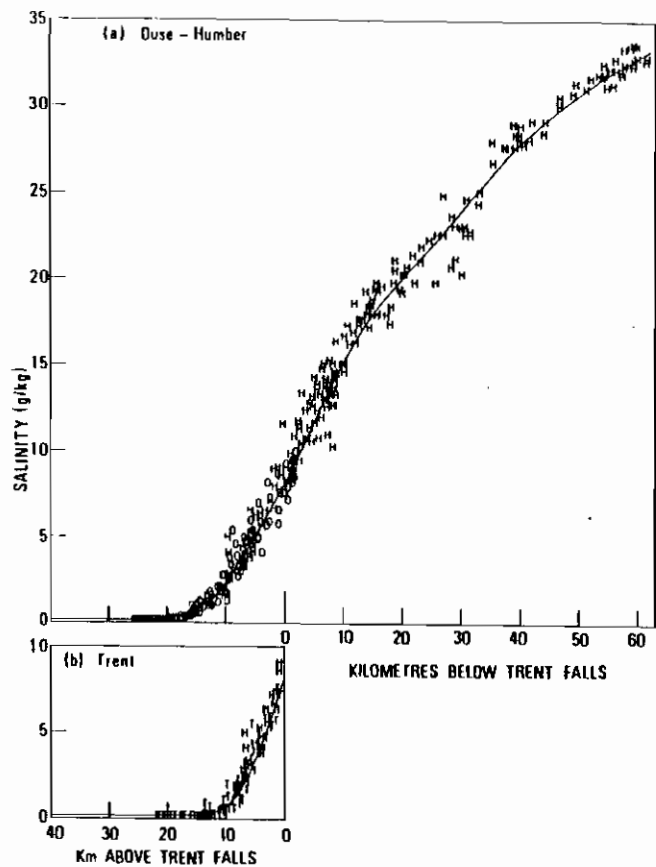


Fig. 63. Distribution of salinity during intensive survey of 20-22 June 1978. Symbols observed data; curves—fitted mean distribution. Positions adjusted to high water (see text)

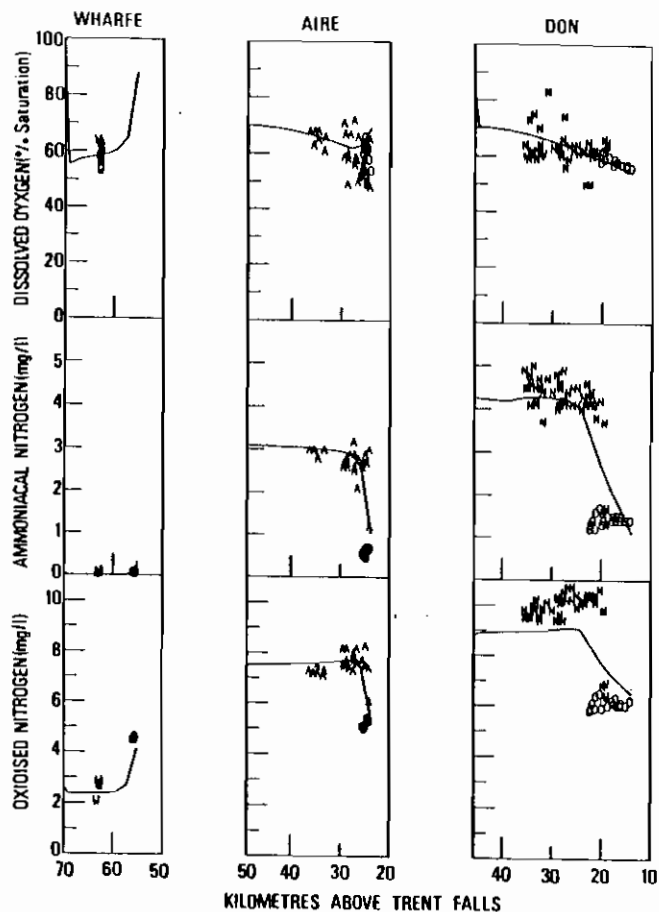


Fig. 65. Comparison of observed and predicted distributions of dissolved oxygen, ammoniacal nitrogen, and oxidised nitrogen during intensive survey of 16-18 May 1978. Curves calculated from steady-state model

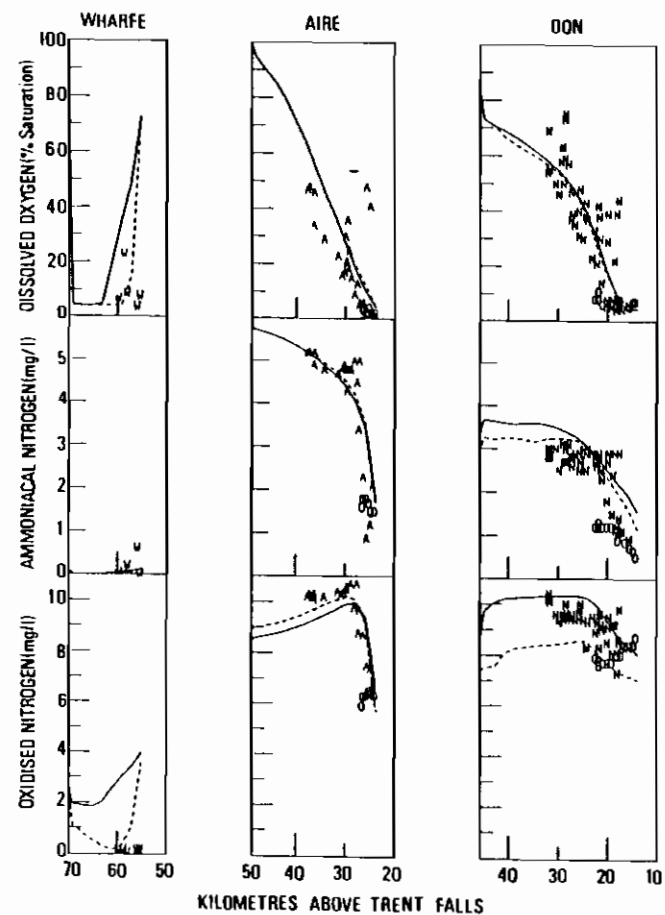


Fig. 64. Comparison of observed and predicted distributions of dissolved oxygen, ammoniacal nitrogen, and oxidised nitrogen during intensive survey of 20-22 June 1978. Broken curves—steady-state model; continuous curves—time-dependent model

derived from other observations or were already known from past experience. Table 25 gives the standard error of estimate between the observed and predicted values, and the number of data points, in each channel, and also in all channels combined, for each substance.

Table 25. Standard error of estimate (SE) and number of data points (N) in each channel for June 1978 calibration using steady-state model

	Dissolved oxygen (% sat.)		Ammoniacal nitrogen (mg/l)		Oxidised nitrogen (mg/l)	
	SE	N	SE	N	SE	N
Wharfe	36	5	0.2	5	1.8	5
Aire	13	30	1.0	27	1.2	26
Don	12	57	0.7	55	1.2	55
Trent	23	126	0.2	124	1.2	126
Ouse-Humber	9	383	0.3	300	1.0	381
Combined	14	601	0.4	511	1.1	593

The overall fit obtained by the model is reasonably good but there are a number of discrepancies which need to be explained. The most serious is a large local discrepancy in the final 20 km of the Trent where dissolved oxygen is overpredicted by about 30% of saturation and oxidised nitrogen underpredicted by about 1 mg/l. Also the predicted distribution of oxidised nitrogen in both the Ouse and the Don are generally too low by about 1 mg/l. The most likely explanations for these discrepancies are (a) the increased loadings of BOD and nitrogen forms to the estuary during the high fresh-water flows on 16-17 June and (b) increased loading owing to resuspension of solids by the spring tides prior to and during the surveys.

To investigate (a), a simulation was made on a time-dependent rather than a steady-state basis and account was taken of the variations in fresh-water flows and concentrations entering the system at the tidal limits over a 9-day period from 12 to 21 June. Areas and widths were calculated at half-hourly intervals using the hydrodynamic model and time-dependent versions of the steady-state equations were solved by a time-stepping method. The results obtained (Figs 39, 40, and 64) show that the time-dependent model gave much improved simulations of dissolved oxygen and oxidised nitrogen. However, the simulation of dissolved oxygen in the final 15 km of the Trent is still not adequate (see Section 3.8 for further discussion).

The comparison of observed and predicted distributions for the May survey are shown in Figs 37, 38, and 65. Table 26 lists the standard error of estimate and the number of data points in each channel and in all channels combined, for each substance. It may be seen that the model has been reasonably successful and there are no major discrepancies as there are in the June survey. There is a tendency to underpredict ammoniacal nitrogen in the Ouse and dissolved oxygen in the Trent but overall the steady-state model gives a satisfactory fit for the May survey data. This is reassuring in view of the large differences in the levels of dissolved oxygen between the May and June surveys.

Table 26. Standard error of estimate (SE) and number of data points (N) for each channel for May 1978 validation using steady-state model

	Dissolved oxygen (% sat.)		Ammoniacal nitrogen (mg/l)		Oxidised nitrogen (mg/l)	
	SE	N	SE	N	SE	N
Wharfe	4	8	0.1	12	0.5	12
Aire	9	41	0.8	36	0.9	36
Don	5	66	0.8	66	1.4	66
Trent	7	123	0.2	126	0.4	126
Ouse-Humber	5	370	0.3	291	0.6	382
Combined	6	608	0.4	531	0.7	622

It was thought useful to use the steady-state model to investigate possible reasons for the much lower levels of dissolved oxygen in the Ouse in June than in May. The factors considered were tidal range, temperature, fresh-water flow, boundary values, and loads. Starting with the June conditions, the effect of changing each factor to that of the May conditions was calculated. For these calculations it was assumed that there was no restriction on nitrification and no denitrification; dissolved oxygen was allowed to fall below zero. (The calculated minimum dissolved oxygen for June was -31% of saturation.) The predicted increase in the minimum dissolved oxygen in the Ouse caused by changing each factor from the June condition to that of the May survey is as follows:

Tidal range	Fresh-water flow	Temperature	Boundary values	Load
-5.3	42.0	32.2	11.9	48.3

Thus the most significant effects were attributed to changes in load, fresh-water flow, and temperature.

#### (d) Computer Programs

Computer programs, written in FORTRAN, as well as data files and output files have been transferred to the YWA computer; the Authority has implemented them

with modifications and is running practical applications on behalf of the three water authorities concerned with the management of the Humber tidal system. A brief description of the three main programs of the moving-segment steady-state model follows.

Program HSSM1 simulates the changes in geometry and position of constant-volume segments moving to and fro with the tide in the system during a tidal period. It operates on data in two frames, one frame fixed to the bank and the other moving with the constant-volume segments. Information on the geometry of the estuary (cross-sectional area and surface width) is read in at equidistant cross-sections in each reach in the fixed frame and the program calculates the variation of various quantities (required by the programs HSSM2 and HSSM3) in the moving frame. The chief quantities of interest are:

- volume of the segments,
- surface area of the segments,
- position of the segments,
- proportion of the time that a segment spends opposite an outfall, and
- proportion of the time that a segment in a tributary spends in the main channel (required to estimate the amount of mixing with the main channel).

Program HSSM2 sets up data files of salinity, temperature, flow, mixing coefficients, and loads for input to HSSM3. It uses the information generated by HSSM1 to calculate the distribution of flows and loads among the moving segments.

Program HSSM3 calculates the steady-state distributions of salinity, dissolved oxygen, and six associated substances (fast carbon, slow carbon, fast nitrogen, slow nitrogen, ammoniacal nitrogen, and oxidised nitrogen) in 144 segments in the Humber system resulting from steady polluting discharges and steady fresh-water inflows. It allows for restricted oxidation of ammonia and for denitrification when the dissolved oxygen is at or below 5 per cent saturation.

#### (e) Further Work

Further modelling work is needed to estimate the influence of suspended solids on the distribution of dissolved oxygen during the spring-neap cycle in the region around Trent Falls. In the first instance this will probably require using the present model to compare observed and predicted distributions for surveys other than May and June 1978. Further work on this aspect may require the acquisition of field data and the carrying out of laboratory experiments. It may be necessary to develop a two-layer model to simulate the movement of the solids.

### D3 Hydrodynamic Model

#### (a) Basic Principles

The model is based on the one-dimensional form of the differential equations expressing continuity of volume and momentum<sup>2</sup>.

$$w \frac{\partial h}{\partial t} + \frac{\partial Q}{\partial x} = q, \quad (8)$$

and

$$\frac{\partial Q}{\partial t} + gA \frac{\partial h}{\partial x} + \frac{gAR}{2\rho_0} \frac{\partial \rho}{\partial x} + \frac{\partial}{\partial x} (UQ) + \frac{f|Q|Q}{8RA} = 0, \quad (9)$$

where  $x$  is the longitudinal co-ordinate and  $t$  is the time,

- $w(x,t)$  = width of estuary at water surface,
- $h(x,t)$  = height of water surface above datum,
- $Q(x,t)$  = discharge through the cross-section at  $x$ ,
- $q(x,t)$  = lateral inflows at  $x$ ,
- $g$  = gravitational acceleration,
- $A(x,t)$  = cross-sectional area,
- $R(x,t)$  = hydraulic radius,
- $\rho(x,t)$  = area-averaged density,
- $\rho_0$  = representative density,
- $U(x,t)$  = average velocity through cross-section,
- $f$  = friction factor.

A finite-difference approximation is used to solve these equations. The estuarine system is considered as a series of cells; each cell centre represents a height boundary (h-pt), a flow boundary (Q-pt), or an internal point of the system where a height (h-pt) or a flow (Q-pt) is to be calculated; h-pts and Q-pts alternate along the system. An h-pt and an adjacent upstream Q-pt are associated with the same suffix, e.g.  $h_7$  and  $Q_7$  are adjacent. The segment between two Q-pts, or, more loosely, the h-pt at the centre of it, is termed a 'storage cell'. Similarly, a Q-pt is also termed a 'conveyance cell'.

There are four junction cells representing the confluences of the tributaries and the main Humber-Ouse artery. Each of these is an h-pt. Any section of the system lying between two junction cells, or a junction cell and a boundary cell, constitutes a reach. There are nine reaches, five in the main artery (Humber-Ouse), and four representing the tributaries (Trent, Don, Aire, Wharfe). The system is numbered in an increasing sense from the sea boundary in the Humber to the flow boundary at the end of the tidal Ouse, and re-starts with the first flow point inside the Trent. The numbering is then continued to the flow boundary of the Trent, then to the first flow point in the Don, and so on. The variables  $A$  and  $U$  are evaluated at Q-pts, and  $w$  at h-pts.

The computations use an implicit method, with a three-level time scheme. The equation of continuity of volume is formulated for an h-pt, and that of continuity of momentum for a Q-pt. The finite difference forms are

$$\frac{w_{m+1} (h_{m+1}^+ - h_{m+1}^-)}{\Delta t} + \frac{Q_{m+1}^+ - Q_m^+ + Q_{m+1}^- - Q_m^-}{2\Delta x} = q_{m+1}, \quad (10)$$

$$\frac{\lambda_m^+ - Q_m^-}{\Delta t} + \frac{gA (h_{m+1}^+ - h_m^+ + h_{m+1}^- - h_m^-)}{2\Delta x} + \frac{gA_m R_m (\partial \rho)}{2\rho_0 \partial x} + \frac{U_m (Q_{m+1} - Q_{m-1})}{2\Delta x} + \frac{Q_m (U_{m+1} - U_{m-1})}{2\Delta x} + \frac{f_m |Q_m^-| Q_m^+}{8R_m A_m} = 0. \quad (11)$$

The equations are obtained by integration over the time interval  $(t_0 - \frac{1}{2} \Delta t, t_0 + \frac{1}{2} \Delta t)$ . Variables evaluated at the centre of the interval are without a superscript, and variables evaluated at the beginning and end of the interval have superscripts  $-$  and  $+$  respectively;  $\Delta x$  represents the distance between successive h-pts, or

successive Q-pts (approximately 2 km) and is the same for all elements of any given reach, although it varies slightly from reach to reach.

Equations 10 and 11 may be re-written by collecting the terms as

$$a_m (h_{m+1}^+ - h_m^+) + b_m Q_m^+ = c_m \quad (12)$$

and

$$d_m H_m^+ + Q_{m-1}^+ = e_m. \quad (13)$$

To start a calculation the water levels and flows are given initial values. The set of linear equations above are solved by elimination and back-substitution and the values obtained are then used as initial values for the next time-step, and so on; a time-step of  $7\frac{1}{2}$  min was used. The solution is driven by the assumed values of the friction factor  $f$ , the tidal curve at the seaward end of the Humber, and the fresh-water flows entering the main channel and tributaries.

### (b) Calibration and Validation

Data on the variation of water level were obtained from 27 tidal-level recorders throughout the system for 16-18 May 1978 (neap tide) and 20-22 June 1978 (spring tide). The tide gauges were distributed as follows: Humber (5), Ouse (8 including tidal limit), Trent (10 including tidal limit), Don (1), Aire (2 including tidal limit) and Wharfe (1). The model was calibrated using the June data and validated using the May data. Basically a schematised version of the system was supplied to the model in the form of tables listing the cross-sectional areas, widths, and hydraulic radii at even increments of level for each of the 143 elements.

Much of the model-development work centred on correctly representing and estimating the frictional stress. The basic calibration parameter used was the Nikuradse roughness height,  $K_s$ , which is related to  $f$  by the Colebrook-White equation,

$$\frac{1}{\sqrt{f}} = -2.0 \log_{10} \left( \frac{K_s}{R} + \frac{2.51}{4 \text{Re} \sqrt{f}} \right), \quad (14)$$

where  $R$  is the hydraulic radius and  $\text{Re} = UR/\nu$  is the Reynolds number,  $\nu$  being the kinematic viscosity of water. An estimate of  $f$  and equivalent surface roughness  $K_s$  in each element was determined from the observed water levels in June by inverting the equations of continuity and motion.

The first stage in the calibration is to produce a height-field throughout the system at 15-min intervals from the observed levels at the tide gauges. This is achieved by employing a four-point cubic interpolation along the main artery, each cell using the data from the four nearest tide gauges either side of it. Near the ends of the artery where the cell could not be so centred the first (or last) four gauges are used. The same procedure is then performed separately for each tributary reach using the height already obtained at the junction cells. The technique then consists of evaluating the flow-field throughout time via the continuity equation and then the substitution of the heights and flows into the momentum equation to evaluate the flow-field. By inversion of Equation 14 a set of values of  $K_s$  is calculated. The final value of  $K_s$  chosen for each cell was an average of the

four median values produced by the inversion technique during four successive ebb tides when conditions were fairly steady. It was not possible to apply this technique to the Wharfe and the Don for June conditions because of the paucity of observed data. Observations of water level at five tide gauges in the Wharfe during a single tide in March 1968, and ten gauges in the Don during a tidal period in October 1967, were made available by HRS. These data were used to evaluate friction values for the Wharfe and Don. Having obtained the complete set of parameters, the model was run for June conditions and the fit assessed.

The comparison between observed and fitted water levels in the Ouse and Humber at high and low water of a spring tide on 21 June 1978 is shown in Fig. 66. The model was run for 5 tides using the seaward-boundary condition and fresh-water inflows corresponding to the May condition (but using the same friction factors as for June) and the comparison of the predicted high and low water levels with the observed for 17 May 1978 is also shown in Fig. 66. It may be seen that the model has been reasonably successful.

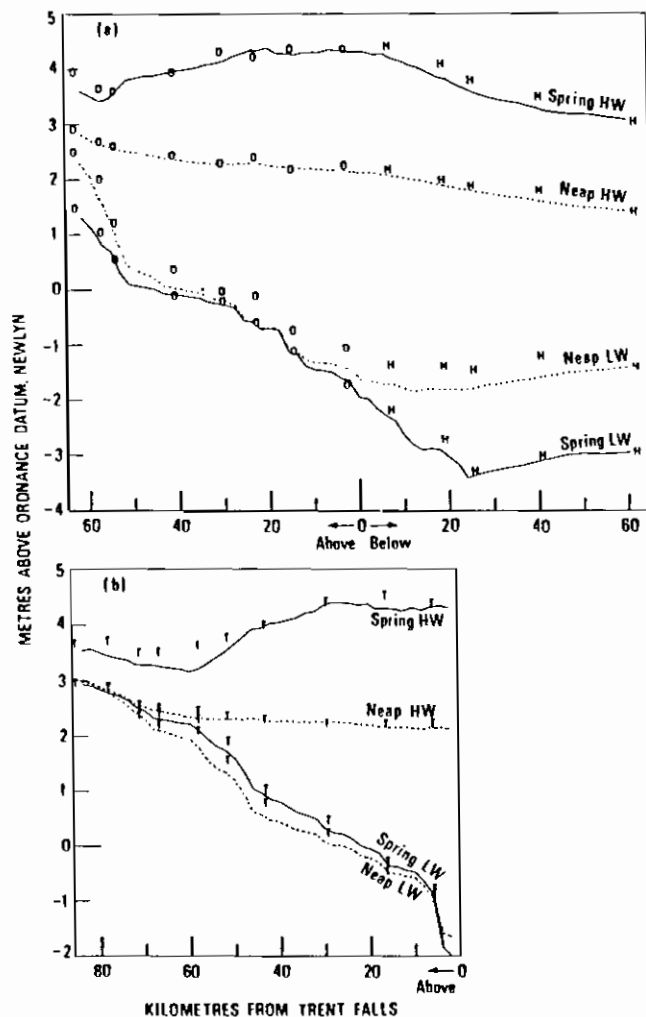


Fig. 66. Comparison of observed and predicted water levels in (a) Ouse-Humber and (b) Trent for a spring tide in June 1978 and a neap tide in May 1978  
Symbols - observed data; curves - predicted from hydrodynamic model

### (c) Further Work

The biggest error in observed and predicted levels occur at low water neap tide when the predicted levels are about 0.3 m too low. An improved fit may be obtained here by using higher friction values at neap tides. A suggested mechanism for causing a variation in the friction parameter,  $K_s$ , with tidal state is sediment transport. On spring tides, velocities are higher and the sediment is suspended, thereby flattening the bed and reducing the friction factor; on the slower neap tides, sediment is deposited with consequent increase in friction. In the present model these effects may be incorporated by employing an empirically based function derived by HRS<sup>2</sup>, which expresses  $K_s$  as a decreasing function of a non-dimensional quantity, the mobility number,  $\gamma$ , is given by

$$\gamma = \frac{U^2}{g(S-1)D_{av}} \quad (15)$$

where  $S$  is the relative density of the sand particles and  $D_{av}$  is a representative diameter of the sand grains forming the sediment.

### Acknowledgements

The author acknowledges the use of a report on the hydrodynamic model by M. C. Whitmore, Water Research Centre. Also acknowledged is the work by D. J. Rabone in setting up the geometry, tidal level, and load data for the models and developing the steady-state fixed-frame model.

### References

1. Mollowney, B. M. *The Moving-Segment Steady-State Model of Dissolved Oxygen in the Humber Tidal System*. Water Research Centre, Paper 366-M, 1982, 30 pp. (plus diagrams).
2. Odd, N. V. M. The predictive ability of one-dimensional estuary models. In *Transport Models for Inland and Coastal Waters* (ed. H. B. Fischer). Academic Press, New York, 1981, p. 39.

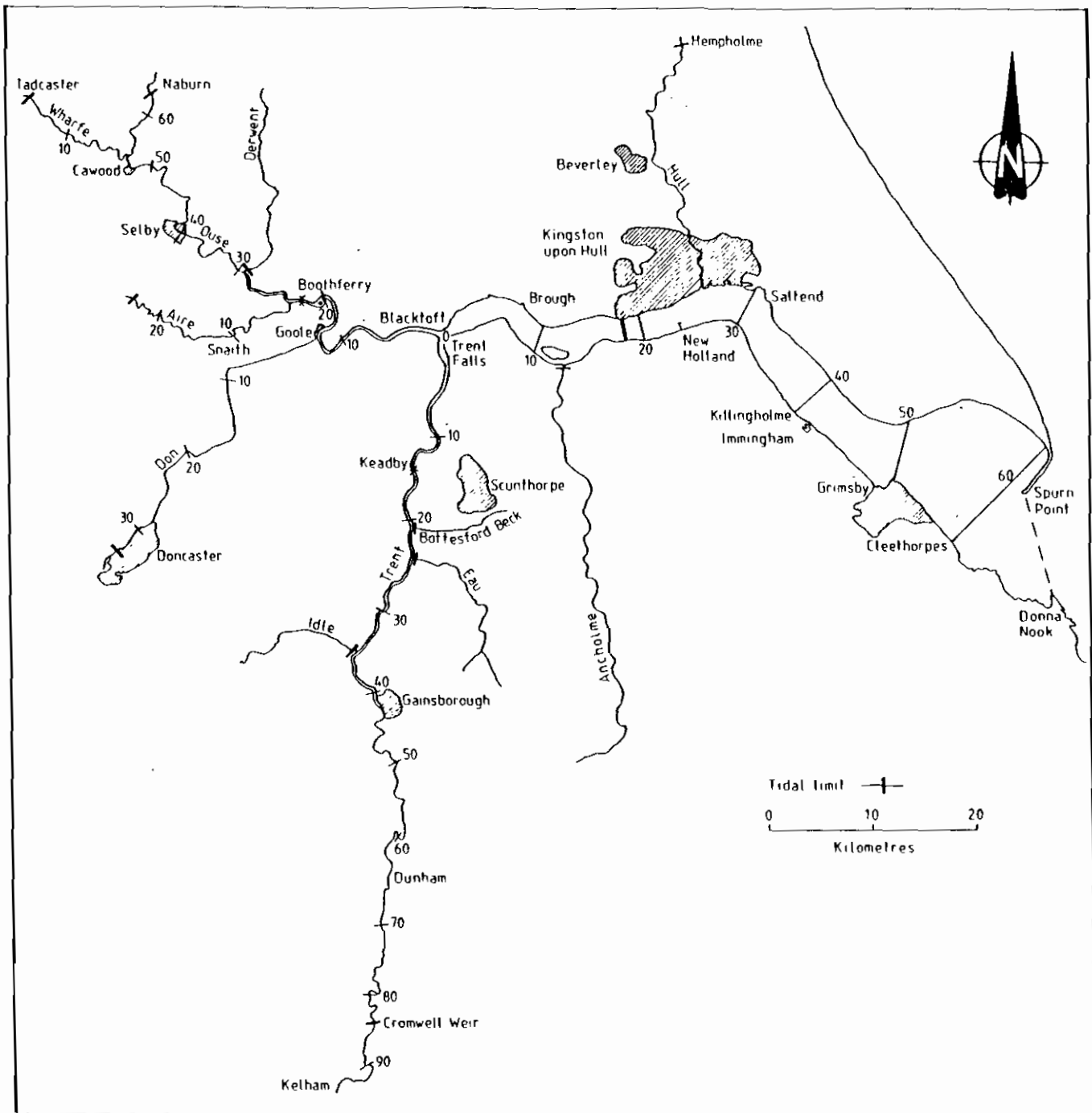


Fig. 2. The Humber Estuary; numbers are kilometres from Trent Falls (Kingston upon Hull is referred to as Hull in text)

Grimsby, Immingham, Hull, and Goole, as well as to private wharves and jetties and to the Aire-Calder and Don canal systems. The Trent is navigable up to Nottingham, over 30 km beyond the tidal limit. Use is made of the estuary as a source of water: six power stations on the tidal rivers and a number of other industrial concerns are licensed to abstract water for cooling purposes, and water is transferred from the tidal Trent to augment the flow in the Ancholme for the benefit of industrial users. There is no abstraction for potable supply, but the barrage across the mouth of the Derwent was constructed as part of a scheme to abstract water for public supply from what, until 1975, had been the tidal portion of the river.

Much greater use is made of the estuary as a recipient for sewage and industrial waste discharges, and it is with the effect of these on the water quality that this report is primarily concerned. Sewage sludge is dumped

some 27 km seaward of Spurn Point and solids dredged from navigation channels are dumped in the Hull-Immingham region. A feasibility study is in progress to reclaim Pyewipe Flats, Grimsby, with colliery spoil and pulverised fuel ash.

The seaside resort of Cleethorpes is the only area within the estuary which is physically suited for bathing. Other recreational uses of the estuary are rather limited, as it is generally considered to be potentially dangerous to small craft because of the strong tides and the presence of commercial craft. The tidal waters are silty, and access to the deep water of the Humber is restricted by mud-flats and partially reclaimed salt-marshes. There are, however, several sailing clubs, and the estuary provides a shelter for pleasure craft using the North Sea and a link with the inland cruising network. A marina is being established in the Old Town docks of Hull. The Humber Bridge, completed in 1981,



APPENDIX G

1-D FIXED ELEMENT MODEL  
WITH PARTICULATE POLLUTANTS  
EXTRACT FROM  
HYDRAULICS RESEARCH LTD  
REPORTS IT 207 and 267



## OXYGEN BALANCE

The model simulates the interactions between the following twelve water quality parameters:

- slow dissolved carbonaceous bio-chemical oxygen demand (CSB);
- fast dissolved carbonaceous bio-chemical oxygen demand (CFB);
- slow organic nitrogen (CSN);
- fast organic nitrogen (CFN);
- ammoniacal nitrogen (CAM);
- nitrate nitrogen (CON);
- dissolved oxygen (CDO)
- salinity (CS);
- temperature (TM);
- suspended solids (inert particulates) (CMUD)
- fast particulate bio-chemical oxygen demand (CFBMUD);
- slow particulate bio-chemical oxygen demand (CSBMUD);

The temperature in each element is used to determine the rates of reactions, and temperature and salinity are used to determine the saturation concentration of dissolved oxygen using Fox's equation.

The interaction between the water quality variables are shown in Fig 1. Organic nitrogen hydrolyses to ammoniacal nitrogen, if there is an oxygen concentration of at least 5% of saturation, then the ammoniacal nitrogen is oxidised to nitrate. The carbonaceous material (BOD) is oxidised using dissolved oxygen provided that oxygen concentrations are greater than 5% saturation. Below this level of dissolved oxygen, nitrate is utilised to provide the necessary oxygen. If there is no nitrate (or insufficient to satisfy all the demand) oxygen is obtained by the reduction of sulphates producing the malodorous gas hydrogen sulphide (the model keeps a log of oxygen obtained in this way as an indicator of anaerobic conditions). The particulate BOD settles at a rate which is dependent on the amount of suspended solids. Particulate organic matter on the bed continues to oxidise, exerting an oxygen demand on the water in the element above.

The use of two components of organic nitrogen and carbon is based on studies which have shown that the rate of oxidation of organic matter, in fresh and saline water, is best represented by a composite

exponential. It is assumed that the organic matter being oxidised consists of several components which are oxidised independently at different rates. Studies by the Water Research Centre (WRC) at Stevenage, indicate that the oxidation of a wide range of organic wastes can be adequately represented by the use of two rate constants, one being one-fifth the value of the other, so that

$$y = E_c [1 - ((1 - p)e^{-kt} + pe^{-kt/5})] \quad (1)$$

where  $y$  is the uptake of oxygen in the time  $t$   
 $k$  is the standard (fast) rate constant;  
 $p$  is the proportion of organic material considered to be oxidised at the slower rate

$E_c$  is the ultimate oxygen uptake, that is the amount of oxygen consumed during the total oxidation of the substance.

The usual BOD determination is over a period of five days so that the value obtained needs to be adjusted to give the ultimate demand. If  $B$  is the five day BOD at  $20^{\circ}\text{C}$  then  $E_c$  is defined as

$$E_c = \lambda B \quad (2)$$

where  $\lambda$  is a constant.

The fast rate constant for carbonaceous material at  $20^{\circ}\text{C}$  is usually taken to be 0.23 per day. Substituting  $y = B$ ,  $t = 5$  and  $k = 0.23 \text{ d}^{-1}$  in equation (2) gives

$$\lambda = \frac{1}{0.69 - 0.48p} \quad (3)$$

In the case of untreated and settled sewage  $p = 0$  so that the appropriate value of  $\lambda$  is 1.45. The rate constants for the reactions in the water quality part of the model are functions of water temperature and are prescribed by equations of the form

$$k_T = k_{20} \left(1 + \frac{\alpha}{100}\right)^{T-20} \quad (4)$$

where  $k_T$  is the value of the constant at  $T^{\circ}\text{C}$

$k_{20}$  is the value of the constant at 20<sup>0</sup>C  
 and  $\alpha$  is the temperature coefficient.

The source-sink term associated with each reaction is of the form

K.V.C

where K is the first order decay rate (s<sup>-1</sup>)  
 V is the element volume  
 C is the concentration of substance

The rate constants for each of the processes simulated in the model are given below. The values of  $k_{20}$  and  $\alpha$  for each process are based on work done at WRC.

The reaction rates for the decay of organic nitrogen and carbon are identical and are prescribed as a function of water temperature as

$$K_{FB} = K_{FN} = 0.23 (1.047)^{T-20} \text{ (day}^{-1}\text{)} \quad (5)$$

$$K_{SB} = K_{SN} = 0.046 (1.047)^{T-20} \text{ (day}^{-1}\text{)} \quad (6)$$

where T is the water temperature in <sup>0</sup>C.

The reaction rate for the decay of ammoniacal nitrogen is

$$K_{AM} = 0.3 (1.047)^{T-20} \text{ (day}^{-1}\text{)} \quad (7)$$

Nitrification of ammonia can only occur when the dissolved oxygen concentration is greater than 5% of the saturated value so the source-sink term has the form

$$\sum S = K_{FN} \cdot V \cdot C_{FN} + K_{SN} \cdot V \cdot C_{SN} - H_1(DO) \cdot K_{AM} \cdot V \cdot C_{AM} \quad (8)$$

where  $H_1(DO) = 1$  if DO is greater than 5%  
 $H_1(DO) = 0$  if DO is less than 5%

If there is insufficient dissolved oxygen to satisfy the carbonaceous oxygen demand then sufficient nitrate is reduced to satisfy the demand. The source-sink term for nitrate is of the form

$$\sum S = H_1 (DO) \cdot K_{AM} \cdot V \cdot C_{AM} - D_B \quad (9)$$

where  $D_B$  is the reduction of nitrates needed to satisfy the oxygen demand when dissolved oxygen levels are less than 5% saturation.

Dissolved oxygen is used in the oxidation of carbonaceous material and in the nitrification of ammonia and is added to the system through reaeration at the water surface. The reaeration rate is

$$K_A = f \frac{A}{V} (1.016)^{T-20} \quad (10)$$

where  $A$  is the plan area of the surface of the element  
 $V$  is the element of volume  
 $f$  is the exchange coefficient for oxygen which has a value of the order of 0.05 m/hour, although this value does vary with the wind speed.

The source-sink term for dissolved oxygen is of the form

$$\begin{aligned} \sum S = K_A \cdot V \cdot DOD - H_2 (DO) \cdot V \cdot (K_{FB} \cdot C_{FB} + K_{SB} \cdot C_{SB}) \\ - 4.57 H_1 (DO) \cdot V \cdot K_{AM} \cdot C_{AM} \end{aligned} \quad (11)$$

where  $H_2 (DO)$  controls the consumption of dissolved oxygen in the oxidation of carbonaceous material  
 $4.57$  is the mass of oxygen consumed in the oxidation of a unit mass of ammonia  
 $DOD$  is the deficit of dissolved oxygen, the amount of oxygen needed to fully saturate the unit mass of water

$$DOD = DOS - DO$$

where  $DOS$  is the saturation concentration of oxygen as calculated from Fox's equation

$$\text{DOS} = 0.00143 \left[ (10.291 - 0.2809 T + 0.006009 T^2 - 0.0000632 T^3) \right. \\ \left. - 0.607 (0.1161 - 0.003922 T + 0.0000631 T^2) S \right] \quad (12)$$

where T is the water temperature in  $^{\circ}\text{C}$

S is salinity ( $\text{kg}/\text{m}^3$ )

#### MUD TRANSPORT

In turbid estuaries it is often necessary to distinguish between pollutants in dissolved and particulate forms. Particulate pollutants are transported, deposited and re-eroded along with natural suspended solids and may remain in an estuary for considerably longer periods than dissolved pollutants. In order to simulate the effect of particulate pollutants, it is necessary to model mud transport in some detail.

There are several time scales and cycles of erosion transport and deposition of mud in turbid estuaries. Seasonal movements of mud depend on the variation of fluvial discharges throughout the year.

Mud transport can also vary significantly during a neap spring cycle. Tidal currents during neap tides are often not large enough to scour and transport significant quantities of mud in suspension. The scouring and transporting capacity of tidal flows can increase rapidly with increasing tidal range so that during spring tides large quantities of mud may be eroded and transported.

The third important cycle of mud transport in an estuary is the semi-diurnal cycle during spring tides. Large quantities of mud may be scoured into suspension by strong tidal currents of the rising tide. During the high water period, the mud in suspension starts to settle. If the mud concentrations are sufficiently high a layer of fluid mud may form on the bed. When the tide turns, there soon becomes a point when the stress in the fluid mud exceeds the critical shear strength of the mud, causing the whole mass to move seaward in suspension. When the fluid mud layer is re-suspended, it can cause a sudden increase in the BOD loading in the over-flowing water, especially if there is a significant oxygen deficit in the mud.

In order to take full account of this phenomenon, the model incorporates a stagnant bed layer with its own pollutant concentrations. The flux of pollutants between the bed layer and the main channel is calculated as a function of the amount of mud deposited or eroded, no flow is allowed in the bed layer. During the flood tide, the whole of the bed layer is likely to be eroded and all the mud found in suspension.

The method by which mud transport is included in the model is described fully in Reference 1 and further details are not included here.

#### MATHEMATICAL MODEL

The main features of the transport and degradation of pollutants in a well-mixed channel can be simulated by solving the one-dimensional, time-dependent mass balance equations together with the equations for the conservation of mass and momentum. In order to simplify the application of these equations, the channel is divided into a series of storage (continuity) elements which overlap a similar set of flow (conveyance) elements. The flow through each element is then governed by the following partial differential equations

$$w \frac{\partial h}{\partial t} + \frac{\partial Q}{\partial x} - q = 0 \quad (13)$$

$$\frac{\partial Q}{\partial t} + g A \frac{\partial h}{\partial x} + Q \frac{\partial \bar{u}}{\partial x} + \bar{u} \frac{\partial Q}{\partial x} + \frac{\tau_o P}{\rho_o} + \frac{A d g}{2 \rho_o} \frac{\partial p}{\partial x} = 0 \quad (14)$$

$$\frac{\partial}{\partial t} (AC) + \frac{\partial}{\partial x} (QC) - \frac{\partial}{\partial x} (AD \frac{\partial c}{\partial x}) + KAC - F_c - L_c = 0 \quad (15)$$

where  $w$  is the water surface width (m)

$h$  is the water surface height (m)

$Q$  is the discharge into the element ( $m^3/s$ )

$\bar{u}$  is the area mean velocity (m/s)

$A$  is the cross-sectional area of the element ( $m^2$ )

$q$  is the lateral inflow per unit length into the element ( $m^2/s$ )

$\tau_o$  is the bed stress ( $N/m^2$ )

$P$  is the wetted perimeter of the element (m)

- C is the concentration of solute ( $\text{kg/m}^3$ )
- D is the effective coefficient of longitudinal dispersion ( $\text{m}^2/\text{s}$ )
- K is the first order decay rate ( $\text{s}^{-1}$ )
- $F_c$  is the flux of solute between the main flow zone and the mud layer ( $\text{kg/m/s}$ )
- $L_c$  is the loading of solutes from lateral inflows per unit length ( $\text{kg/m/s}$ )

The equations are solved using finite difference techniques as described in IT 267.

#### APPLICATION OF THE MODEL

The model was used to simulate the oxygen balance of the River Parrett (Fig 2) estuary in Somerset (Ref 2). The estuary has a strongly semi-diurnal tide with a spring tide range of 13m at its mouth, one of the highest in the UK. The depth of water in the lower and middle estuary at low water spring tides is about 1m, so that there is a large tidal range to depth ratio. This results in strong shallow water effects, the tide is highly distorted with a rapidly rising flood tide forming a small tidal bore.

#### Representation of the estuary

The volume of water contained in the estuary at low water is only a few per cent of that at high water. The model was therefore extended 16km seaward of the mouth of the estuary at Stert Point to contain the tidal volume of the estuary within the calculation.

For the purposes of the numerical model, the estuary was divided into three reaches - downstream of the confluence at Burrow Bridge, the River Parrett, upstream of the confluence, and the tidal tributary River Tone. The channel network was divided into fifty-five, 1km long continuity elements, overlapping with an equal number of flow elements of the same length. At the seaward limit of the model a tide curve was prescribed using tidal harmonic constants interpolated from those for Watchet, Weston-Super-Mare, Barry and Flatholm. The concentration of suspended solids at the seaward boundary was calculated as the sum of two tidal components,  $M_2$  and  $S_2$ , this ensured that the concentrations

The modified scheme prevents the separation of the two solutions. It is important that the odd time step solution is then considered as an intermediate solution, any transport calculations are only carried out at even time steps.

### 3.3 Salinity and mud

The mass balance equations for an arbitrary substance are solved using the six point implicit finite difference scheme operating only on the even time steps:

$$\frac{\partial}{\partial t} (AC) = \frac{A_1^+ C_1^+ - A_1^- C_1^-}{2\Delta t} \quad (35)$$

$$\begin{aligned} \frac{\partial}{\partial x} (QC) = & \frac{1}{2\Delta x_{u_{1-1}}} [Q_1^+ ((1-\theta) C_1^+ + \theta C_{1-1}^+) + Q_1^- ((1-\theta) C_1^- + \theta C_{1+1}^-)] \\ & - Q_{1-1}^- ((1-\theta) C_{1-1}^- + \theta C_1^-) - Q_{1-1}^+ ((1-\theta) C_{1-1}^+ + \theta C_1^+) \end{aligned} \quad (36)$$

$$\begin{aligned} \frac{\partial}{\partial x} (AD \frac{\partial C}{\partial x}) = & \frac{1}{2\Delta x_{u_{1-1}}} ([\frac{AD}{\Delta x_h}]_1^+ (C_{1+1}^+ - C_1^+) + [\frac{AD}{\Delta x_h}]_1^- (C_{1+1}^- - C_1^-)) \\ & - [\frac{AD}{\Delta x_h}]_{1-1}^+ (C_1^+ - C_{1-1}^+) - [\frac{AD}{\Delta x_h}]_{1-1}^- (C_1^- - C_{1-1}^-) \end{aligned} \quad (37)$$

where  $\theta$  is a weighting factor allowing the advective term to be based on upstream concentration,  $0.5 < \theta < 1$ .  $\theta = 0.5$  is equivalent to centre differencing,  $\theta = 1.0$  is equivalent to fully upstream differencing. The use of centred differencing where the concentration gradient is steep can give rise of oscillations in concentration gradients. The use of upstream differencing smooths out these oscillations but the off centering of the space derivative introduces numerical diffusion which could swamp the physical dispersion.

Substituting the finite difference approximations into equation (8) and re-arranging gives:

$$a_1 C_{1-1}^+ + b_1 C_1^+ + c_1 C_{1+1}^+ = d_1 C_{1-1}^- + e_1 C_1^- + f_1 C_{1-1}^- + g_1 \quad (38)$$

Define

$$\beta_1 = \frac{\Delta x_{u_{1-1}}}{\Delta t} \quad (39)$$

$$\delta_1^\pm = \left[ \frac{AD}{\Delta x_h} \right]_1^\pm \quad (40)$$

then

$$a_1 = \alpha_1 A_{1-1}^+ - (1 - \theta) Q_{1-1}^+ - \delta_{1-1}^+ \quad (41)$$

$$b_1 = \beta_1 A_1^+ + (1 - \theta) Q_1^+ - \theta Q_{1-1}^+ + \delta_1^+ + \delta_{1-1}^+ \quad (42)$$

$$c_1 = \gamma_1 A_{1+1}^+ + \theta Q_1^+ + \delta_{1-1}^- \quad (43)$$

$$d_1 = \alpha_1 A_{1-1}^- + (1 - \theta) Q_{1-1}^- + \delta_{1-1}^- \quad (44)$$

$$e_1 = \beta_1 A_1^- + \theta Q_{1-1}^- - (1 - \theta) Q_1^- - \delta_1^- - \delta_{1-1}^- \quad (45)$$

$$f_1 = \gamma_1 A_{1+1}^- - \theta Q_1^- + \delta_1^- \quad (46)$$

$$g_1 = 2L c_1 \quad (47)$$

where  $\alpha_1$  and  $\gamma_1 = 0$  for the difference scheme described but are included to facilitate the use of other finite difference schemes, eg. Brian and Stone.

The tri-diagonal system equations defined by equation (38) is solved using recurrence relationships and sweeps along the reaches in a similar manner to which the flow equations are solved.

For a forward sweep along a reach the recurrence relationship used is:

$$C_{1-1}^+ = p_{1-1} + q_{1-1} C_1^+ + r_{1-1} C_{1s}^+ \quad (48)$$

Substituting into (38) and re-arranging gives:

$$C_1^+ = \frac{RI_1 - a_1 p_{1-1} - c_1 C_{1+1}^+ - a_1 r_{1-1} C_{1s}^+}{b_1 + a_1 q_{1-1}} \quad (49)$$

Where  $RI_1 = d_1 C_{1-1}^- + e_1 C_1^- + f_1 C_{1+1}^- + g_1$

so that for a forward sweep

$$p_i = \frac{RI_i - a_i p_{i-1}}{b_i + a_i q_{i-1}}, \quad q_i = \frac{-c_i}{b_i + a_i q_{i-1}}, \quad r_i = \frac{-a_i r_{i-1}}{b_i + a_i q_{i-1}} \quad (50)$$

For a backward sweep the recurrence relationship is

$$C_{i+1}^+ = p_{i+1} + q_{i+1} C_i^+ + r_{i+1} C_{1ee}^+ \quad (51)$$

Substitution into (38) and rearranging gives

$$C_i^+ = \frac{RI_i - c_i p_{i+1} - a_i C_{i-1}^+ - c_i r_{i+1} C_{1ee}^+}{b_i + c_i q_{i+1}} \quad (52)$$

so that for a backward sweep

$$p_i = \frac{RI_i - c_i p_{i+1}}{b_i + c_i q_{i+1}}, \quad q_i = \frac{-q_{i+1}}{b_i + c_i q_{i+1}}, \quad r_i = \frac{-c_i r_{i+1}}{b_i + c_i q_{i+1}} \quad (53)$$

Where a number of substances are modelled simultaneously the values of  $q_i$  and  $r_i$  are common to all the substances, the values of  $p_i$  are different for each substance as they include loadings.

At a junction the mass balance equation gives:

$$\begin{aligned} \frac{\Delta x_j}{2\Delta t} (A_j^+ C_j^+ - A_j^- C_j^-) &= \sum_1^s \left[ \frac{Q_{1e}^+}{2} ((1-\theta)C_{1e}^+ + \theta C_j^+) + \frac{Q_{1e}^-}{2} ((1-\theta)C_{1e}^- + \theta C_j^-) \right] \\ &- \sum_1^j \left[ \frac{Q_{1s}^+}{2} (\theta C_{1s+1}^+ + (1-\theta)C_j^+) + \frac{Q_{1s}^-}{2} (\theta C_{1s+1}^- + (1-\theta)C_j^-) \right] \\ &+ \sum_1^s \left[ \frac{\delta_{1e}^+}{2} (C_{1e}^+ - C_j^+) + \frac{\delta_{1e}^-}{2} (C_{1e}^- - C_j^-) \right] \\ &+ \sum_1^j \left[ \frac{\delta_{1s}^+}{2} (C_{1s+1}^+ - C_j^+) + \frac{\delta_{1s}^-}{2} (C_{1s+1}^- - C_j^-) \right] \\ &+ L_c \end{aligned} \quad (54)$$

Substituting for  $C_{1e}^+$  and  $C_{1s+1}^+$  from the relevant recurrence relationships gives:

$$\begin{aligned}
\frac{\Delta x_j}{\Delta t} A_j^+ C_j^+ &= \frac{\Delta x_j}{\Delta t} A_j^- C_j^- + \sum_1^s [Q_{ie}^+ ((1-\theta)(p_{ie} + q_{ie} C_j^+ + r_{ie} C_{is}^+) + \theta C_j^+)] \\
&+ \sum_1^s [Q_{ie}^- ((1-\theta)C_{ie}^- + \theta C_j^-)] \\
&- \sum_1^j [Q_{is}^+ (\theta(p_{is+1} + q_{is+1} C_j^+ + r_{is+1} C_{iee}^+) + (1-\theta)C_j^+)] \\
&- \sum_1^j [Q_{is}^- (\theta C_{is+1}^- + (1-\theta)C_j^-)] \\
&+ \sum_1^s [\delta_{ie}^+ (p_{ie} + q_{ie} C_j^+ + r_{ie} C_{is}^+ - C_j^+) + \delta_{ie}^- (C_{ie}^- - C_j^-)] \\
&+ \sum_1^j [\delta_{is}^+ (p_{is+1} + q_{is+1} C_j^+ + r_{is+1} C_{iee}^+ - C_j^+) + \delta_{is}^- (C_{is+1}^- - C_j^-)] \\
&+ 2 L_c
\end{aligned} \tag{55}$$

collecting up terms gives:

$$\begin{aligned}
C_j^+ \left( \frac{\Delta x_j}{\Delta t} A_j^+ - \sum_1^s [Q_{ie}^+ ((1-\theta)q_{ie} + \theta) - \delta_{ie}^+ (1 - q_{ie})] \right) \\
+ \sum_1^j [Q_{is}^+ (\theta q_{is+1} + (1-\theta)) + \delta_{is}^+ (1 - q_{is+1})] \\
- \sum_1^s C_{is}^+ [Q_{ie}^+ (1-\theta) + \delta_{ie}^+] r_{ie} \\
+ \sum_1^j C_{iee}^+ [Q_{is}^+ \theta - \delta_{is}^+] r_{is+1} \\
= \frac{\Delta x_j}{\Delta t} A_j^- C_j^- + \sum_1^s [Q_{ie}^+ (1-\theta) + \delta_{ie}^+] p_{ie} - \sum_1^j [Q_{is}^+ \theta - \delta_{is}^+] p_{is+1} \\
+ \sum_1^s [Q_{ie}^- ((1-\theta)C_{ie}^- + \theta C_j^-) + \delta_{ie}^- (C_{ie}^- - C_j^-)] \\
- \sum_1^j [Q_{is}^- (\theta C_{is+1}^- + (1-\theta) C_j^-) - \delta_{is}^- (C_{is+1}^- - C_j^-)] \\
+ 2 L_c
\end{aligned} \tag{56}$$

As in the case of the flow equations the matrix coefficients for the junction equations are built up sweep by sweep. When all the necessary sweeps have been completed the resultant junction matrix equation:

$$M.C = B$$

is solved using standard matrix techniques to give the substance concentrations at all the junctions. Sweeps along the reaches using the calculated recurrence coefficients complete the calculation.

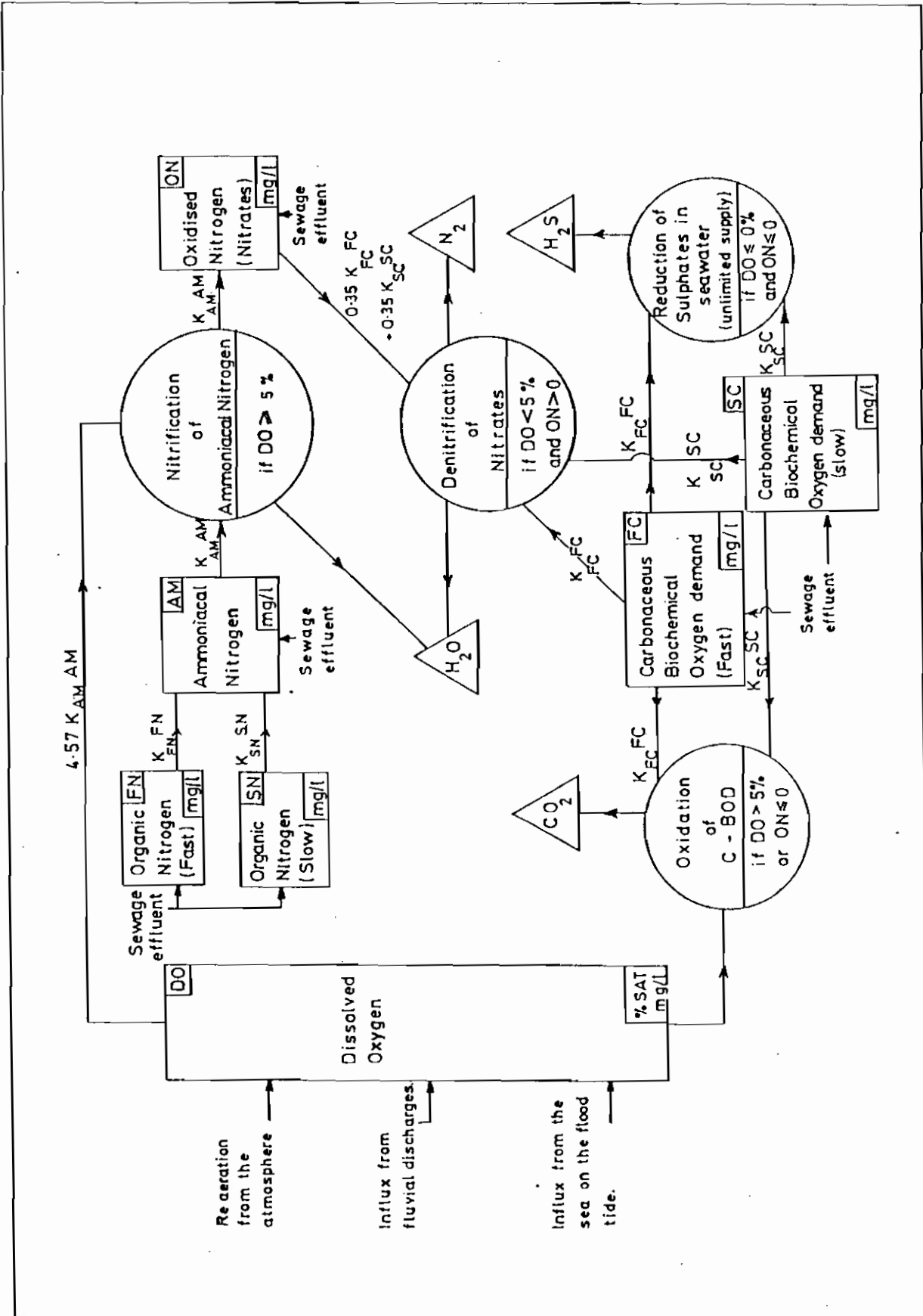
### 3.4 Deposition and erosion of mud

The deposition and erosion of mud is taken into account in the mass balance equation by the term  $F_c$ . Deposition and erosion are governed by the bed shear stress

$$\tau_D = \frac{\rho g}{8} |u|u f_{bed}$$

where  $F_{bed}$  is the overall friction factor, which for an effectively smooth mud bed has a value of about 0.008.

The deposition or erosion is governed by the relative magnitude of  $\tau_b$  in relation to the critical shears for erosion and deposition. The rate of deposition or erosion is calculated according to the theory described earlier.



Water quality interactions



APPENDIX H

2-D IN-DEPTH MODEL  
EXTRACT FROM  
IMPERIAL CHEMICAL INDUSTRIES  
PAPER TO  
WPRL TECH PAPER 13

Hobbs, G D and Fawsewt A. Two-dimensional  
Estuarine Models. Proceedings Sym on  
Mathematical and Hydraulic Modelling of  
estuarine pollution. WPRL, April 1972.



# Two-dimensional Estuarine Models

*Imperial Chemical Industries, Ltd, Petrochemicals Division, Billingham*

This paper describes a class of two-dimensional mathematical models for the investigation of water quality in estuaries of the partially mixed or stratified type<sup>1</sup>. In such estuaries the vertical and longitudinal variations of relevant water-quality parameters are of comparable magnitude, but transverse variations are small. Salt-wedge or fjord-type estuaries fall into this category but, because the model equations are solved by finite-difference methods and an excessively fine vertical grid would be required to resolve the interface, their study by this class of model is not advocated.

The models are particularly suitable for estuaries which are sufficiently narrow for the time taken for an effluent to mix across the width to be short compared with its time of residence within the estuary, and in which bends or Coriolis forces do not induce gross asymmetries. There should be a single, well defined, but not necessarily regular, channel and no extensive tidal mud flats. Subject to these conditions the shape of the estuary can be arbitrary.

The models are dynamic in that tidal motion is taken into account explicitly. Such models are particularly valuable when effluent or tracer discharges are time-dependent or when the residence time of a pollutant is comparable with the tidal period. The latter condition can arise when outfalls are within one or two tidal excursions of the estuary mouth.

The models are based on the hydrodynamic equation of continuity<sup>1,2</sup> (a statement of mass balance) and are therefore deterministic in character. The greater flexibility and range of applications achievable with this type of model give it important advantages over the alternative statistical type based on regression analysis.

For each water-quality parameter of interest (e.g. BOD, dissolved oxygen, temperature, salinity) one mass-balance equation must be specified. The resulting set of equations will be coupled in various ways, the main coupling being due to biochemical interactions.

A water-quality model can conveniently be considered to be a synthesis of two sub-models—the hydrodynamic and the biochemical. The hydrodynamic sub-model determines where a substance goes after its discharge to, or solution in, the estuary water. Its complexity is strongly dependent on the channel shape (the hydrography) and the number of dimensions being considered. The biochemical sub-model determines the fate of the substance during its journey. Since its form is little different in one or two dimensions and since other papers at the Symposium<sup>3-5</sup> discuss in detail its most important aspect, the oxygen balance, the biochemical sub-model will not be described further in this paper.

The hydrodynamic basis of the models is first described. The equations are then formulated mathematically and methods outlined for calculating the advective and diffusive transport, after which a finite-difference solution method for use when advection is the dominant transport mechanism is described. Finally, verification against field data is discussed.

## The hydrodynamic basis

The processes by which dissolved substances are transported from point to point can be classified under two headings: advection—motion with the mean water velocity; and diffusion—motion relative to the mean water velocity.

### Advection

The net advective motion can be divided into periodic and drift components. The periodic motion is a direct consequence of the tides. It includes the semidiurnal and neap/spring effects<sup>1</sup> and in general is not sinusoidal. The integrated flow through any transverse cross-section is directly related to the volume changes induced by the rise and fall of the water surface and is completely determined once the hydrography and the tidal wave characteristics are specified. The vertical and transverse variations of this flow will not be so determined and must be computed from momentum-balance considerations or specified empirically. The models described here make use of empirical distributions.

The drift component is defined as the residual velocity field after the subtraction of the periodic component. It consists of (1) the fresh-water flow, which may be distributed in a non-uniform manner over the cross-section, the predominant variation being with depth, (2) the densimetric (or gravitational) circulation driven by salinity and temperature induced density gradients, and (3) the 'hydrographic' circulation, induced by major irregularities in the channel shape. The net drift integrated over a transverse cross-section will equal the fresh-water flow, but again its distribution over the cross-section

must be either calculated or established empirically. The specification of the velocity field is discussed in more detail on pp. 130–132.

### Diffusion

The predominant cause of diffusion is turbulence induced by the bulk water motion. It has been shown<sup>2,6,7</sup> that mass transport due to turbulent fluctuations can be represented by a Fickian diffusion coefficient  $K$ . This coefficient depends on position and time, its magnitude being related to velocity shear and an appropriate mixing length<sup>2,8</sup>. The shear depends on the tidal characteristics, channel roughness, etc.; the mixing length on river depth, width, and a characteristic eddy size. In near-surface layers wind and wave-induced turbulence may also make a significant contribution to the diffusive transport<sup>8</sup>. At intermediate depths vertical diffusion can be inhibited by stratification<sup>8–10</sup>, energy being extracted from the turbulence in order to lift material from regions of high to regions of low density.

The mathematical representation of the turbulent diffusion process in two-dimensions is discussed in more detail on pp. 132–133.

### Sources

Included under this heading are all sources external to the channel which contribute to the material balance. For each pollutant of interest there must be a specification of the load (mass per unit time) and the position of its discharge in the channel. In general an effluent carries with it water, oxygen, salt, and heat, each of which contributes a source in the relevant equation. If a warm, low-salinity effluent is discharged through an outfall at fixed depth into relatively cold, saline estuary water it may be best represented as being discharged directly into a surface layer.

A major source of oxygen is that diffusing through the water surface. The rate of reaeration depends on temperature and on the deviation of the oxygen concentration from the local saturation value, itself depending on temperature and salinity. Similarly heat passes through the water surface due to convective heat transfer and solar radiation. In the models described the rates of oxygen and heat addition are computed from the surface conditions and then 'discharged' into a thin surface layer in a way similar to that of other buoyant effluents. The consumption of oxygen by mud respiration can be accommodated in an analogous manner, as a negative source discharging into a thin bottom layer.

## Mathematical formulation

### Hydrography

Cartesian coordinates are chosen with  $x$  directed seawards along the axis of the river channel,  $y$  directed vertically upwards, and  $z$  directed across the channel. The depth of the river bed below datum ( $y = 0$ ), defined relative to the deepest point in the transverse cross-section, is specified by the function  $y_b(x)$ , while the height of the water surface above datum is defined by  $y_s(x, t)$ —see Fig. 1. The total water depth  $h(x, t)$  is  $y_s + y_b$ . The function  $y_s(x, t)$  describes the surface elevation resulting from the combined effects of tidal wave propagation and fresh-water flow and is assumed known. The landward ( $x = 0$ ) and seaward ( $x = L$ ) extremities of the channel are vertical planes chosen at convenient positions along the estuary. The transverse cross-section is defined in terms of the width  $w(x, y)$ .

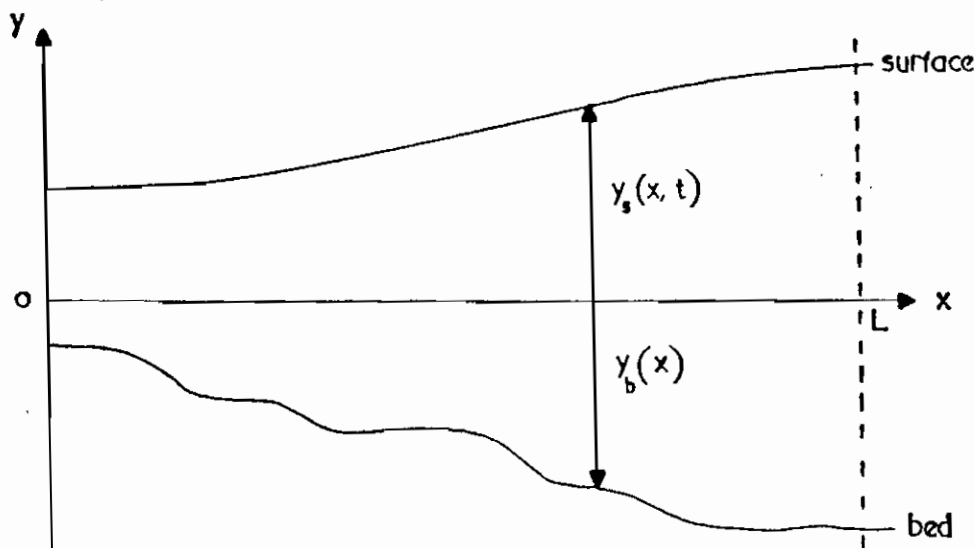


FIG. 1. An axial cross-section of an estuary

### Mass balance

When averaged over the width of the channel, the mass-balance equation describing the distribution of a substance dissolved in the turbulently flowing water is<sup>6,7</sup>:

$$\begin{aligned} \frac{\partial}{\partial t} \int_w c \, dz &= -\frac{\partial}{\partial x} \int_w uc \, dz - \frac{\partial}{\partial y} \int_w vc \, dz + \\ &+ \frac{\partial}{\partial x} \int_w K_x \frac{\partial c}{\partial x} \, dz + \frac{\partial}{\partial y} \int_w K_y \frac{\partial c}{\partial y} \, dz + \\ &+ \left( \frac{\partial}{\partial t} \int_w c \, dz \right)_1 + \left( \frac{\partial}{\partial t} \int_w c \, dz \right)_2, \end{aligned} \quad (1)$$

where  $c(x, y, z, t)$  is the concentration,  $u$  and  $v$  are the longitudinal and vertical water velocities (averaged over turbulent fluctuations),  $K_x$  and  $K_y$  are the longitudinal and vertical turbulent diffusion coefficients, and the last two terms represent the time rate of change of concentration due to (1) addition of material from external sources and (2) creation of material due to biochemical reactions. One equation of this type is required for each substance of interest.

Small variations in the water density due to dissolved solids (e.g. salt) and temperature are ignored. As a consequence of incompressibility,  $u$  and  $v$  must satisfy

$$\frac{\partial}{\partial x} \int_w u \, dz + \frac{\partial}{\partial y} \int_w v \, dz = 0. \quad (2)$$

It has been assumed here that there are no external sources of water. The generalization to take account of tributaries and major outfalls is straightforward.

Writing  $c = \bar{c} + c'$ ,  $u = \bar{u} + u'$ ,  $v = \bar{v} + v'$ , where

$$\bar{c} = \frac{1}{w} \int_w c \, dz,$$

etc., are transverse means and  $c'$ ,  $u'$ ,  $v'$  are deviations from the mean, and assuming  $K_x$  and  $K_y$  to be independent of  $z$  (a good approximation for large width-to-depth ratios), Equations 1 and 2 become

$$\begin{aligned} \frac{\partial}{\partial t} w \bar{c} &= -\frac{\partial}{\partial x} \bar{u} w \bar{c} - \frac{\partial}{\partial y} \bar{v} w \bar{c} + \frac{\partial}{\partial x} K_x w \frac{\partial \bar{c}}{\partial x} + \frac{\partial}{\partial y} K_y w \frac{\partial \bar{c}}{\partial y} - \\ &- \frac{\partial}{\partial x} w \overline{u'c'} - \frac{\partial}{\partial y} w \overline{v'c'} + \left( \frac{\partial}{\partial t} w \bar{c} \right)_1 + \left( \frac{\partial}{\partial t} w \bar{c} \right)_2 \end{aligned} \quad (3)$$

and

$$\frac{\partial}{\partial x} w \bar{u} + \frac{\partial}{\partial y} w \bar{v} = 0. \quad (4)$$

The first two terms on the right-hand side of Equation 3 represent the advective transport of material in the mean velocity field ( $\bar{u}$ ,  $\bar{v}$ ) and the second two the transport due to longitudinal and vertical turbulent diffusion (the form of these terms is correct only if  $c' \ll \bar{c}$ ). The third pair of terms represents the transport due to longitudinal and vertical dispersion<sup>11</sup>, that is mixing in those directions arising from transverse variations in  $u$ ,  $v$ , and  $c$ .

### Advection

In the models described here the longitudinal velocities are specified *a priori* from a combination of experimental information and the constraints implied by Equation 4. Integration of this equation with respect to  $y$  from bed to surface, with respect to  $x$  from the tidal limit  $x_0$  to an arbitrary position  $x$ , and then with respect to time from  $t_n$  to  $t_{n+1}$  gives

$$P(x) = \int_{t_n}^{t_{n+1}} \int_{-y_b(x)}^{y_s(x)} \bar{u} w \, dy \, dt = \int_{t_n}^{t_{n+1}} Q \, dt - \left[ V(x, t_{n+1}) - V(x, t_n) \right], \quad (5)$$

where

$$Q(t) = \int_{-y_b(x_0)}^{y_s(x_0, t)} \bar{u} w \, dy$$

is the fresh-water flow entering the estuary at the tidal limit and

$$V(x, t) = \int_{x_0}^x \int_{-y_b(x')}^{y_s(x', t)} w dy dx'$$

is the volume of water downstream of the tidal limit but upstream of  $x$ .

The quantity  $P(x)$  is the volume of water flowing through the wet cross-section at distance  $x$  in the time interval  $\Delta t = t_{n+1} - t_n$ . It will be assumed for simplicity in the rest of this paper that the water surface elevation  $y_s(x, t)$  is unaffected by fresh-water flow and that  $P$  can be divided into fresh-water and periodic tidal components:

$$P_F^{n+1} = \int_{t_n}^{t_{n+1}} Q dt$$

and

$$P_T^{n+1} = V(x, t_n) - V(x, t_{n+1}).$$

If the hydrography (i.e.  $w$ ,  $y_s$ , and  $y_b$ ) and the fresh-water flow  $Q$  are specified the total volume of water flowing through a particular cross-section during any period is completely determined, the only arbitrariness remaining being the distribution of that flow over the depth. It will be shown later that a finite-difference approximation to Equation 3 can be written in terms of segmented flows  $p_{jk}^{n+1}$ , where

$$p_{jk}^{n+1} = \frac{1}{2\Delta y \Delta t} \int_{t_n}^{t_{n+1}} \int_{y_k - \Delta y}^{y_k + \Delta y} \bar{u} w dy dt \quad (6)$$

and  $\bar{u}$ ,  $w$  are computed at  $x = x_j$  (Fig. 2).

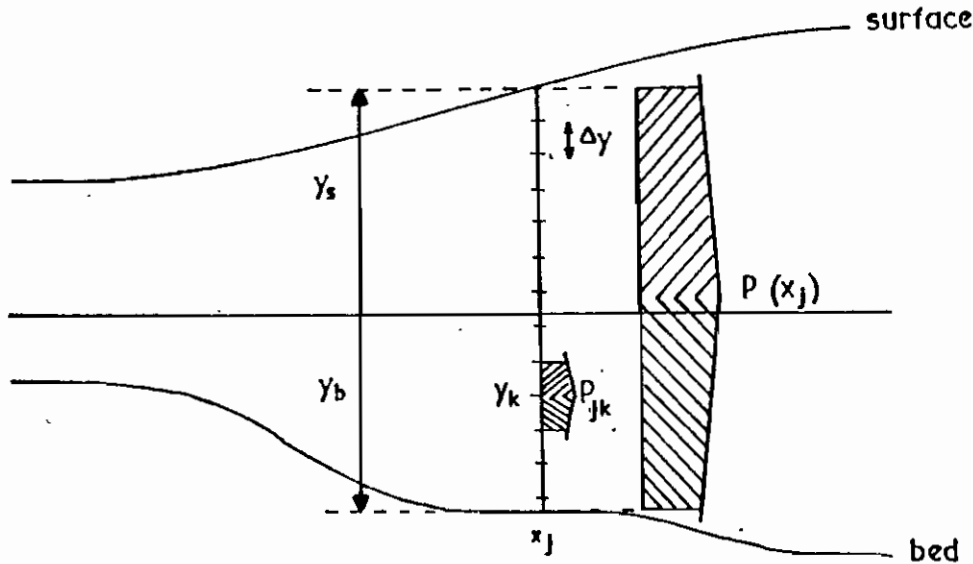


FIG. 2. Illustrating relation between segmented and total flows

It is now assumed that  $p_{jk}^{n+1}$  can be written in the form

$$2\Delta y \Delta t p_{jk}^{n+1} = P_T^{n+1}(x_j) G_T(x_j, y_k, t_{n+1}) + P_F^{n+1}(x_j) G_F(x_j, y_k, t_{n+1}) + G_D(x_j, y_k, t_{n+1}), \quad (7)$$

where the functions  $G$  are defined by

$$G(x, y, t) = \frac{1}{h} \int_{y-\Delta y}^{y+\Delta y} H(x, y', t) dy'. \quad (8)$$

The functions  $H$  can be chosen arbitrarily provided they satisfy the conditions

$$\frac{1}{h} \int_{-y_s}^{y_s} H_T dy = \frac{1}{h} \int_{-y_s}^{y_s} H_F dy = 1$$

and

$$\frac{1}{h} \int_{-y_s}^{y_s} H_D dy = 0.$$

These conditions ensure that the sum of all segmented flows through a given cross-section exactly equals the total flow  $P$ ;  $H_T$ ,  $H_F$ , and  $H_D$  characterize the vertical distribution of tidal, fresh-water, and other drift velocities respectively. In practice  $H_T$ ,  $H_F$ , and  $H_D$  are chosen to be readily integrable analytic functions, each containing a small number of parameters which can be determined by comparison with field data.

With the  $p_{jk}^{n+1}$  specified, the vertical velocities can be determined from Equation 4 which, on integration over a volume  $2\Delta x \cdot 2\Delta y$  centred on  $(x_j, y_k)$  and a time interval  $\Delta t$ , can be written in the form

$$\Delta x(q_{jk+1}^{n+1} - q_{jk-1}^{n+1}) + \Delta y(p_{j+1k}^{n+1} - p_{j-1k}^{n+1}) = 0, \quad (9)$$

where

$$q_{jk}^{n+1} = \frac{1}{2\Delta x \Delta t} \int_{t_n}^{t_{n+1}} \int_{x_j - \Delta x}^{x_j + \Delta x} \bar{v} w \, dx \, dt$$

are vertical segmented flows.

Equation 9 provides a simple recurrence formula for the evaluation of the  $q_{jk}$ . The starting value can be determined by integrating Equation 4 over the volume illustrated in Fig. 3 and applying the boundary condition of zero flow through the water surface. The result is

$$q_{jk-1}^{n+1} = \frac{\Delta y}{\Delta x} \left[ p_{j+1k}^{n+1} - p_{j-1k}^{n+1} \right] + \frac{1}{2\Delta x \Delta t} \left[ V(x_{j+1}, t_{n+1}) - V(x_{j-1}, t_{n+1}) - V(x_{j+1}, t_n) + V(x_{j-1}, t_n) \right], \quad (10)$$

where

$$p_{jk}^{n+1} = \frac{1}{2\Delta y \Delta t} \int_{t_n}^{t_{n+1}} \int_{y_k - \Delta y}^{y_k(x_j, t)} \bar{u}(x_j, y, t) w \, dy \, dt$$

and the second term arises from the change in volume of the segment during the time  $\Delta t$ . The partial segmented flows  $p_{jk}^{n+1}(s)$  can be computed by integrating  $H$  between the same limits, i.e.  $y_k - \Delta y$  to  $y_k(x_j, t)$ .

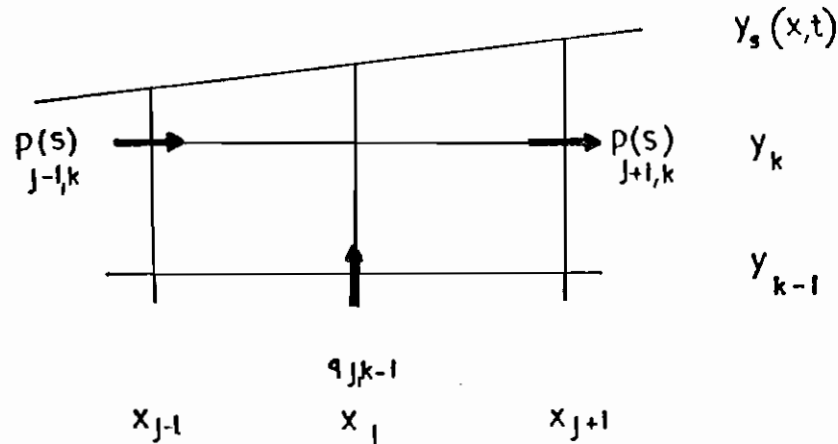


FIG. 3. Water flow through a surface segment

This procedure specifies the total velocity field  $(\bar{u}, \bar{v})$  such that it is an exact solution of Equation 4, exactly satisfies the boundary conditions of zero flux through the estuary bed and surface, can be fitted easily to experimental data, and is in a form convenient for the finite-difference solution of Equation 3.

#### Diffusion and dispersion

The relative magnitudes of the diffusive and dispersive terms in Equation 3 depend on the particular estuary being modelled. In general the longitudinal diffusion is negligible in comparison with the dispersion resulting from the combined effects of advection and vertical or lateral diffusion<sup>11</sup>. It can also be shown that the vertical dispersion term  $\partial(w\bar{v}'c')/\partial y$  is of negligible importance. This leaves two terms of general significance: vertical transport due to turbulent diffusion and longitudinal dispersion due to the deviation from their transverse means of the horizontal velocity and concentration, the latter being dependent on the magnitude of the transverse diffusion coefficient.

Mixing-length arguments can be used<sup>2,8</sup> to express the vertical turbulent diffusion coefficient in the form

$$K_v = \alpha l^2 \left| \frac{\partial \bar{u}}{\partial y} \right|.$$

The 'mixing length'  $l$  is given<sup>8</sup> by

$$l = 0.4 h \frac{(y_b + y)(y_s - y)}{h^2} (1 + \beta Ri)^{-1},$$

where  $\alpha$  and  $\beta$  are empirical constants and  $Ri$  is the Richardson Number

$$Ri = \frac{g}{\rho} \frac{\partial \rho}{\partial y} / \left( \frac{\partial \bar{u}}{\partial y} \right)^2;$$

$\rho$  is the water density and  $g$  the acceleration due to gravity. The factor  $(1 + \beta Ri)^{-1}$  allows for the partial suppression of vertical turbulent fluctuations due to density gradient effects.

In the absence of significant density gradients,  $K_v$  has a depth-mean value of

$$K_v = 0.011 \alpha h U,$$

where  $\partial \bar{u} / \partial y$  has been replaced by  $2U/h$ ,  $U$  being the horizontal velocity at mid-depth averaged over the tidal cycle. An estimate of  $\alpha$  can be obtained by comparing this result with that obtained from other studies<sup>12-14</sup> of turbulent mixing in wide straight channels, where it has been found that

$$K_v = 0.067 h u_s,$$

where  $u_s$ , the shear velocity, can be approximated by

$$u_s = 3.9(n/h^{1/6})U;$$

$n$  is the Manning roughness. Equating the two results gives

$$\alpha = 25(n/h^{1/6}). \quad (11)$$

For many estuaries  $n \simeq 0.035$ , hence  $\alpha = 0.88h^{-1/6}$ , where  $h$  is in feet.

It has been shown<sup>12,15</sup> that the longitudinal dispersion term  $\partial \bar{u}'c' / \partial x$  can be approximated by the introduction of an 'effective longitudinal dispersion coefficient'  $E_x$  where

$$-E_x \frac{\partial \bar{c}}{\partial x} = \overline{u'c'}.$$

In many estuaries  $E_x$  can be estimated<sup>11</sup> from

$$E_x = 0.16 h u_s \left( \frac{UT}{w} \right)^2 \left( \frac{\bar{u}'^2}{\bar{U}^2} \right), \quad (12)$$

where  $T$  is the tidal period. In Equation 12 allowance has been made for the oscillatory nature of the flow and for the fact that  $T \ll w^2/K_v$ , the time for full transverse diffusion. For any particular estuary the applicability of the result should be examined critically taking due note of the assumptions implicit in its original derivation. To obtain numerical values an estimate of  $\bar{u}'^2$  must be obtained from field data.

### Boundary conditions

There can be no flux of material through the river bed or surface. If the velocities are specified as shown on p. 132, this condition is automatically satisfied as far as advection is concerned. Since  $K_v = 0$  at  $y = y_s$  and since, in general, the water surface will not deviate far from the horizontal, the diffusive flux through the water surface is also zero. Similarly, at the bed,  $K_v = E_x = 0$  (since  $\bar{u}'^2 \rightarrow 0$  as  $y \rightarrow -y_b$ ) and again the boundary condition is automatically satisfied.

On the planes  $x = 0$  and  $x = L$  a linear combination of the concentration and longitudinal flux must be specified as a function of  $y$  and  $t$ . If these boundaries can be made sufficiently remote from the region in which concentration gradients are significant, appropriate boundary conditions are  $\bar{c}(0, y, t) = c_0$  and  $\bar{c}(L, y, t) = c_L$ , where  $c_0$  and  $c_L$  are constants. When gradients persist right up to the estuary mouth, special methods may have to be adopted to ensure that realistic boundary conditions are available, e.g.<sup>16</sup>.

### Numerical solution

The numerical methods employed to solve

$$\frac{\partial}{\partial t} w \bar{c} = -\frac{\partial}{\partial x} \bar{u} w \bar{c} - \frac{\partial}{\partial y} \bar{v} w \bar{c} + \frac{\partial}{\partial x} E_x w \frac{\partial \bar{c}}{\partial x} + \frac{\partial}{\partial y} K_v w \frac{\partial \bar{c}}{\partial y} + \left( \frac{\partial}{\partial t} w \bar{c} \right)_1 + \left( \frac{\partial}{\partial t} w \bar{c} \right)_2 \quad (13)$$

depend on the relative magnitudes of the individual terms. The equation of continuity (4) implies that the two advective terms can be of comparable magnitude and, relative to them, the two source terms

will be small (time scale of days rather than hours). Utilizing the results of the previous section the advection, horizontal dispersion, and vertical diffusion terms will be in the ratios

$$1:3\left(\frac{h}{w}\right)^2\left(\frac{\bar{u}^2}{U^2}\right)\left(\frac{\alpha L}{100h}\right):\left(\frac{\alpha L}{100h}\right).$$

Taking typical values of  $L/h = 200$ ,  $h/w = 10$ ,  $\alpha = 0.05$  and  $\bar{u}^2/U^2 = 0.01$  gives ratios 1:0.3:0.1.

Consistent with this result, the finite-difference method of solution outlined in this paper places the greatest emphasis on the advective terms. If, for a particular application the advection is not clearly dominant, it may be necessary to use more sophisticated methods than those described to represent the dispersion and diffusion terms.

### Advection

Finite-difference methods of representing the advective part of Equation 13 have been discussed in detail by Roberts and Weiss<sup>17</sup>. The methods advocated by them are conservative (no loss or gain of material due to numerical approximation), stable and non-dissipative (amplification matrix of the Fourier modes has unit modulus), and minimally dispersive (only minor inaccuracies in the Fourier mode propagation speeds). The schemes have truncation errors of order  $\Delta x^4$ ,  $\Delta y^4$ , and  $\Delta t^2$  thereby permitting the use of a relatively coarse space net. A rectangular staggered mesh is recommended (Fig. 4) on which variables are computed at points denoted by crosses at integral times  $t_n, t_{n+1}, t_{n+2}$ , etc., and at points denoted by circles at half-integral times  $t_{n+\frac{1}{2}}, t_{n+\frac{3}{2}}$ , etc.

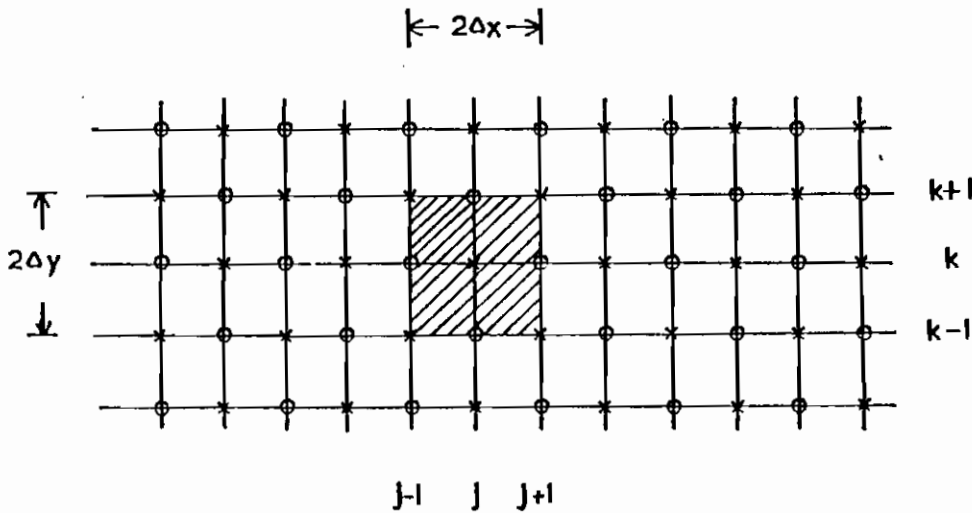


FIG. 4. A rectangular staggered mesh

After integration over an elemental volume  $4\Delta x\Delta y w_{jk}$ , centred on  $(x_j, y_k)$ , and time  $\Delta t$ , the advective part of Equation 13 becomes

$$4\Delta x\Delta y w_{jk}(c_{jk}^{n+1} - c_{jk}^n) = -2\Delta y\Delta t(F_{j+1k}^x - F_{j-1k}^x) - 2\Delta x\Delta t(F_{jk+1}^y - F_{jk-1}^y), \quad (14)$$

where

$$c_{jk}^n = \frac{1}{4\Delta x\Delta y} \int_{x_{j-1}}^{x_{j+1}} \int_{y_{k-1}}^{y_{k+1}} \bar{c}(x, y, t_n) dx dy$$

and

$$F_{jk}^x = \frac{1}{2\Delta y\Delta t} \int_{t_n}^{t_{n+1}} \int_{y_{k-1}}^{y_{k+1}} w(x_j, y) \bar{u}(x_j, y, t) \bar{c}(x_j, y, t) dy dt.$$

$F_{jk}^x$  is the flux of material in the  $x$ -direction flowing through a segment 'wall' in time  $\Delta t$ . There is a similar expression for  $F_{jk}^y$ , the vertical flux, in which  $\bar{u}/\Delta y$  is replaced by  $\bar{v}/\Delta x$  and the space integral is with respect to  $x$ . For simplicity the average width  $w_{jk}$  will be set equal to  $w(x_j, y_k)$ . If  $w$  varies rapidly in space a more sophisticated expression must be used.

The fluxes can now be written

$$F_{jk}^x = c_{jk}^x p_{jk}^{n+\frac{1}{2}} + \frac{1}{48} \left( (c_{jk+\frac{1}{2}}^{n+\frac{1}{2}} - c_{jk-\frac{1}{2}}^{n+\frac{1}{2}}) (p_{jk+\frac{1}{2}}^{n+\frac{1}{2}} - p_{jk-\frac{1}{2}}^{n+\frac{1}{2}}) \right) + O(\Delta t^2) + O(\Delta y^4), \quad (15)$$

where

$$c_{jk}^x = \frac{1}{2\Delta y \Delta t} \int_{t_n}^{t_{n+\frac{1}{2}}} \int_{y_{k-1}}^{y_{k+1}} \bar{c}(x_j, y, t) dy dt$$

and  $p_{jk}^{n+\frac{1}{2}}$  is defined by Equation 6. In terms of the volume average  $c_{jk}^n$ , the 'contracted' average  $c_{jk}^x$  can be written in two alternative forms:

$$c_{jk}^x = \frac{1}{6} \left[ 8c_{jk}^{n+\frac{1}{2}} - (c_{j-1k}^{n+\frac{1}{2}} + c_{j+1k}^{n+\frac{1}{2}}) \right] + O(\Delta y^4) + O(\Delta x \Delta t), \quad (16a)$$

or

$$= \frac{1}{6} \left[ 8c_{jk}^{n+\frac{1}{2}} - (c_{j-1k}^n + c_{j+1k}^n) \right] + O(\Delta y^4) - O(\Delta x \Delta t). \quad (16b)$$

The truncation error  $O(\Delta x \Delta t)$  is the same in both cases and can be reduced to  $O(\Delta x \Delta t^2)$  by using Equations 16a and 16b on alternate time-steps.

Substitution of Equations 15 and 16 into Equation 14 gives an explicit expression for  $c_{jk}^{n+\frac{1}{2}}$  in terms of known concentrations at the previously computed time levels  $n$  and  $n + \frac{1}{2}$ . When Equation 16a is used the mesh is scanned with  $j$  and  $k$  incremented positively; if 16b, the scanning direction is reversed. In order to preserve the non-dissipative properties of the solution the time-step  $\Delta t$  must satisfy

$$-2 \leq \frac{u \Delta t}{\Delta x} + \frac{\bar{v} \Delta t}{\Delta y} \leq \frac{6}{5}.$$

### Diffusion

If, as is assumed here, the diffusion and dispersion terms are sub-dominant, they can be represented by a finite-difference approximation of lower-order accuracy. An explicit unconditionally stable scheme is that of Du Fort and Frankel<sup>17,18</sup>. Integration of the diffusive parts of Equation 13 over an elemental volume  $\Delta x \Delta y w_{jk}$ , centred on  $(x_j, y_k)$ , gives

$$\Delta x \Delta y w_{jk} (c_{jk}^{n+\frac{1}{2}} - c_{jk}^n) = \Delta y \Delta t (D_{j+\frac{1}{2}k}^x - D_{j-\frac{1}{2}k}^x) + \Delta x \Delta t (D_{jk+\frac{1}{2}}^y - D_{jk-\frac{1}{2}}^y). \quad (17)$$

The  $D^x$  and  $D^y$  are diffusive fluxes defined by

$$D_{j+\frac{1}{2}k}^x = \frac{1}{2\Delta x} \left[ (E_{nw})_{j+\frac{1}{2}k}^{n+\frac{1}{2}} (c_{j+1k}^{n+\frac{1}{2}} - c_{jk}^n) + (E_{nw})_{j+\frac{1}{2}k}^n (c_{j+1k}^n - c_{jk}^{n+\frac{1}{2}}) \right], \quad (18a)$$

$$D_{j-\frac{1}{2}k}^x = \frac{1}{2\Delta x} \left[ (E_{nw})_{j-\frac{1}{2}k}^{n+\frac{1}{2}} (c_{jk}^n - c_{j-1k}^{n+\frac{1}{2}}) + (E_{nw})_{j-\frac{1}{2}k}^n (c_{jk}^{n+\frac{1}{2}} - c_{j-1k}^n) \right], \quad (18b)$$

with similar expressions for  $D_{jk+\frac{1}{2}}^y$  and  $D_{jk-\frac{1}{2}}^y$ .

To obtain this result it has been assumed that

$$\frac{1}{\Delta x \Delta y} \int_{x_{j-\frac{1}{2}}}^{x_{j+\frac{1}{2}}} \int_{y_{k-\frac{1}{2}}}^{y_{k+\frac{1}{2}}} \bar{c} dx dy = \frac{1}{4\Delta x \Delta y} \int_{x_{j-1}}^{x_{j+1}} \int_{y_{k-1}}^{y_{k+1}} \bar{c} dx dy = c_{jk}^n. \quad (19)$$

Thus the total change in  $c_{jk}$  over the time interval  $\Delta t$  is

$$(c_{jk}^{n+\frac{1}{2}} - c_{jk}^n) = (c_{jk}^{n+\frac{1}{2}} - c_{jk}^n)_{\text{advection}} + (c_{jk}^{n+\frac{1}{2}} - c_{jk}^n)_{\text{diffusion}}. \quad (20)$$

The advantage of integrating the diffusion terms over  $\Delta x \Delta y$  rather than  $4\Delta x \Delta y$  is that the integral and half-integral grids become tied together. Without this diffusive 'relaxation' the numerical integration would proceed quite independently on the two grids, cumulative rounding errors causing the solutions to drift apart.

### Boundary conditions

For ease of computation it is convenient to continue the solution beyond the boundaries for distances of order  $2\Delta x$  and  $2\Delta y$ , two rows of 'guard points' being introduced to this end. The fourth-order scheme can then be used up to and on the boundary. At the water surface and bed a simpler second-order scheme<sup>17</sup> can be used to determine the solution on the first external mesh line, values on the second line being determined when required by extrapolation.

## Model verification

What has been described in the preceding paragraphs is a theoretical structure. On its own this has only limited value. It can be used as it stands to explore the qualitative behaviour of hypothetical estuaries—the relative importance of longitudinal dispersion and densimetric flow, for example.

The major value of the model lies, however, in its use as a quantitative planning tool—as a tool with which to evaluate alternative effluent-disposal policies. For use in this area the theoretical structure must be supported on a firm foundation of experimental information and field data. And there must be a continuous review and revision of model parameters as additional data become available.

The use of field data to determine the water-velocity distribution has already been mentioned. The magnitude of the turbulent diffusion coefficients is not well known but can be estimated from a comparison of model predictions with field data for biochemically inert substances, such as salt and injected tracers. The biochemical sub-model also contains parameters of uncertain magnitude. These must be determined, perhaps partly from laboratory experiments, since they will not be strongly dependent on geometry, but mainly by comparison of predicted and observed distributions of indicators of biochemical activity, for example dissolved oxygen. For this to be a meaningful exercise there must be available complete and accurate data on the location of waste outfalls and the quantity and quality of the effluents discharged.

## REFERENCES

1. IPPEN, A. T. Estuary and coastline hydrodynamics. McGraw-Hill, New York, 1966.
2. PRANDTL, L. The essentials of fluid dynamics. Blackie, London, 1969.
3. ALABASTER, J. S. Oxygen in estuaries: requirements for fisheries. *This Symposium*, p. 15.
4. OWENS, M. Sources of oxygen in estuaries. *This Symposium*, p. 25.
5. BARRETT, M. J. Utilization of oxygen in estuaries. *This Symposium*, p. 39.
6. PRITCHARD, D. W. The equations of mass continuity and salt continuity in estuaries. *J. mar. Res.*, 1958, 17, 412.
7. OKUBO, A. Equations describing the diffusion of an introduced pollutant in a one-dimensional estuary. In 'Studies on oceanography' (ed. Kozo Yoshida). Hidaka Jubilee Committee, Univ. of Washington Press, 1964, p. 216.
8. KENT, R. E., and PRITCHARD, D. W. A test of mixing length theories in a coastal plain estuary. *J. mar. Res.*, 1959, 18, 62.
9. PRITCHARD, D. W. The movement and mixing of contaminants in tidal estuaries. *Proc. 1st Conf. on Waste Disposal in the Marine Environment*. Pergamon Press, 1959, p. 512.
10. BOWDEN, K. F. Stability effects on turbulent mixing in tidal currents. *Physics Fluids Suppl.* (Boundary Layers and Turbulence), 1967, S.278.
11. FISCHER, H. B. Dispersion in homogeneous estuary flow. *J. hydraul. Div. Am. Soc. civ. Engrs*, 1970, 96, 1691.
12. ELDER, J. W. The dispersion of marked fluid in turbulent shear flow. *J. Fluid Mech.*, 1959, 5, 554.
13. FISCHER, H. B. Dispersion predictions in natural streams. *J. sanit. Engng Div. Am. Soc. civ. Engrs*, 1968, 94 (SA5), 927.
14. SAYRE, W. W., and CHANG, F. M. A laboratory investigation of open channel dispersion processes for dissolved, suspended and floating dispersants. Open File Report. U.S. Geological Survey, Colorado, 1966.
15. TAYLOR, G. I. Dispersion of matter in turbulent flow through a pipe. *Proc. R. Soc., A*, 1954, 223, 446.
16. HOBBS, G. D. The mathematical modelling of a stratified estuary. *Proc. 5th int. Conf. Wat. Pollut. Res., San Francisco & Hawaii, 1970*, Vol. 2, III-8.
17. ROBERTS, K. V., and WEISS, N. O. Convective difference schemes. *Maths Comput.*, 1966, 20, 272.
18. RICHTMYER, R. D., and MORTON, K. W. Difference methods for initial-value problems. Interscience, New York, 2nd Edn, 1967.

---

Mr Hobbs said, in his opening remarks, that there was a wide range of mathematical models available to those wishing to study estuarine pollution, ranging from the very simplest (such as taking the effluent concentration in a river to be given by the ratio of the effluent mass flow to the river flow) to the most complex—based on the multi-dimensional advective-diffusion equation. The type of model chosen had to be matched to the circumstances. The modeller, in making his choice, had to ask what were the objectives of the investigation, how important were the answers (usually in financial terms), and what estuarine processes were going to have significant effects on the predictions. Within the constraints implied by the answers to these questions the model ought to be the simplest possible.



APPENDIX I

3-D SEGMENTED MODEL WITH PHOTOSYTHESIS  
EXTRACT FROM  
HYDRAULICS RESEARCH LTD  
REPORT EX 1274 and EX 1105



## CONTENTS

1. INTRODUCTION
2. MODEL DATA REQUIREMENTS
3. EQUATIONS OF MOTION
4. APPLICATION OF THE TIDE AVERAGED EQUATIONS
5. LONGITUDINAL MIXING
6. VERTICAL MIXING
7. SOLUTION PROCEDURE
8. SCHEMATISATION OF THE LAKE GEOMETRY
9. REFERENCES

## TASGM

### A tide-averaged numerical model of saline intrusion and water balance in lagoon system

#### 1. INTRODUCTION

This report describes the theoretical basis, main assumptions and numerical method employed in TASGM, a three-dimensional tidally-averaged model of gravitational circulation, saline intrusion, thermal and water balance in a lagoon system. The model, which was originally developed to simulate conditions in Tolo harbour, Hong Kong (Ref 1) with prescribed seasonal variations in the water temperature, was modified to simulate evaporation and thermal balance of the North Lakes in Benghazi (Ref 8) and Tunis North Lake (Ref 9).

#### 2. MODEL DATA REQUIREMENTS

In addition to the geometric data and logical data describing the dimensions and positions of the model elements, TASGM requires data specifying the variation of several dynamic parameters during the period of time to be simulated. These parameters are: (i) the rainfall in each segment; (ii) freshwater inflow to each segment; (iii) metrological conditions; (iv) the salinity and water temperature at the seaward boundary and (v) the mean tidal level at the seaward boundary. It is assumed that each of these parameters will be functions of time and that rainfall and freshwater inflow will vary daily; the evaporation rate will vary every 3 hours and boundary salinity, temperature and level will only vary seasonally, if at all. The equations solved in TASGM contain surface wind stress terms and a term describing the evaporation rate.

Initial conditions are also required by TSAGM. This is data specifying the values of velocity, salinity and water level throughout the model area which will be used as the starting point for the model simulation. These initial conditions can be "flat" (i.e. zero velocities and sea salinity everywhere and all water surface levels equal to the boundary value and can be set up automatically by the model) or specified by the user or, since TASGM stores all relevant data at the end of each run, the model can be restarted from the final output from a previous run.

In order to solve these equations for the complex flows encountered in real estuaries it is necessary to make several simplifying assumptions which can be justified for the particular application being considered. In TASGM, as in most estuary models, the pressure is assumed to be hydrostatic: i.e. vertical accelerations are assumed small and are ignored and the pressure at any point is assumed to depend solely on the weight of overlying water. Equation (5) then simplifies to:

$$\frac{\partial p}{\partial z} + \rho g = 0$$

In an analogous way to the study of turbulent flows, in studying tidally-averaged flows it is useful to express the variables in terms of a tide averaged component (denoted by  $\bar{\quad}$ ) and a tidally varying component (denoted by  $\prime$ ) by defining:

$$\begin{aligned} u &= \bar{u} + u' \\ v &= \bar{v} + v' \\ w &= \bar{w} + w' \\ \rho &= \bar{\rho} + \rho' \\ s &= \bar{s} + s' \end{aligned} \tag{8}$$

where for example  $\bar{u} = \frac{1}{T} \int_t^{t+T} u dt$  where  $T$  is the tidal period and, by definition:

$$\bar{u}' = \frac{1}{T} \int_t^{t+T} u' dt = 0$$

The equations for tide averaged flow can now be obtained by substituting equation 8 into equations 1 to 7 and integrating the resulting equations over the tidal period. Further simplifying assumptions can now be made. In the remaining momentum equations (3) and (4), variations in the density are ignored except in the pressure term (the Boussinesq approximation) and longitudinal derivatives of correlations of fluctuating velocity components are assumed small compared with the vertical derivatives and are ignored. The viscous term is also small compared with the other terms and is dropped from the equations.

Equations 1, 2, 3, 4 and 7 become:

### 3. EQUATIONS OF MOTION

The model is based upon the equations describing conservation of mass and momentum. Ignoring source and sink terms, these equations can be written as:

#### Conservation of mass

$$\frac{\delta s}{\delta t} + \frac{\delta us}{\delta x} + \frac{\delta vs}{\delta y} + \frac{\delta ws}{\delta z} = 0 \quad (1)$$

#### Incompressible flow

$$\frac{\delta u}{\delta x} + \frac{\delta v}{\delta y} + \frac{\delta w}{\delta z} = 0 \quad (2)$$

#### Conservation of Momentum

x-direction

$$\frac{\delta \rho u}{\delta t} + \frac{\delta \rho u^2}{\delta x} + \frac{\delta \rho uv}{\delta y} + \frac{\delta \rho uw}{\delta z} + \frac{\delta P}{\delta x} = \nu \left( \frac{\delta^2 u}{\delta x^2} + \frac{\delta^2 u}{\delta y^2} + \frac{\delta^2 u}{\delta z^2} \right) \quad (3)$$

y-direction

$$\frac{\delta \rho v}{\delta t} + \frac{\delta \rho uv}{\delta x} + \frac{\delta \rho v^2}{\delta y} + \frac{\delta \rho vw}{\delta z} + \frac{\delta P}{\delta y} = \nu \left( \frac{\delta^2 v}{\delta x^2} + \frac{\delta^2 v}{\delta y^2} + \frac{\delta^2 v}{\delta z^2} \right) \quad (4)$$

z-direction

$$\frac{\delta \rho w}{\delta t} + \frac{\delta \rho uw}{\delta x} + \frac{\delta \rho vw}{\delta y} + \frac{\delta \rho w^2}{\delta z} + \frac{\delta P}{\delta z} + \rho g = \nu \left( \frac{\delta^2 w}{\delta x^2} + \frac{\delta^2 w}{\delta y^2} + \frac{\delta^2 w}{\delta z^2} \right) \quad (5)$$

where (u,v,w) are the longitudinal, lateral and vertical velocity components in the (x,y,z) directions; s is the salinity; ρ is the density of the water; P is the pressure; ν is the viscosity of water and g is the acceleration due to gravity. In addition to these equations, an equation of state is required relating water density to salinity. The density is also a function of temperature and can be written as:

$$\rho = 1000 + (0.797 - 0.001875T)S - 1000(0.562(T-4)/277)^{1.85} \text{ (kg/m}^3\text{)} \quad (6)$$

where:

T is the water temperature (<sup>0</sup>C) where 12<sup>0</sup> < T < 34<sup>0</sup>C.

$$\frac{\delta \bar{s}}{\delta t} + \frac{\delta \bar{u} \bar{s}}{\delta x} + \frac{\delta \bar{v} \bar{s}}{\delta y} + \frac{\delta \bar{w} \bar{s}}{\delta z} = \frac{\delta F_x}{\delta x} + \frac{\delta F_y}{\delta y} + \frac{\delta F_z}{\delta z} \quad (10)$$

$$\frac{\delta \bar{u}}{\delta x} + \frac{\delta \bar{v}}{\delta y} + \frac{\delta \bar{w}}{\delta z} = 0 \quad (11)$$

$$\frac{\delta \bar{u}}{\delta t} + \frac{\delta \bar{u}^2}{\delta x} + \frac{\delta \bar{u} \bar{v}}{\delta y} + \frac{\delta \bar{u} \bar{w}}{\delta z} + \frac{1}{\bar{\rho}} \frac{\delta \bar{P}}{\delta x} = \frac{1}{\bar{\rho}} \frac{\delta \tau_x}{\delta z} \quad (12)$$

$$\frac{\delta \bar{v}}{\delta t} + \frac{\delta \bar{u} \bar{v}}{\delta x} + \frac{\delta \bar{v}^2}{\delta y} + \frac{\delta \bar{v} \bar{w}}{\delta z} + \frac{1}{\bar{\rho}} \frac{\delta \bar{P}}{\delta y} = \frac{\delta \tau_y}{\delta z} \quad (13)$$

$$\frac{\delta \bar{P}}{\delta z} + \bar{\rho} g = 0 \quad (14)$$

where:

$F_x = \overline{s'u'}$ ,  $F_y = \overline{s'v'}$  and  $F_z = \overline{s'w'}$  are mass fluxes resulting from mixing and  $\tau_x = -\rho \overline{u'w'}$  and  $\tau_y = -\rho \overline{v'w'}$  are shear stresses resulting from exchanges of momentum.

If an accurate solution is to be obtained to these equations, then since  $u'$ ,  $v'$ ,  $w'$  and  $s'$  are not calculated,  $\tau_x$ ,  $\tau_y$  and  $F_x$ ,  $F_y$ ,  $F_z$  must be prescribed in terms of the tide averaged values of  $\bar{u}$ ,  $\bar{v}$ ,  $\bar{w}$  and  $\bar{s}$ . The manner in which these terms are prescribed is given in more detail in the section on longitudinal and vertical mixing.

Equations 10 to 14, after some simplification described below, form the basis for Tasgm.

#### 4. APPLICATION OF THE TIDE AVERAGED EQUATIONS

In the model, layers of finite thickness are used (Figs. 1) the equations 9 to 11 are integrated over the depth ( $\Delta Z$ ) and width (B) of each element.

This integration results in equations for the area averaged velocity components  $u$  and  $v$  defined as:

$$u = \frac{1}{AX} \int \int \bar{u} dy dz \quad (15)$$

$$v = \frac{1}{AY} \int \bar{v} dx dz \quad (16)$$

where  $\left\{ \begin{smallmatrix} AX \\ AY \end{smallmatrix} \right\}$  = cross sectional area of an element face perpendicular to the  $\left\{ \begin{smallmatrix} x \\ y \end{smallmatrix} \right\}$  direction.

For an element in the interior of the flow, for the small slowly varying tide averaged velocities, equations (12) and (13) can be further simplified by noting that horizontal derivatives of products of velocities will be much smaller than vertical derivatives. These terms are therefore dropped and equation (12) becomes:

$$\frac{\delta u AX}{\delta t} + (\bar{u}\bar{w}B)_u - (\bar{u}\bar{w}B)_D + \frac{AX}{\bar{\rho}} \frac{\delta \bar{P}}{\delta x} = \frac{1}{\bar{\rho}} (\tau_x^B)_u - (\tau_x^B)_D \quad (17)$$

where vertical derivatives have now become differences between the upper (subscript u) and lower (subscript D) element faces. In the interior of the flow, the cross sectional area is constant in time and equation 17 can be written as:

$$\frac{\delta u}{\delta t} + \frac{(\bar{u}\bar{w}B)_u - (\bar{u}\bar{w}B)_D}{AX} + \frac{1}{\bar{\rho}} \frac{\delta \bar{P}}{\delta x} = \frac{1}{\bar{\rho}} \frac{(\tau_x^B)_u - (\tau_x^B)_D}{AX} \quad (18)$$

Similarly equation (11) becomes:

$$\frac{\delta v}{\delta t} + \frac{(\bar{v}\bar{w}B)_u - (\bar{v}\bar{w}B)_D}{AY} + \frac{1}{\bar{\rho}} \frac{\delta \bar{P}}{\delta y} = \frac{1}{\bar{\rho}} \frac{(\tau_y^B)_u - (\tau_y^B)_D}{AY} \quad (19)$$

In the surface element, the depths and therefore cross sectional areas are no longer constant. The equations can still be integrated over the depth of the surface element and can be simplified by using the equation describing conservation of volume in a surface element, namely:

$$\frac{\delta h}{\delta t} + u \frac{\delta h}{\delta x} + v \frac{\delta h}{\delta y} - \bar{w} = 0$$

where h is the depth of the surface layer. Using this equation and integrating equations (12) and (13) over the width and depth of a surface element gives:

$$\frac{\delta u}{\delta t} + \frac{1}{\bar{\rho}} \frac{\delta \bar{P}}{\delta x} = \frac{(\tau_w^B)_v - (\tau_x^B)_D}{\bar{\rho} AX} \quad (20)$$

$$\frac{\delta v}{\delta t} + \frac{1}{\bar{\rho}} \frac{\delta \bar{P}}{\delta y} = \frac{(\tau_w^B)_v - (\tau_y^B)_D}{\bar{\rho} AY} \quad (21)$$

where  $\tau_w$  = wind stress on a surface element and the same assumptions before have been used to neglect horizontal derivatives of products of velocity components.

In an element at the bed (subscript b), it is assumed that  $\bar{u}_b = \bar{v}_b = \bar{w}_b = 0$  and equations (18) and (19) become:

$$\frac{\delta u}{\delta t} + \frac{(\bar{u}\bar{w}B)_u}{AX} + \frac{1}{\bar{\rho}} \frac{\delta \bar{P}}{\delta x} = \frac{(B\tau_x)_u - (B\tau_x)_D}{\rho AX} \quad (22)$$

$$\frac{\delta v}{\delta t} + \frac{(\bar{v}\bar{w}B)_v}{AX} + \frac{1}{\bar{\rho}} \frac{\delta \bar{P}}{\delta x} = \frac{(B\tau_y)_u - (B\tau_y)_D}{\rho AX} \quad (23)$$

where, at the bed  $\tau_x = \frac{\rho f |u_T| u}{8}$  and  $\tau_y = \frac{\rho f |v_T| v}{8}$  where  $u_T, v_T$  are the peak tidal velocities and  $f$  is the friction factor.

The equation of conservation of mass eq (10) is integrated over the volume of each element giving:

$$\begin{aligned} & \frac{\delta sV}{\delta t} + (suAX)_k - (suAX)_{kw} + (svAY)_{kn} - (svAY)_k + (swAZ)_{ku} - (swAZ)_k \\ & = (F_z AZ)_{ku} - (F_z AZ)_k + (F_x AX)_k - (F_x AX)_{kw} + (F_y AY)_{kn} - (F_y AY)_k \end{aligned} \quad (24)$$

where  $V$  = volume of the element.

This equation is applicable to all elements where in the surface  $(F_z)_{ku} = w_{ku} = 0$  and in the bed  $(\bar{F}_z)_k = w_k = 0$ . In deriving this equation it has been assumed that  $\bar{us} = us$  etc. This assumption in fact neglects additional diffusion terms which are probably small compared to the diffusion resulting

from averaging over the tidal period ( $F_x$ ,  $F_y$ ,  $F_z$ ). The final empirical representation of these mixing terms includes the mixing resulting from all spacial and temporal averaging.

Similarly, the equation describing incompressible flow (Eq 11) is required in the interior elements and is integrated over the volume of an element to give:

$$(uAX)_k - (uAX)_{kw} + (vAY)_{kn} - (vAZ)_k + (wAZ)_{ku} - (wAZ)_k = 0 \quad (25)$$

where the subscripts refer to element faces as in figure 1. Equation 24 is also used in the bed layer where  $w_k = 0$ , i.e. no flow through the bed.

The pressure terms in equations 18 to 23 can be split into two parts: a pressure gradient resulting from the water surface slope and a pressure gradient resulting from density gradients and can be written in the form:

$$\frac{1}{\rho} \frac{\delta P}{\delta x} = \frac{\rho_s}{\rho} g \frac{\delta h}{\delta x} + P(\rho) \quad (26)$$

(See Appendix )

Using this representation of the pressure term, equations 18 to 26 form the basis for TASGM.

As shown in equations 10, 12 and 13, averaging over the tidal period results in terms ( $F$  and  $\tau$ ) which represent the net exchange of mass and momentum resulting from the tide averaging of the equations. These terms are important and must be evaluated in terms of the tide averaged parameters determined by the model.

#### LONGITUDINAL MIXING

The horizontal diffusive flux through an element face is expressed in the usual form as:

$$F_{x_k} = AX_k D_k \frac{\delta s}{\delta x} \quad (27)$$

where  $D_k$  is the coefficient of longitudinal diffusion.

The coefficient of longitudinal mixing has the form:

$$D_k = \frac{A}{A_T} D_{k1} + Q_k \frac{\Delta x}{A_T} \quad (28)$$

where  $D_{k1}$  = values, table, ref 1;  $\Delta x$  = distance between element centres;  $Q_k$  = discharge;  $A$  = cross-sectional area and  $A_T$  = total cross-sectional area.

#### VERTICAL MIXING

The presence of vertical density gradients greatly reduces the rate of transfer of mass and momentum in the vertical direction and in order to evaluate the vertical exchange terms, a mixing length method has been used which can dynamically vary the mixing according to the calculated density and velocity gradients. Using this approach, the interfacial shear stress and mass flux are:

$$\tau_x = \rho l_m^2 \left| \frac{\partial u}{\partial z} \right| \frac{\partial u}{\partial z} \quad (29)$$

$$F_z = l_m l_c \left| \frac{\partial u}{\partial z} \right| \frac{\partial c}{\partial z} \quad (30)$$

(where  $l_m$  = momentum mixing length;  $l_c$  = solute mixing length,  $c$  = solute concentration)

In neutral conditions (in the absence of density gradients) the mixing lengths are simply a function of the relative depth,  $z/D$ :-

$$l_m = l_c = l_{m0} = 0.4 z \left(1 - \frac{z}{D}\right)^{\frac{1}{2}} \quad (31)$$

where  $D$  = total depth

In stably stratified conditions the mixing lengths  $l_m$  and  $l_c$  also become a function of the Richardson Number,  $R_1$ , where:

$$R_1 = - \frac{g}{\rho} \frac{\frac{\partial \rho}{\partial z}}{\left| \frac{\partial u}{\partial z} \right|^2} \quad (32)$$

Rossby and Montgomery's hypothesis (Ref 3) that the sum of the kinetic and potential energies per unit mass should be the same in stratified and homogeneous flows with identical shearing rates gives rise to the following relationship between  $l_m/l_{mo}$  and  $R_1$ .

$$\frac{l_m}{l_{mo}} = (1 + \beta R_1)^{-\frac{1}{2}} \quad (33)$$

The value of  $\beta$  depends on the vertical structure of the flow, the degree of time averaging and the definition of  $R_1$  (Ref 4).

Bowden and Hamilton, Ref (5), reported that the tide-averaged value of  $(l_m/l_{mo})^2$  and  $R_1$  in the Mersey estuary were 0.1 and 0.5, respectively. This indicates that  $\beta$  has a value of about 20 for tide averaged conditions.  $l_m$  is not thought to fall below a minimum value of about 0.1m so if the result of equation (33) is less than 0.1m,  $l_m$  is set to 0.1m.

The ratio  $l_c/l_m$  decreases with increasing Richardson Number Ref (4).

Tide averaged data published by Bowden and Gilligan, Ref (6), has been used to define the following empirical relationship:

$$l_c = 1.15 l_m e^{-0.70R_1} \quad \text{for } R_1 < 3$$

or

$$l_c = 0.14 l_m \quad \text{for } R_1 \geq 3 \quad (35)$$

The effect of the water temperatures on the water density was allowed for in the equation of state (eq (6)).

#### SOLUTION PROCEDURE

The equations resulting from the finite difference representation of equations 18 to 26 are used to determine the velocity field, water surface level and salt concentration subject to given initial conditions and boundary conditions.

The finite difference method involves a time stepping procedure. That is, knowing the solution at the time  $t$ , the solution at time  $(t + \Delta T)$  is obtained by solving the difference equations. The length of the timestep  $(\Delta T)$  is restricted by considerations of stability and accuracy of the

numerical scheme and by the rate of variation of the boundary conditions. In Tasgm, this timestep will be of the order of several hours.

The solution procedure can therefore be summarised as follows:

- (i) solve for intermediate variables  $u^*$ ,  $v^*$ , (Appendix A);
- (ii) solve for velocities  $u$ ,  $v$  and water surface level incorporating lateral inflows etc;
- (iii) use  $u$ ,  $v$  to find  $w$ ;
- (iv) using calculated velocities and levels, solve for salt concentrations;
- (v) use velocities and salinities (and therefore density) to update mixing coefficients;
- (vi) repeat steps (i) to (v) until the model has simulated the prescribed period.

#### SCHEMATISATION OF THE LAKE GEOMETRY

The Songkhla Lake system consists of a series of large, shallow lagoons connected to each other and to the sea by relatively long narrow deep channels. A large low lying swamp lies to the north of Thale Luang.

For the purposes of the model the system was divided into 16 segments as shown in Figure 2. The size and boundaries of the segments were chosen, taking into account the natural geometry of the system and the size and importance of the connecting channels. The water body was divided vertically into a number of horizontal 1m thick layers (Fig. 3) to take into account the vertical structure of gravitational circulations in the deep channels and two layer wind driven circulations in the Lakes.

A single representative cross-section was used to define the geometry of each of the connecting links between the segments.

The datum for the purposes of the model was taken to be the chart datum for the lake as defined by the Harbour Department to be 0.3m below mean sea

level. However, the results from the model are presented in terms of levels relative to mean sea level to be compatible with observations made by RID.

The larger lakes were sub-divided into two or more segments in order to resolve salinity variations within the water bodies and the effect of wind set-up. Songkhla Channel and Klong Luang were represented as separate segments in order to simulate the gravitational circulation and vertical mixing in these deep channels. The swamp area to the north of Thale Luang were represented as two separate segments 10 and 11 in order to resolve water surface slopes in the swamp.

The slices formed by layering each section formed a total of 89 continuity elements. The model systematically calculates the movement of water, salt and thermal energy between each of the linked elements timestep by timestep throughout a whole year.

The volumes of the elements lying below mean sea level were based on the observed bathymetry of the lakes. This was based on surveys made by the Harbour Department in 1974 and 1975 of the lakes, and in 1981 of Songkhla Channel. Additional cross-sectional information was taken from a check survey of the lakes undertaken by Redcon in August 1984.

## REFERENCES

1. Hydraulics Research Station, Report No EX 1045, Tolo water quality model, Hong Kong, Hydraulic aspects, February 1982.
2. Miles, G V. Formulation and development of a multi-layer model of estuarine flow. Hydraulics Research Station Report No IT 155.
3. Rossby, C G and Montgomery, R B. The layer of Functional Influence in Wind and Ocean currents, Pap Phys Oceanogr, Vol 3, No 3, 1935
4. Odd, N V M O and Rodger, J G. Vertical mixing in stratified tidal flows, J Hyd Div, ASCE, Vol 104, Hy3, Proc Paper 13599, Nov 1978.
5. Bowden, K F and Hamilton, P. Some experiments with a numerical model of circulation and mixing in a tidal estuary. Estuarine and Coastal Marine Science (1975) 3, 281-301.
6. Bowden, K F and Gilligan, R M. 1971. Characteristic features of estuarine circulation as represented in the Mersey estuary. Limnology and Oceanography/6, 490-502.
7. Defant A. Physical Oceanography Vol 1, 1961, p379-381.
8. Hydraulics Research Limited, Report No EX 1178, Benghazi North Lake Project. Effect of proposed schemes on the temperature and salinity of the lagoon.
9. Hydraulics Research Limited, Report No EX 1214, Restoration and Development of Tunis North Lake: Effect of proposed schemes on the rate of flushing of the lagoon.

## Appendix

### Representation of the pressure term

The description of the representation of the pressure gradient term in the momentum equations described below is taken from Miles, Ref 2.

From equation (14), the hydrostatic pressure at any level  $z$  in the fluid is:

$$P = g \int_z^h \rho dz \quad (B1)$$

where  $h$  is the fluid surface.

The pressure gradient in the  $x$  (or  $y$ ) direction can be obtained by differentiating equation (B1) to give (in the  $x$  direction)

$$\frac{\delta \bar{P}}{\delta x} = g \rho_s \frac{\delta h}{\delta x} + g \int_z^h \rho \frac{\delta \bar{\rho}}{\delta x} dz \quad (B2)$$

where  $\rho_s$  = density in the surface layer.

Alternatively, the pressure gradient at level  $z$  may be related to the pressure gradient at a higher level  $z_1$  and the integrated contribution between  $z_1$  and  $z$  as:

$$\left(\frac{\delta \bar{P}}{\delta x}\right)_z = \left(\frac{\delta \bar{P}}{\delta x}\right)_{z_1} + \int_z^{z_1} \frac{\delta \bar{\rho}}{\delta x} dz \quad (B3)$$

From equation (B2), the acceleration of the surface layer resulting from the pressure gradient can be found by integrating B2 over the depth of the surface layer to give:

$$\frac{1}{\rho_s} \left(\frac{\delta \hat{P}}{\delta x}\right) = \frac{1}{\rho_s \Delta z_s} \int_{h-\Delta z_s}^h \frac{\delta \bar{P}}{\delta x} dz = g \frac{\delta h}{\delta x} + \frac{\Delta z_s}{2 \hat{\rho}_s} g \frac{\delta \hat{\rho}_s}{\delta x} \quad (B4)$$

where  $\Delta z_s$  is the depth of the surface layer and  $\hat{\phantom{x}}$  indicates a layer averaged value.

From equations (B3) and (B4) the pressure gradient in layer  $k$  can be expressed in terms of the pressure gradient in the overlying layer ( $ku$ ) as:

$$\frac{\delta P_k}{\delta x} = \frac{\delta \hat{P}_{ku}}{\delta x} + \frac{g}{2} \Delta z_{ku} \frac{\delta \hat{\rho}_{ku}}{\delta x} + g(z_u - z) \frac{\delta \hat{\rho}_k}{\delta x} \quad (B5)$$

Therefore, the acceleration resulting from the pressure gradient in the  $k$ th layer can be written as:

$$\frac{1}{\hat{\rho}_k} \frac{\delta \hat{P}_k}{\delta x} = \frac{1}{\rho_k} \frac{\delta \hat{P}_{ku}}{\delta x} + \frac{g}{2 \hat{\rho}_k} \left[ \Delta z_{ku} \frac{\delta \hat{\rho}_{ku}}{\delta x} + \Delta z_k \frac{\delta \hat{\rho}_k}{\delta x} \right] \quad (B6)$$

Although the lower limit of integration for the mean pressure in the bed layer is a function of  $x$ , the contribution resulting from the variation of the lower limit is cancelled by the back pressure exerted by the bed. Equation (B6) therefore applies in all layers.

The formulation of the pressure gradient is used as follows:

- (i) Equation (B4) is used in the surface layer;
- (ii) The solution of the difference equations begins in the surface layer and proceeds towards the bed summing the terms in equation (B6) to obtain the pressure gradient in each layer in turn.

### Finite difference equations

A second order six point implicit finite difference scheme has been used to obtain a numerical solution to the differential equations (18) to (25). Figure 2 shows a typical model element to which the finite difference scheme is applied and the meaning of all subscripts used in this section can be found in Figure 2.

The derivatives in equations (18) to (26) are represented as, for example:

Temporal:

$$\frac{\delta u}{\delta t} \Big|_k = \frac{u_k^+ - u_k^-}{\Delta T} \quad (A1)$$

Spacial:

$$\frac{\delta h}{\delta x} \Big|_k = \frac{h_{kE}^+ + h_{kE}^- - h_k^+ - h_k^-}{(\Delta x_k + \Delta x_{kE})} \quad (A2)$$

where + refers to time  $t + \Delta T$

and - refers to time  $t$

### Momentum equations

The equations describing conservation of momentum in the x and y directions are similar and in this section only the x (or u) direction equation is considered. The treatment of the v momentum equation is identical to that described below.

The momentum equations contain the layer or element face area averaged velocity  $\bar{u}$  and the value of the velocity ( $u$ ) on the upper and lower element faces. It is assumed that:

$$\bar{u}_k = (R_k u_k + R_{kD} u_{kD})$$

$R_k$  and  $R_{kD}$  are interpolation factors.

In the following equations the  $R_k$  are assumed equal to  $\frac{1}{2}$  for clarity although the model uses the appropriate value. Using the form of the derivatives described above, the momentum equations — using the pressure term expanded as in equation 26 — can now be written in finite difference form:

Equation 18 becomes:

$$\begin{aligned} & \frac{u_k^+ - u_k^-}{\Delta T} + \frac{(u_{ku}^+ + u_k^+)(w_{ku}^- + w_{kuE}^-)B_{ku} - (u_k^+ + u_{kD}^+)(w_k^- + w_{kE}^-)B_k}{4AX_k} \\ & + \frac{2\rho_s}{\rho_k} g \frac{[(h_{kE}^+ - h_k^+)\theta + (h_{kE}^- - h_k^-)(1 - \theta)]}{(\Delta x_k + \Delta x_{kE})} \\ & = \frac{4l^2 m_{ku} (u_{ku}^+ - u_k^+) |u_{ku}^- - u_k^-|}{AX_k (\Delta z_k + \Delta z_{ku})^2} \quad (A4) \\ & - \frac{4l^2 m_k (u_k^+ - u_{kD}^+) |u_k^- - u_{kD}^-|}{AX_k (\Delta z_k + \Delta z_{kD})^2} - P(\rho) \end{aligned}$$

where  $\theta$  is a parameter  $0.5 \leq \theta \leq 1$  used to damp short period oscillations which could arise,  $\rho_s$  = density in surface element,  $P(\rho)$  is the density gradient term described in Appendix B.

Regrouping terms, A4 becomes:

$$f_{kD} u_{kD}^+ + f_k u_k^+ + f_{ku} u_{ku}^+ + g_k (h_{kE}^+ - h_k^+) = E_k^- \quad (A5)$$

Similarly in the surface layer, equation (20) can be reduced to:

$$f_{kD} u_{kD}^+ + f_k u_k^+ + g_k (h_{kE}^+ - h_k^+) = E_k^- \quad (A6)$$

and in the bed layer, equation (22) can be reduced to:

$$f_k u_k^+ + f_{ku} u_{ku}^+ + g_k (h_{kE}^+ - h_k^+) = E_k^- \quad (A7)$$

where the  $f_k$ ,  $f_{ku}$ ,  $g_k$  and  $E_k^-$  are different in each equation (A5, A6 and A7) but represent expressions whose values are known. For example, from equation A4,

$$f_{kD} = \frac{-(w_k^- + w_{kE}^-)B_k}{4\bar{A}X_k} - \frac{4l_{mk}^2(u_k^- - u_{kD}^-)}{\bar{A}X_k(\Delta z_k + \Delta z_{kD})^2}$$

a similar set of equations for momentum in the 'y' direction containing  $v_k^+$  and  $h_k^+$  can be obtained and these equations plus equations A5, A6 and A7 form a complete set of linear equations which could be solved directly for all the  $u_k^+$ ,  $v_k^+$  and  $h_k^+$ . This would be a relatively slow and costly procedure and to save time and to facilitate the introduction of lateral inflows, rainfall and evaporation, the following method was used.

New variables defined as:

$$u_k^* = u_k^+ + g_k (h_{kE}^+ - h_k^+)$$

are introduced and are substituted into the momentum equations A5, A6 and A7. Similarly, define:

$$v_k^* = v_k^+ + g_k (h_{kE}^+ - h_k^+) \quad (A9)$$

for substitution into the equivalent y-momentum equations. After some simplification and using the actual form of the coefficients  $f_k$ ,  $f_{ku}$ , etc, the u momentum equations can be simplified.

Equation A5 becomes:

$$f_{kD} u_{kD}^* + f_{ku} u_k^* + f_{kv} u_{kv}^* = e_k^- \quad (A10)$$

Equation A6 becomes:

$$f_{kD} u_{kD}^* + f_k u_k^* = e_k^- \quad (A11)$$

Equation A7 becomes:

$$f_k u_k^* + f_{kD} u_{kD}^* = e_k^- \quad (A12)$$

where, again to second order,  $e_k^-$  have a known set of values. Equations (A10) to (A12) form a much simpler set of equations than (A5) to (A7). Similar equations can be obtained for  $v_k^*$ . These equations form a tridiagonal set which can be solved independently in each vertical in turn using standard efficient methods to yield the values of  $u_k^*$  and  $v_k^*$  throughout the model area.

In order to recover  $u_k^+$  and  $v_k^+$  from  $u_k^*$  and  $v_k^*$ , the equations for  $u_k^*$  and  $v_k^*$  are integrated over the cross-sectional area of each element and summed over the depth: ie for each vertical, in the u direction,

$$\Sigma u_k^* A X_k = \Sigma u_k^+ A X_k + \Sigma g_k A X_k (h_{kE}^+ - h_k^+) \quad (A13)$$

If  $Q_i^+$  is the total area averaged discharge over vertical i, then  $Q_i^+ = \Sigma u_k^+ A X_k$ . Writing  $Q_i^* = \Sigma u_k^* A X_k$  and rearranging equation (A13) gives:

$$Q_i^* = Q_i^+ + A l h_{kE}^+ - B l h_k^+ \quad (A14)$$

where AI and BI are known. A similar equation can be derived for the total discharge in the y direction.

This equation, (A14), and the equivalent  $v^*$  equation can now be used with the area averaged (one-dimensional) equation describing conservation of volume integrated over each segment, ie

$$\frac{\delta h_k A z_k}{\delta t} + Qu_k - Qu_{kw} + Qv_{kn} - Qv_k = L + P - E \quad (A15)$$

where  $Az_k$  = segment surface plan area,  $L$  = lateral inflows,  $P$  = precipitation,  $E$  = evaporation;  $Qu$ ,  $(Qv)$  = total discharges in the u, (v) direction. Writing  $Qu = (Qu^+ + Qu^-)/2$ , etc equation (A9) in finite difference form is

$$\frac{2Az_k h_k^+}{\Delta T} + Qu_k^+ - Qu_{kw}^+ + Qv_{kn}^+ - Qv_k^+ = e^- + L + P - E \quad (A16)$$

where  $e^-$  is a collection of known terms on the '-' timestep.

Equations (A16), (A14) and the equivalent v direction equation form a complete set of equations which can be solved for all the  $h_k^+$ ,  $Qu^+$  and  $Qv^+$ . Then knowing all the  $u_k^+$ ,  $v_k^+$  and  $h_k^+$ ,  $u_k^+$  and  $v_k^+$  can be found from their equations:

$$u_k^+ = u_k^+ + g_k(h_{ke}^+ - h_k^+) \quad (A17)$$

and

$$v_k^+ = v_k^+ + g_k(h_{kw}^+ - h_k^+) \quad (A18)$$

The vertical velocity components  $w_k$  can now be found from equation (25). Starting in the bed layer where  $w_k = 0$ ,  $w_{kw}$  can be found and so all the  $w_k$  in each vertical can be found by working from the bed towards the surface.

### Salt transport equation

The calculated velocities can now be used to drive the equation of conservation of salt (equation (24)). The finite difference representation of the terms in this equation can be summarised as for example:

$$\frac{\delta sV}{\delta t} = \frac{s^+ V^+ - s^- V^-}{\Delta T} \quad (A19)$$

$$(suAX)_k = \frac{(u_k^+ AX_k^+ + u_k^- AX_k^-)(R_k s_k^+ + R_k s_k^- + R_{kE} s_{kE}^+ + R_{kE} s_{kE}^-)}{2} \quad (A20)$$

where  $R_k$ ,  $R_{kE}$  are interpolation factors required to find  $s$  on an element face.

$$(F_x AX)_k = \frac{D_k AX_k (s_{kE}^+ + s_{kE}^- - s_k^+ - s_k^-)}{(\Delta X_k + \Delta X_{kE})} \quad (A21)$$

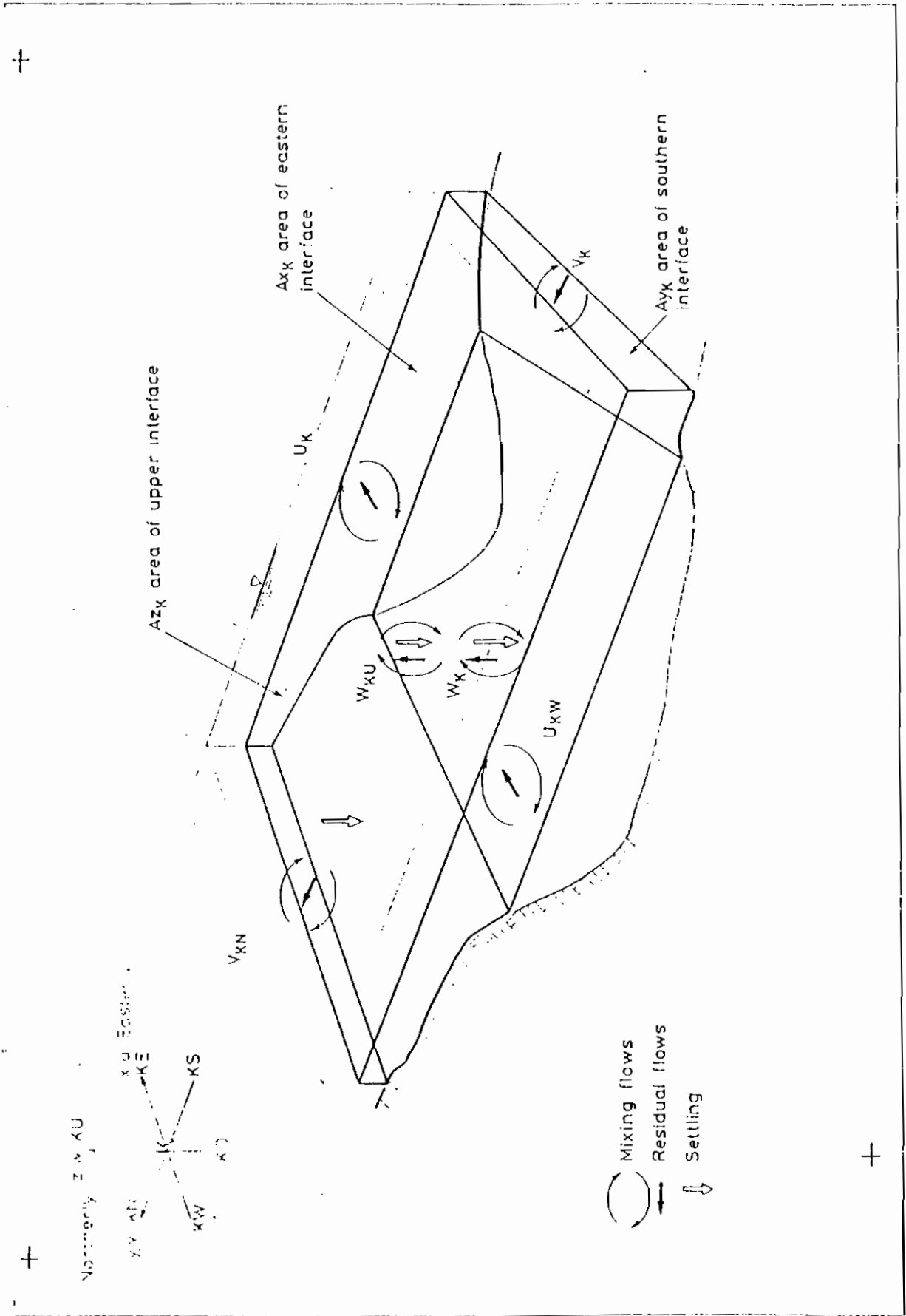
$$(F_z AX)_k = \frac{l_m l_c |\delta u / \delta z| (s_k^+ + s_k^- - s_{kD}^+ - s_{kD}^-)}{(\Delta Z_k + \Delta Z_{kD})} \quad (A22)$$

Substituting for all terms in equation (25) in this way and re-arranging gives for each element:

$$f_{kn} s_{kn}^+ + f_{ks} s_{ks}^+ + f_{kw} s_{kw}^+ + f_{kE} s_{kE}^+ + f_{ku} s_{ku}^+ + f_{kD} s_{kD}^+ + f_k s_k^+ = E_k^- \quad (A23)$$

where all the  $f_k$  and  $E_k^-$  are known.

In the general case, there is no simple or fast method of solving the complete set of equations represented by equation (A11) and the matrix of coefficients must be inverted using standard methods.



Notation and sign convention for a typical element (K)

# 1 Introduction

This appendix describes the theoretical basis, main assumptions and the numerical methods used in QUEST, a three-dimensional, tidally-averaged model of water quality, turbidity and ecosystem in a lagoon system. The model was originally developed to simulate conditions in Tolo Harbour, Hong Kong where two versions were used:- a simple algal growth model (QUEST1) (Ref 1) and a full ecosystem model (QUEST2) (Ref 2) which had prescribed seasonal variations for fish and the higher carnivores. The simpler model was used as a basis for the present study but freshwater weeds (macrophytes) and benthic algae were added to create QUESTP a model tailored for the Songkhla system.

## 2 Equations of transport

The model applies mass balance equations for each of the substances under consideration in each of a series of inter-connected elements. The division of the system into elements is described in Ref 3. The elements were chosen so that they were large enough to make tide averaged calculations meaningful yet small enough to allow variations within the system to be modelled.

In each element the mass balance equation for an arbitrary substance can be written as

$$\begin{aligned} \frac{\partial C}{\partial t} + \frac{\partial}{\partial x} uC + \frac{\partial}{\partial y} vC + \frac{\partial}{\partial z} wC \\ = K_x \frac{\partial^2 C}{\partial x^2} + K_y \frac{\partial^2 C}{\partial y^2} + K_z \frac{\partial^2 C}{\partial z^2} + \frac{\partial}{\partial z} \omega C + \Sigma S \end{aligned} \quad (1)$$

where

C is the concentration of substance

u, v, w are the components of velocity

$K_x$ ,  $K_y$ ,  $K_z$  are the components of the coefficient of eddy diffusivity

$\omega$  is the settling velocity for particulate substances

$\Sigma S$  is the net effect of all the source and sink terms simulated in the water quality and ecosystem interactions for the substance

Using a fully centred implicit finite difference scheme and defining the velocities and concentrations in an element in the manner shown in Fig 2 it is possible to rewrite equation (1) in finite difference form as

$$\begin{aligned}
\frac{V_k^+ C_k^+ - V_k^- C_k^-}{\Delta t} = & \Sigma S_k + \omega_{ku} A_{ku} C_{ku} - \omega_k A_k C_k \\
& + \frac{Q_{x_{kw}}}{2} (r_{x_{kw}} C_{kw}^+ + r_{x_{kw}} C_{kw}^- + r_{x_k} C_k^+ + r_{x_k} C_k^-) \\
& - \frac{Q_{x_k}}{2} (r_{x_k} C_k^+ + r_{x_k} C_k^- + r_{x_{ke}} C_{ke}^+ + r_{x_{ke}} C_{ke}^-) \\
& + \frac{Q_{y_k}}{2} (r_{y_{kw}} C_{kw}^+ + r_{y_{kw}} C_{kw}^- + r_{y_k} C_k^+ + r_{y_k} C_k^-) \\
& - \frac{Q_{y_{kn}}}{2} (r_{y_k} C_k^+ + r_{y_k} C_k^- + r_{y_{kn}} C_{kn}^+ + r_{y_{kn}} C_{kn}^-) \\
& + \frac{Q_{z_k}}{2} (r_{z_{kd}} C_{kd}^+ + r_{z_{kd}} C_{kd}^- + r_{z_k} C_k^+ + r_{z_k} C_k^-) \\
& - \frac{Q_{z_{ku}}}{2} (r_{z_k} C_k^+ + r_{z_k} C_k^- + r_{z_{ku}} C_{ku}^+ + r_{z_{ku}} C_{ku}^-) \\
& + \frac{QDX_{kw}}{2} (C_{kw}^+ + C_{kw}^- - C_k^+ - C_k^-) \\
& - \frac{QDX_k}{2} (C_k^+ + C_k^- - C_{ke}^+ - C_{ke}^-) \\
& + \frac{QDY_k}{2} (C_{kw}^+ + C_{kw}^- - C_k^+ - C_k^-) \\
& - \frac{QDY_{kn}}{2} (C_k^+ + C_k^- - C_{kn}^+ - C_{kn}^-) \\
& + \frac{QDZ_k}{2} (C_{kd}^+ + C_{kd}^- - C_k^+ - C_k^-) \\
& - \frac{QDZ_{ku}}{2} (C_k^+ + C_k^- - C_{ku}^+ - C_{ku}^-)
\end{aligned} \tag{2}$$

where

$C^+$  and  $C^-$  indicate values of concentration at the new and old time levels

$V$  is the volume

$Q_x, Q_y, Q_z$  are the advective discharges across the element faces

$QDX, QDY, QDZ$  are the dispersive discharges across the element faces

$r_{x_k}, r_{y_k}, r_{z_k}$  are interpolation coefficients which are used to determine the concentration at an element face from the values at the centres of adjacent elements

$A_{ku}, A_k$  are the areas of the upper and lower faces of the element.

Collecting up terms in equation (2) gives an equation of the form

$$\begin{aligned}
A_{k,k} C_k^+ + A_{k,kw} C_{kw}^+ + A_{k,ke} C_{ke}^+ + A_{k,ks} C_{ks}^+ + A_{k,kn} C_{kn}^+ \\
+ A_{k,kd} C_{kd}^+ + A_{k,ku} C_{ku}^+ = B_k
\end{aligned} \tag{3}$$

The left hand side of equation (3) contains only advective and dispersive terms and is thus the same for all substances. The right hand side of (3) contains all the interactions as well as some advective and dispersive terms and so is different for each substance.

$$\begin{aligned}
A_{k,k} = & \frac{V_k}{\Delta t} + \frac{Q_{xk} r_{xk}}{2} - \frac{Q_{xkw} r_{xkw}}{2} \\
& + \frac{Q_{yk} r_{yk}}{2} - \frac{Q_{ykw} r_{ykw}}{2} \\
& + \frac{Q_{zk} r_{zk}}{2} - \frac{Q_{zkw} r_{zkw}}{2} + \frac{QDX_{kw}}{2} + \frac{QDX_k}{2} + \frac{QDY_k}{2} \\
& + \frac{QDY_{kw}}{2} + \frac{QDZ_k}{2} + \frac{QDZ_{kw}}{2} \quad (4)
\end{aligned}$$

$$A_{k,kw} = -\frac{Q_{xkw} r_{xkw}}{2} - \frac{QDX_{kw}}{2} \quad (5)$$

$$A_{k,ke} = \frac{Q_{xk} r_{xk}}{2} - \frac{QDX_k}{2} \quad (6)$$

$$A_{k,ks} = -\frac{Q_{yk} r_{yk}}{2} - \frac{QDY_k}{2} \quad (7)$$

$$A_{k,kn} = \frac{Q_{ykw} r_{ykw}}{2} - \frac{QDY_{kw}}{2} \quad (8)$$

$$A_{k,kd} = -\frac{Q_{zk} r_{zk}}{2} - \frac{QDZ_k}{2} \quad (9)$$

$$A_{k,ku} = \frac{Q_{zkw} r_{zkw}}{2} - \frac{QDZ_{kw}}{2} \quad (10)$$

$$\begin{aligned}
B_k = & \frac{V_k}{\Delta t} C_k^- - A_{k,k} C_k^- - A_{k,kw} C_{kw}^- - A_{k,ke} C_{ke}^- - A_{k,ks} C_{ks}^- - A_{k,kn} C_{kn}^- \\
& - A_{k,kd} C_{kd}^- - A_{k,ku} C_{ku}^- + \omega_{ku} A_{ku} C_{ku} - \omega_k A_k C_k + \Sigma S_k \quad (11)
\end{aligned}$$

Combining the mass balance equations for all the elements gives the matrix equation

$$A \cdot X = B \quad (12)$$

where A is a (n x n) matrix and B is the n x m matrix of right hand sides for the m substances considered, and n is the number of active elements

The solution of (12) can be expedited by writing

$$B = B_a + B_r + B_s \quad (13)$$

where

B<sub>a</sub> contains advective/dispersive terms

B<sub>r</sub> the interactions, and

B<sub>s</sub> the settling terms

The solution procedure is then

1. Solve A · X = B<sub>a</sub> to give the advected concentrations C\*
2. Apply the settling procedure for particulate substances to give an amended C\*
3. Calculate the reactions based on C<sup>-</sup>, check that ΣS would not make C<sup>+</sup> negative, restrict reactions if necessary

$$C_k^+ = C_k^* + \frac{\Sigma S_k}{V_k^+} \quad (14)$$

## 4 Ecosystem

As a first step to simulating the ecosystem, QUEST1 includes a simple algal growth model. Ultimately all of the interactions contained in the GEMBASE model developed at the Institute for Marine Environmental Research (IMER) will be incorporated in QUEST2. A description of the full GEMBASE model is outside the scope of this report but details can be found in Ref 4 and will be included in the report describing QUEST2. This section describes the simple algal growth model. The equations relating to respiration and primary production are however those used in GEMBASE.

The algal growth model includes the effect of 6 substances these are

- Algal carbon (AC)
- Detrital carbon (DC)
- Nitrate (CON)
- Orthophosphate (CPH)
- Silica (CSI)
- Dissolved oxygen (CDO)

Nitrate and dissolved oxygen are the 'link substances' between the water quality and algal growth parts of the model. Concentrations of these substances ( $C^*$ ) are calculated from water quality considerations and amended according to the algal growth to give  $C^+$ .

The processes simulated are

**Primary production** Productivity is calculated from the temperature dependent maximum productivity for the species of phytoplankton considered. The maximum productivity is then modified to take account of the limiting effects of nutrient concentrations using Michaelis-Menten relationships.

$$\text{PROD} = P_{MAX}(T) \cdot \mu_1 \cdot \min(\mu_2, \mu_3, \mu_4) \quad (27)$$

where

$P_{MAX}(T)$  is maximum productivity for species

$$P_{MAX}(T) = \exp(2.30259m T + c) \text{ where } m \text{ and } c \text{ are constants} \quad (28)$$

$\mu_1$  is limitation due to light intensity (1)

$$\mu_1 = \frac{e}{k_3(b_2 - b_1)} \left[ \exp\left(-\frac{I}{I_m} e^{-k_3 b_2}\right) - \exp\left(-\frac{I}{I_m} e^{-k_3 b_1}\right) \right] \quad (29)$$

$b_2$  is depth of bottom face of element from the water surface (m)

$b_1$  is depth of top face of element from the water surface (m)

$I_m$  is light intensity required for maximum productivity

$k_3$  is an equivalent extinction coefficient which takes account of turbidity in the overlying water

$\mu_2$  is limitation due to nitrate concentration

$$\mu_2 = \frac{\text{CON}}{\text{CON} + \text{MON}} \quad (30)$$

$\mu_3$  is limitation due to phosphate concentration

$$\mu_3 = \frac{\text{CPH}}{\text{CPH} + \text{MPH}} \quad (31)$$

$\mu_4$  is limitation due to silica concentration

$$\mu_4 = \frac{CSI}{CSI + MSI} \quad (32)$$

MON, MPH, MSI are the nutrient concentrations which would permit 50% of maximum productivity.

**Respiration** Losses due to respiration are calculated as a function of temperature as

$$RESP = RP_{10} \cdot Q_{10} \frac{(T-10)}{10} \times AC \quad (33)$$

$RP_{10}$  is respiration rate at 10°C.

$Q_{10}$  is the rate of increase of respiration for 10°C rise in temperature

**Mortality of algae** In the algal growth model mortality includes the losses due to grazing by zooplankton which in GEMBASE are modelled explicitly

$$INAK = Mp \cdot AC \quad (34)$$

$Mp$  is the mortality of algae ( $\text{day}^{-1}$ )

**Decomposition of detritus** Detritus is considered to decay in a similar manner to BOD

$$DECC = KR \cdot DC \quad (35)$$

where

$$KR = K_{DC} \cdot (1 + \alpha_{DC})^{T-20} \quad (36)$$

$K_{DC}$  and  $\alpha_{DC}$  are constants.

**Settling of algae and detritus**

As algae and detritus are particulate the model allows for settlement in the settling procedure. Particles either settle into a lower element and are then incorporated into the equations for that element or are deposited on the bed where a log is kept of the masses deposited. This calculation is performed before the ecosystem reactions are calculated.

From these processes the resultant concentrations of algal growth parameters are

$$AC_k^+ = AC_k^* + (PROD - INAK - RESP) \times VOLRAT \quad (37)$$

$$DC_k^+ = DC_k^* + (INAK - DECC) \times VOLRAT \quad (38)$$

$$CON_k^+ = CON_k^* + JNPN (DECC - PROD) \times VOLRAT \quad (39)$$

$$CPH_k^+ = CPH_k^* + JNPP (DECC - PROD) \times VOLRAT \quad (40)$$

$$CSI_k^+ = CSI_k^* + JNPS (DECC - PROD) \times VOLRAT \quad (41)$$

$$CDO_k^+ = CDO_k^* + 2.67 (PROD - RESP) \times VOLRAT \quad (42)$$

where JNPN, JNPP, JNPS are the nutrient to carbon ratios in the algae for the relevant nutrient and 2.67 is the carbon to oxygen conversion factor.

$$VOLRAT = \frac{V_k^-}{V_k^+}$$

**Coliforms** It is possible to include an indication of coliform distribution in the system using QUEST. A more accurate assessment is impossible because the elements are large, the advective and dispersive discharges relatively small and the mortality rate of coliforms high. As with other substances the concentration of coliforms due to advection/dispersion is calculated and this concentration  $CF^*$  amended to allow for mortality

$$CF_k^+ = CF_k^* - MORT \times VOLRAT \quad (43)$$

$$MORT = M_{CF} \times CF_k^- \quad (44)$$

$M_{CF}$  is mortality of coliforms ( $\text{day}^{-1}$ )

